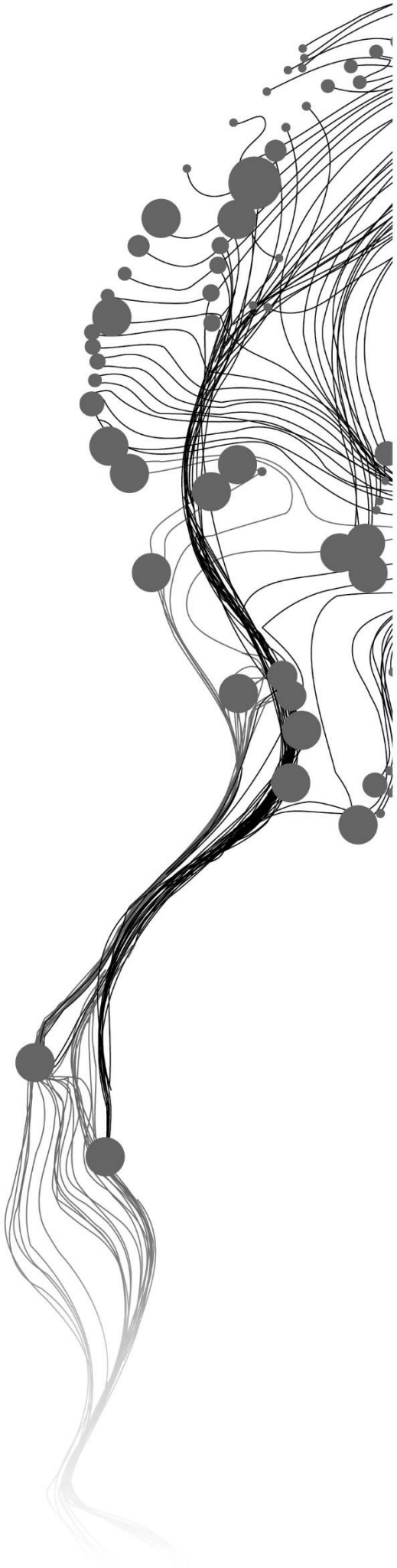
ACCURACY OF TREE HEIGHT DERIVED FROM POINT CLOUDS OF UAV COMPARED TO AIRBORNE LiDAR AND ITS EFFECT ON ESTIMATING BIOMASS AND CARBON STOCK IN PART OF TROPICAL FOREST IN MALAYSIA

JOHN REUBEN

Enschede, The Netherlands, February, 2017

SUPERVISORS:
Dr. Y. A. Hussin
Drs. E. H. Kloosterman



ACCURACY OF TREE HEIGHT DERIVED FROM POINT CLOUDS OF UAV COMPARED TO AIRBORNE LiDAR AND ITS EFFECT ON ESTIMATING BIOMASS AND CARBON STOCK IN PART OF TROPICAL FOREST IN MALAYSIA

JOHN REUBEN
Enschede, The Netherlands, February, 2016

Thesis submitted to the Faculty of Geo-Information Science and Earth Observation of the University of Twente in partial fulfilment of the requirements for the degree of Master of Science in Geo-information Science and Earth Observation.
Specialization: [Name course (e.g. Applied Earth Sciences)]

SUPERVISORS:
Dr. Y. A. Hussin
Drs. E. H. Kloosterman

THESIS ASSESSMENT BOARD:
Dr. A. G. Toxopeus (Chair)]
Dr. T. Kauranne (External Examiner, Lappeenranta University of Technology Finland)

DISCLAIMER

This document describes work undertaken as part of a programme of study at the Faculty of Geo-Information Science and Earth Observation of the University of Twente. All views and opinions expressed therein remain the sole responsibility of the author, and do not necessarily represent those of the Faculty.

ABSTRACT

Forests occupy about one-third of the land area of the earth and have been playing crucial role in regulating the adverse effect of increased emission of greenhouse gasses. Tropical rain forests have higher capacity to sequester carbon dioxide and hence play a role in stabilization of the concentration of greenhouse gasses in the atmosphere. Forest inventory parameters require accurate information for biomass and carbon stock estimation. However, acquiring of forest inventory parameter data especially tree height for estimation of biomass and carbon stock is often a major challenge in tropical forest. A conventional method that is data acquisition using handless tool is tiresome, labor intensive, not applicable in large area and cumbersome approach due to the complexity of tropical forest. On the other hand, data collection using LiDAR technology, is expensive and therefore not readily available. However, rapid advancement in photogrammetry technology in both hardware (i.e., Unmanned Aerial Vehicle) and software (i.e., image matching algorisms) led on data acquisition of fine spatial resolution imagery of less than a meter with notably improved revisit time at affordable cost. Therefore, this study aimed to assess the accuracy of measuring tree height using drone in comparison to that of Airborne LiDAR and assessing its effect on estimating forest biomass and carbon stock.

The accuracy of photogrammetry image matching DTM of UAV and that of LiDAR was assessed by using height (z value) recorded by Differential Global Positioning System (DGPS) and it was revealed that RMSE of UAV DTM was 3.84 m or 7.96% and $R^2 = 0.96$. While the same measures for LiDAR RMSE, RMSE% and R^2 were 1.25 m, 2.75% and 0.99. Then the accuracy of the DTM of UAV was assessed by comparison to the DTM of ALS in all six flight of UAV, and the results revealed that RMSE, RMSE%, R^2 were 0.31 to 1.49 m, 1.57% to 8.34% and 0.53 to 0.82 respectively. The accuracy assessment went further and assessed DTM generated from photogrammetry image matching of UAV in the area which shows small difference between UAV and LiDAR DTM. In this case the RMSE was 0.19 m, RMSE%=0.5%, R^2 was 0.99. While at the same area, estimated tree height of UAV images compared to tree height from airborne LiDAR showed RMSE of 1.56 m and RMSE% of 8.7 with R^2 of 0.80.

Tree height measurements were conducted by using three main methods: field measurement using Leica DISTO, UAV and ALS. The accuracy of estimating tree height of the field and UAV was validated by using the tree height derived from ALS. The validation of field measured tree height revealed that the RMSE was 2.55 m RMSE% of 15.25 and R^2 of 0.62. When estimated tree height of UAV was regressed with derived tree height from ALS, R^2 was 0.78 while RMSE was 1.7 m and RMSE% was 9.63. Furthermore, the AGB and carbon stock was computed using an allometric equation which utilized Diameter at Breast height (DBH), tree height and wood density. The AGB and carbon stock did not show statistically significant difference, the total biomass computed was 189.48 Mg, 177.13 Mg and 172.97 Mg for ALS, UAV and field respectively. The accuracy assessment revealed that 97% of field biomass was accurately modeled by ALS computed biomass, with RMSE of 0.11 Mg (24%). While 99% of calculated UAV biomass was accurately predicted by ALS computed biomass, with RMSE of 0.06 Mg and RMSE% of 13.The measured tree heights were later adjusted to reveal its influence on the calculated AGB and carbon stock. The field trees height was adjusted based on RMSE of 3m while tree height derived from photogrammetry image matching of UAV was adjusted by RMSE = 4m.

Keywords: Tree height, Biomass, Carbon stock, Unmanned Aerial Vehicle, Photogrammetry, Airborne LiDAR, Ortho-mosaic, Digital Terrain Model, Digital Surface Model, Sensitivity Analysis REDD+MRV

ACKNOWLEDGEMENTS

I would like to take this crucial opportunity to express my gratitude appreciation to Almighty God for protection and care since the commencement and completion of my study here in Netherland. I would love to express my heartfelt appreciation to ITC, University of Twente and Netherland Fellowship Program (NFP) who granted me a space for study and scholarship opportunity to pursue the MSc degree. Also, I would like to convey my thanks to MJUMITA executive director Rahima Njaidi and TFCG executive director Mr. Charles Meshack for their encouragement during my entire time of study.

Words are not enough to express my gratitude thank to my supervisors, Dr. Yousif Ali Hussin, my first supervisor and Drs E. Henk Kloosterman, second supervisor for your constructive criticism, advice, guidance and readily being available any time during the whole time of the research. Without your guidance, advice and encouragement this research would hardly come to an end. Working with you was unique experience in my life since I learned how to reason critically and try to visualize things in different angle.

My sincere thanks go to Dr. Thomas and Dr. A.G. Toxopeus, for their constructive and genuine comments during the first term and mid-term of proposal defense. I would like to extend my thankful to Drs. Raymond Nijmeijer, NRM, Course Director for tireless continuous of feedback.

I would like to acknowledge the University Putra Malaysia (UPM) for systematic logistics support during field work. Sincerely special thanks should go direct to Dr. Mohd Hasmadi for constructive comments during presentation of my proposal at UPM. My gratitude appreciation should go to UPM team (rangers and drivers); Mrs. Sitti Zurina Zakaria, Mr. fazli Shariff, Mr. Fazrul Azree, Mr. Jelani Alias and Mrs. Noor Azlina Azizdim for their tireless support during field execution in Ayare Hitam Forest Reserve, without their support, data collection would be more difficult.

I would like to extend my appreciation to my fieldwork teammates Mariam, Muluken, Solomon and Juvenal for the team working spirit and encouragement being around you was unique experience and had invaluable meaning in my study. I wish to thank all NRM classmates for the time and cooperation during the entire time of the study. Special thanks go to my friends Aman Desta, Ghebregziabher, Benjamini, Paulina, and Jefferson for their friendly advice.

Last but not least I would like to express my heartfelt gratitude to my lovely wife Rhoda Richard Lema and our beautiful baby Grace John Reuben for unconditional love you have been showing me during the entire time of the research. Special thanks go to my father (Reuben Hongoa) and mother (Pascalia Celestine) for their moral support and encouragement. I would love to convey my gratitude appreciation to the family of Mr. Charles Meshack Mulimila for supporting my study since primary education to undergraduate which built up the foundation my academic career. I would like to express my thanks to the family of aunt, Felista Celistine and uncle Kahana Celestine for their advice and encouragement during my study.

TABLE OF CONTENTS

LIST OF FIGURES iv
LIST OF TABLES vi
LIST OF EQUATIONS vii
LIST OF APPENDICES viii
LIST OF ACRONYMS ix
1. INTRODUCTION 1
1.1. Background 1
1.2. Literature review 3
1.3. Research problem and Justification 5
1.4. Objectives 6
1.5. Research questions 7
1.6. Hypothesis or anticipated results 7
2. STUDY AREA 8
2.1. Geographic location of the study area 8
3. METHODS 11
3.1. UAV data acquisition and processing 12
3.2. LiDAR data processing 18
3.3. Field data collection 19
3.4. Comparing results and sensitivity analysis 21
4. RESULTS 23
4.1. UAV Digital Terrain Model (DTM) Generation 23
4.2. Comparison of ALS and photogrammetric image matching DTM'S 23
4.3. Comparison of DTM's in relatively close altitude 27
4.4. Biometric data 29
4.5. Accuracy assessment for airborne LiDAR CHM 30
4.6. Accuracy of assessing tree height measurement 31
4.7. Assessing tree height measurement differences (ALS, UAV and Field) 35
4.8. Biomass estimation 36
4.9. Carbon Stock estimation 37
4.10. Sensitivity analysis 38
5. DISCUSSION 45
5.1. Accuracy of UAV DTM 45
5.2. Tree height estimation using Leica DISTO 48
5.3. UAV tree height estimation 50
5.4. Tree height derived from Airborne Lidar 52
5.5. Estimation of above ground biomass 52
5.6. Carbon stock estimation 53
5.7. Sensitivity Analysis of tree height measured error to the biomass and carbon stock estimation 53
6. CONCLUSION AND RECOMMENDATION 55
6.1. Conclusion 55
6.2. Recommendation 56
LIST OF REFERENCES 59
APPENDICES 67

LIST OF FIGURES

Figure 1: UAV surveying in forest 3
Figure 2: Study area 9
Figure 3: Phantom4 DJI UAV/Drone 10
Figure 4: Placing tags before tree measurements 10
Figure 5: Methods simplified in the flowchart 11
Figure 6: UAV flight mission and parameters set in the study area. 13
Figure 7: Marking ground control point for the DGPS measurements 14
Figure 8: Adding of ground control points in the UAV images 14
Figure 9: Example of UAV images uploaded in the Agisoft PhotoScan Professional 15
Figure 10: Photoalignment and sparse point clouds 15
Figure 11: Dense point clouds reconstructing parameter and Dense Point Clouds 16
Figure 12: DSM (a), Orthomosaic (b) and DTM (c) for first flight 16
Figure 13: UAV CHM on screen segmentation 18
Figure 14: UAV CHM for first and second flight 18
Figure 15: LiDAR data segmentation 19
Figure 16: Airborne LiDAR-derived CHM 19
Figure 17: Plot delineation 20
Figure 18: Buttress and folk tree 21
Figure 19: Relationship between ALS DTM and DGCP height 24
Figure 20: Relationship between UAV DTM and DGCP height 25
Figure 21: Comparison of UAV from ALS DTM height based on the centroid pixel value (DTM height). 27
Figure 22: Comparison of UAV from ALS DTM height based on perfect height match. 27
Figure 23: Relationship between ALS DTM height and UAV DTM height 28
Figure 24: Histogram showing positive skewness of the DBH 30
Figure 25: Scatter plot of the relationship between UAV and Airborne LiDAR 32
Figure 26: Scatter plot of the relationship between field height and UAV tree height 33
Figure 27: Scatter plot of the relationship between ALS height and Field height 34
Figure 28: Effect of differences of field measured tree height on AGB estimation 39
Figure 29: Bar chart indicating the effect of differences of field tree height measurements on AGB estimation 41
Figure 30: Bar chart indicating the effect of differences of field trees height measurements on carbon stock 41
Figure 31: Bar chart indicating effect of differences of UAV tree height measurements on biomass estimation 42
Figure 32: Sensitivity analysis of AGB to tree height adjusted based on the RMSE 42
Figure 33: Bar chart indicating effect of error in tree height on carbon stock 43
Figure 34: The effect of differences of UAV estimated trees height on AGB 44
Figure 35: Effects of differences of tree height measurement in ALS, UAV and field on biomass estimation. 44
Figure 36: Scatterplots showing the relationship between GPS surveyed plot center points against DTM_{SfM} (left) and DTM_{lidar} (right). 46
Figure 37: Comparison of Airborne LiDAR and photogrammetry points cloud 48

Figure 38: Effect of occlusion in tree height measurements 49
Figure 39: Relationship between ALS and field tree height..... 50
Figure 40: The relationship between SfM against field measured tree (left) and ALS tree height (right) 51
Figure 41: LiDAR, UAV and field measurements 54

LIST OF TABLES

Table 1: Parameter used for UAV data collection 12
Table 2: Summary of photogrammetry features of the generated of all flight DTM 23
Table 3: Accuracy assessment of ALS DTM using GCP collected by DGPS 24
Table 4: Accuracy assessment of UAV DTM using GCP collected by DGPS 24
Table 5: Summary for comparison of ALS and UAV DTMs height extracted from centroid pixel value for all flights 25
Table 6: Summary of comparison of ALS and UAV tree height extracted from all flights 26
Table 7: Summary for comparison of ALS and UAV biomass and carbon stock extracted from all flights 26
Table 8: Descriptive statistics of the ALS and UAV measured tree height in the area where DTMs have slightly difference 28
Table 9: Comparison of UAV and ALS tree height where UAV and ALS DTMs have slight difference in height 28
Table 10: Descriptive statistics of DBH height 29
Table 11: DBH normality test 29
Table 12: Summary statistics for matched trees 31
Table 13: Descriptive statistics for Lidar and UAV tree height 32
Table 14: Relationship between ALS height and UAV estimated tree height 33
Table 15: Descriptive statistics for UAV and field height 33
Table 16: Relationship between UAV height and Field height 34
Table 17: Descriptive statistics for ALS and field height 34
Table 18: Relationship between ALS height and Field height 35
Table 19: Descriptive statistics for ALS, UAV and Field biomass 37
Table 20: Relationship and accuracy of UAV computed biomass 37
Table 21: Relationship and accuracy of field computed biomass 37
Table 22: Summary of ALS, UAV and field carbon stock 38
Table 23: Summary of relationship and accuracy of UAV computed carbon stock 38
Table 24: Relationship and accuracy of field computed carbon stock 38
Table 25: Effect of differences of measured field tree height on biomass estimation 39
Table 26: Effect of differences of trees height measurements on estimation of carbon stock estimation 40
Table 27: Effect of differences of field height measurement on AGB and carbon stock estimation 40
Table 28: Effect of differences of UAV estimated trees height on biomass estimation 41
Table 29: Effect of differences of UAV estimated tree height on estimation of carbon stock 43
Table 30: Change in biomass and carbon stock due to field measurement error 43
Table 31: Comparison of photogrammetry and ALS DTM using GPS surveyed 46
Table 32: The error variables of the DTMs interpolated by the five different methods for the four test sites 47
Table 33: Comparison of individual tree height models (n = 86) based on photo-CHM and LiDAR-CHM metrics. 51

LIST OF EQUATIONS

Equation 1: Over segmentation equation model 17
Equation 2: Under segmentation equation model 17
Equation 3: Measure of goodness 17
Equation 4: RMSE computation 21
Equation 5: Allometric equation for above ground biomass 22
Equation 6: Carbon stock estimation 22

LIST OF APPENDICES

Appendix 1: Field Measurement form 67
Appendix 2: Common LiDAR sensor parameters for natural resource applications 68
Appendix 3: List of equipment which was used in field equipment 68
Appendix 4: List of software and its principle function 68
Appendix 5: t-test to compare height for ALS and UAV DTMs 69
Appendix 6: t-test to compare tree height for ALS and photogrammetric image matching DTMs where DTM had small difference 69
Appendix 7: One way analysis of variance (ANOVA) for field, UAV and ALS tree height 70
Appendix 8: F test for variance 70
Appendix 9: t-test for ALS and UAV tree height 70
Appendix 10: F test of UAV and field tree height 71
Appendix 11: t-test for field and UAV tree height 71
Appendix 12:F test for ALS and field tree height 71
Appendix 13: t-test for Airborne Lidar and Field height 72
Appendix 14: Relationship between ALS and UAV biomass 72
Appendix 15: t-test: for ALS and UAV biomass 72
Appendix 16: Relationship between ALS and field biomass 73
Appendix 17: t-test: for ALS and field biomass 73
Appendix 18: Relationship between ALS and field carbon stock 74
Appendix 19: Relationship between ALS and UAV carbon stock 74
Appendix 20: Sampled trees with their GPS coordinate of individual tree and DBH and tree height measurement 75
Appendix 21: Field photos 84

LIST OF ACRONYMS

AGB:	Above Ground Biomass
ALS:	Airborne LiDAR System
CAA:	Civil Aviation Authority
CF:	Carbon Fraction
CHM:	Canopy Height Model
DBH:	Diameter at Breast Height
DEM:	Digital Elevation Model
DGPS:	Differential Global Position System
DOD:	Department Of Defence
DSM:	Digital Surface Model
DTM:	Digital Terrain Model
GCP:	Ground Control Points
GPS:	Global Position System
GSD:	Ground Sample Distance
IMU:	Inertia Measurement Unit
IPCC:	Intergovernmental Panel on Climate Change
LiDAR:	Light Detection And Ranging
MRV:	Measurement Report and Verification
nDSM:	Normalized Digital Surface Model
OBIA:	Object Based Image Analysis
REDD:	Reduce Emission from Deforestation and forest Degradation
RMSE:	Root Mean Square Error
SfM:	Structure from Motion
TIN:	Triangulation Irregular Network
TLS:	Terrestrial Laser Scanning
UAV:	Unmanned Aerial Vehicle
UAS:	Unmanned Aerial System
UNFCCC:	United Nations Framework Conversion on Climate Change
UPM:	University Putra Malaysia

1. INTRODUCTION

1.1. Background

Forests occupy about one-third of the land area of the earth and play crucial role in regulating the adverse effects of increased emission of greenhouse gasses in the atmosphere. Trees and forests play an important role in human livelihoods, as well as in ecosystem services and health (Lindquist et al., 2012). Among ecosystem services offered by the forest include regulation of hydrological cycles, mitigation of global climate change, recreation and biodiversity conservation (Sabogal et al., 2013). Therefore, sustaining these services under increasing community demand depends on effective forest management, which is in turn based on concrete scientific understanding of the natural processes of carbon cycling (Masek et al., 2015). In addition, Winjum et al. (1992) stated that forests play a crucial role in the global carbon cycle, and forest vegetation and soils comprise about 60% of the total terrestrial carbon stock. Furthermore, Gibbs et al. (2007) emphasized that forests sequester and store more carbon than any other terrestrial ecosystem and therefore play potential role in regulating the effect of climate change. The severe impact on biodiversity has been contributed by ongoing anthropogenic activities. *"Human influence on the climate system is clear, and recent anthropogenic emissions of greenhouse gasses are the highest in history. Recent climate changes have had widespread impacts on human and natural systems"* (IPCC, 2014). This has clearly been shown on the recently changing in climate in combination with mathematical model prediction (Bellard et al., 2012), through multiple terrestrial (Bonan, 2008) and marine ecosystems (Moberg & Folke, 1999), with significant influence on human settlements and variable but often negative and significant socio-economic consequences across regional scales (Lane et al., 2013). Additionally, increasing impact of climate change will have significant adverse consequences for biodiversity and ecosystem functions (Getzin et al., 2012), and may also imply multiple negative impacts on their socio-economic value and benefits such as food production, public health and people's livelihood sustainability (Moberg & Folke, 1999).

According to Angelsen (2009), Molto et al. (2013) and Nations (1998) global initiative aimed to reduce the impact of climate change through establishing reducing emissions from deforestation and forest degradation, and enhancing forest carbon stocks in developing countries (REDD+) which involve payment for environmental services (PES). The UNFCCC signed by 150 countries to conventionally commit to have an update, publish and make available their national assessment of the forests, however, the current review indicated that very few countries meet the minimum ability needed for MRVs (Angelsen, 2009). Additionally Herold & Schiller (2009) insisted that most of developing countries have limited capacity to assess accurately their biomass and carbon stock. Nabuurs et al. (2008) explained that for biomass and carbon estimation, the inventory-based approach is conducive and reliable. Therefore, REDD+ established measurement report and verification (MRVs) as a way to quantify biomass pools in which above ground biomass is the part of it. In order to assess above ground biomass and carbon stock REDD+ through MRVs require accurately data measurements of the forest parameters, which is important for accurately estimation of the AGB and carbon stock (IPCC, 2014). The accurate methods on estimating AGB in REDD+ scheme especially on evaluating the baseline for national carbon has been stated by (Gibbs et al., 2007; Chave et al., 2015).

The role of tropical forests in global climate change, especially the carbon cycle and its relation to the greenhouse effect, has increased interest in estimating the biomass density (Henry et al., 2011). Because of their high carbon density, tropical forests are increasingly viewed as the place for mitigation of climate

change (Hunter et al., 2013). In an effort to reduce deforestation and degradation by creating monetary value for the carbon in forests, the United Nations Framework Conversion on Climate Change (UNFCCC) introduced Reduce Emission from Deforestation and Forest Degradation (REDD+) program in developing countries as strategy to regulate the effect of greenhouse gasses in the atmosphere (Gibbs et al., 2007). One important component of REDD+ is Measuring Report and Verification (MRVs). This mechanism refers to prolonged measurement and collection of data on the anthropogenic forest related greenhouse gas emissions. In addition to that Henry et al. (2011) argued that because of interest in the global carbon cycle, estimating aboveground biomass with the required accuracy to establish the increase or decrease of carbon stored in forests is very important. However, they stated that the largest errors in estimates of the terrestrial carbon balance are believed to result from uncertain rates of tropical deforestation.

Accurate estimates of forest biomass can offer valuable facts about the productivity and functioning of the forest ecosystem and have been vital due to its impact on ecosystem process and carbon cycles (Sadadi, 2016). In estimation of forest biomass, most biomass prediction models utilize the tree height as one of the fundamental predictor variables (Chhetri & Fowler, 1996). Tree height is one of essential variable in the quantitative assessment of forest biomass and carbon stocks (Andersen et al., 2006). Additionally, Chhetri & Fowler (1996) urged that tree height can be estimated in forest stand, however, the activities would be tedious, time consuming and costly. Consequently, due to its importance in biomass estimation and eventually carbon stock computation, research on tree height estimation has been given more priorities. Previous work has shown that the inclusion of height in biomass allometries, compared to the sole use of DBH, would significantly improve biomass estimation accuracy (Hunter et al., 2013).

Several studies have been carried out to measure or estimate tree height. These techniques range from traditional field work using hypsometers to the more advanced approaches of using remote sensing. In the traditional field work, measuring tree height is generally more cumbersome and time consuming than measuring diameter at breast height (Mugasha et al., 2016). Direct measurement of forest parameters for estimation of aboveground biomass is very expensive and therefore the measurements are limited to 10-year intervals (Houghton, 2005). Many studies have been using field data as ground truth, wider ranges of equipment have been used in traditional method of measuring tree height. This equipment includes: Haga altimeter, Abney level, Blume-Leiss altimeters and Suunto clinometer. Measuring tree height using Haga and then checking up with actual measurement did not show the significant different in temperate forest, especially when trees are scattered. Their measurement accuracy is approximately ± 1-2 meters (Solomon & Nolet, 1968). Trigonometry principles have been employed to estimate tree height using these equipment (Chave, 2005). Sicking (1998) revealed that the accuracy of tree height measurement can be enhanced by using laser finder with its accuracy approximately ± 0.50 – 0.75 meters. Therefore, high uncertainties in measuring field data are a very sensitive issue because these data are essential for the validation of remotely sensed data. The controlled experiment done prior to this study revealed that there was a variation in the measurement of the height of the tree reported by observers due to invisibility of the tree top caused by intermingling of the tree crown.

However, Fritz et al. (2013) stated that, compared to other platforms such as airborne sensors, UAV shows comparatively low costs for acquisition of information and high flexibility with Unmanned Aerial Vehicles (UAVs) devices led to intense research in the field. Recently, UAVs have developed to off the shelf platforms for remote sensing applications and photogrammetric data acquisition (Fritz et al., 2013). UAVs have been proven to be valuable platforms for mounting cameras to create photogrammetric point clouds through the structure from motion technique (Maltamo et al., 2014).

1.2. Literature review

1.2.1. UAV photogrammetry overview

Unmanned Aerial Systems (UAS) is famous with different names and acronyms, such as "Unmanned Aerial Vehicle" (UAV), "aerial robot" or simply "drone," with "UAV" and "drone" being the most known. The term UAS was adopted by the US Department of Defense (DOD) and the Civil Aviation Authority (CAA) of the UK (Colomina & Molina, 2014). UAVs have primarily been used in the military domain. With the increased availability of low-cost and lightweight Global Positioning System (GPS) receivers, Inertial Measurement Units (IMUs), digital cameras, and autopilot systems, the civilian use of UAVs has increased dramatically in recent times (Zhang et al., 2016; Colomina & Molina, 2014; Fritz et al., 2013). In particular, the use of UAVs for photogrammetry and remote sensing presents many new and exciting opportunities (Jaime et al., 2014). The collection of ultra-high resolution data (~1 cm/pixel) with centimeter level accuracy is one area in which small UAVs offer the greatest potential.

UAV photogrammetry provides a potential usefulness in aerial photography, surveillance, live video motion, research, mapping services and ecosystem monitoring (Figure 1). To be able to capture UAV stereo pictures, the camera is configured to produce 12.2 megapixels with 8-bit radiometric resolution stored in the digital card, the camera has 14 – 42 mm zoom lens although it was fixed at 14 mm focal length for these works. The camera's sensor size is 17.3 x 13.0 mm and the pixel size is 0.0043 mm. These parameters are needed to calculate the image resolution on the ground/ground sample distance (GSD) is affected by the flight altitude.



Figure 1: UAV surveying in forest

Source: DJI- Phantom – Drones

1.2.2. UAV flight mission

UAV requires flight plan setting before data imagery acquisition. It involves setting of the extent boundary where the UAV will pass through and across during data collection. In a study conducted by (Torres-sánchez et al., 2015). UAV was configured with visible light camera in such a way that the camera continuously took the photo at the interval of 1 second. Mayr (2011) emphasize that for unmanned aerial system mission plan and management system are very important components for geodata acquisition. It has been noted that logical and careful design of aircraft trajectories such as speed, attitude, strips, waypoint and real-time mission management are crucial in succeeding on data acquisition. The typical features of UAV plan mission are 80% forward and 60 – 80% cross overlap to compensate for instability of the aircraft (Colomina & Molina, 2014).

1.2.3. Overview of previous work on UAV

In the study conducted by Seul et al. (2015) UAV was used to estimate tree height and compared with tree height which was estimated using haga and suunto hypsometer because it estimates tree height more accurately. In this study, ground survey field and UAV extracted tree height measurements did not show a significant different. The study showed that the average difference between the tree heights measured by hypsometer and that by the UAV was 0.53m in test area 1 and 2.07m in test area 2. According to Lisein et al. (2014) the use of UAV photogrammetry in the forest inventory play crucial role in monitoring of the forest ecosystem through high temporal image acquisition on a local scale.

Additionally, orthophoto mosaics image which is provided by UAV stereo images can be used to demarcate forest stand. In the study done by Zarco-Tejada et al. (2014), UAV acquire 750 and 679 images in two sites of 95 ha and 56 ha respectively and ortho-mosaic and DSMs were developed. The validation was done using 152 trees measured in the field using GPS system. The results of estimating tree height using UAV shown that VHR DSMs yielded R^2= 0.83, while root mean square error (RMSE) of 35 cm. In the study conducted by Torres-sánchez et al. (2015) tree height was estimated with higher accuracy with the root mean square error reported was ranging from 0.17–0.18 m from the UAV stereo image which was acquired with the camera and of 0.22–0.53 m from the images recorded with the multi-spectral camera. In this study, the object based image analysis was used, which mainly had the advantage of aggregating the pixels to create a new segment (tree). Also, the study done by Zarco-tejada et al. (2014) and Kattenborn et al. (2014) revealed that tree height estimation using UAV technology recorded RMSE of 0.33–0.39 m and of 0.44–0.59 m in olive-tree and palm-tree plantations, respectively. An essential difference with these investigations refers to the image analysis technique used to compute the tree parameters in each case. In this study, the tree delineation used pixel based filtering algorism.

1.2.4. Airborne LiDAR

Airborne LiDAR refers to the Light Detection and Ranging. It is also called airborne laser scanning (ALS) system which is active remote sensing technology. In forest, LiDAR technology has been given more attention since its applicability has been improving since 1980s. But LiDAR technology had already been used for the generation of digital elevation models (DEMs) which is important in extracting of CHM (Ritchie, 2016). Currently, GIS software has developed tools that provide easy way of processing and analyzing LiDAR data (Zawawi et al., 2015).

Airborne LiDAR provides better vertical profile of bare land and vegetation structure and therefore helped to acquire more accurate information of forest tree height surveying (Koch et al., 2006). Additionally Ruiz et al. (2014) revealed that LiDAR technology has provided the best way of representing the height structure of the canopy of the forest and therefore enable description of complex structure of the forest ecosystem and offer valuable information to improve their management. To perform its function more efficiency, LiDAR system has three basic fundamental components which are (1) a laser

scanner, (2) a Global Positioning System (GPS) and (3) an Inertia Measurement Unit (IMU) (Yang & Li, 2012). Because of IMU system which corrects the error of each point cloud the vertical accuracy for commercial applications can reach few centimeters on discrete points.

Furthermore, LiDAR technology allows ranging of objects which is accomplished by measuring the time of flight between emitted pulses and their received reflections. In combination with accurate position and attitude sensors, LiDAR allows the remote measure of forest structure from airborne or spaceborne platforms (Leeuwen & Nieuwenhuis, 2010).

1.2.4.1. LiDAR application

In tree height estimation using LiDAR system, determination of distance from the targeted object is based on generation of short duration laser pulses (nanosecond or less) which are transmitted toward a targeted object (trees). A target is defined as any object that reflects back the light pulse (or part of it) and triggers the receiver. The receiver measures the lapse time between pulse initiation and its return. Highly accurate timing (less than a nanosecond) is required. Time is converted to distance using the velocity of light Laser pulse width and timing electronics determine vertical resolution. Current timers allow the determination of surface topography with a vertical resolution of less than 5 cm (Ritchie, 2016). Additionally Evans et al. (2009) stated that Lidar system operates on the fundamental principle that the time taken for a laser pulse to travel from the sensor to a target and back again to the sensor enables calculation of the distance between the instrument and the scattering object(s). In data acquisition, scanning angle is very important because when the scanning angle is higher it can reduce the cost associated with the operation since more ground is covered in a single line (Holmgren et al., 2003).

1.2.5. Acquisition parameters

Lidar system generates number of pulses per second (pulse repetition frequency) such as 50,000 pulses per second. On a single flight swath, pulse repetition frequency (PRF) is a basic factor that determines pulse density that can be attained (Evans et al., 2009). Numbers of returns are very important. Within a single laser pulse discrete return LiDAR can record number of measurements and depending on the sensor 3 – 5 returns are possible per laser pulse. In the study done by Evans et al. (2009) the simulation results of angle indicated that when the scanning angle is greater than 10 off-nadir error is introduced (Appendix 2).

1.3. Research problem and Justification

Tree height and Diameter at Breast height (DBH) are important parameters of the forest that used as input in the allometric equation for quantification of forest biomass and carbon stock. Andersen et al. (2006) reported that tree height is one of essential variable in the quantitative assessment of forest biomass and carbon stocks. According to Chave (2005) as cited by Hunter et al. (2013) revealed that in the estimation of biomass and carbon stock, inclusion of tree height in the model can significantly improve the accuracy of estimating carbon stock. Additionally, Chhetri & Fowler (1996) urged that tree height can be estimated in forest stand, however, the activities would be tedious, time-consuming and costly. Previous work has shown that the inclusion of height in biomass allometries, compared to the sole use of DBH, would significantly improve biomass estimation (Hunter et al., 2013). Several studies have been carried out to measure or estimate tree height. These techniques range from traditional field work using hypsometers to the more advanced approaches of using remote sensing. In the traditional field work, measuring tree height is generally more cumbersome and time consuming due to intermingling of the crown of the trees (Mugashaet al., 2016; Zawawi et al., 2015;Rahman et al., 2015) . Direct measurement of forest parameters for estimation of aboveground biomass is expensive and therefore the measurements are limited to 10-year intervals (Houghton, 2005). In the controlled field experiment which was done prior to this research where observers were measuring tree height at different distance from the tree, it was revealed that there were variations in tree height measurements reported by different observers. The error

was attributed to the increase in the distance from the tree, obscured of tree top due to occlusion of the crown of the tree.

In remote sensing, Airborne LiDAR System (ALS) has been used as a fundamental remote sensing technique to estimate tree height and consequently carbon stock. Jensen & Mathews (2016) and Zhang et al. (2016) reported that ALS and space satellite are remote sensing technique which has been used to estimate aboveground biomass and subsequently carbon stock. In the study done by Kumar (2012), ALS was used to estimate tree height. Also Sadadi (2016) reported that ALS was considered the most accurate and efficient way of assessing field measured tree height and subsequently biomass and carbon stock. His results revealed that RMSE of the field measured tree was 4.2 m (21.45%) when compared to ALS estimated tree height and coefficient of determination was 0.61. The fact that ALS is the most accurate and efficient way of assessing tree height provided reliable DTM is available, but LiDAR is an expensive tool and therefore not readily available.

Recently, advances in photogrammetry image matching of UAV 3D point cloud extraction technology from very high-resolution images potentially offer a cheap and flexible alternative for ALS. Fritz et al. (2013) stated that, compared to other platforms such as airborne sensors, UAV shows comparatively low costs for acquisition of information and high flexibility with Unmanned Aerial Vehicles (UAVs) devices led to intense research in this field. Currently, UAVs have developed to off the shelf platforms for remote sensing applications and photogrammetric data acquisition (Fritz et al., 2013). UAV provide extremely fine resolutions and thus allow the identification of previously undetected object details, and images are rarely affected by cloud cover because flying altitudes are usually low. Flight missions can be timed very flexible and they are very cost-effective (Getzin et al., 2012; Fritz et al., 2013). UAV imagery is characterized by a high image overlap and therefore, has the potential to accurately model the canopy surface and tree height at a very high spatial and temporal resolution (Lisein, et al., 2014). Many types of research have been done in estimating AGB using UAV in temperate forest and very little in tropical forest. Limited numbers of research have been comparing UAVs from ALS and assess its accuracy in AGB estimation, especially in tropical forest.

1.4. Objectives

1.4.1. Research objective

To investigate the accuracy of tree height extracted from 3D point clouds of photogrammetry image matching of UAV in comparison to tree height estimated with ALS imagery and assessing its effect on estimation of biomass and carbon stock.

1.4.2. Specific objectives

1. To generate DTM from 3D photogrammetric point clouds of UAV images and compare it with DTM from LiDAR.
2. To assess the accuracy of estimating tree heights derived from 3D point clouds of UAV and field height in comparison to LiDAR trees height.
3. To compare the estimated biomass from sampled trees derived from photogrammetry image matching of UAV and field estimated biomass using Airborne LiDAR dataset.
4. To assess the effect of differences in tree height associated with photogrammetry image matching approach of UAV and field measurement methods on biomass and carbon stock estimation.

1.5. Research questions

1. What is the accuracy of DTM derived from 3D photogrammetric point clouds of UAV in comparison to DTM of LiDAR?
2. What is the difference in the accuracy of tree height estimated from UAV and field data in reference to that of Airborne LiDAR?
3. What is the difference in the amount of biomass from sampled trees which derived from estimated height and DBH parameter of field measurements and UAV in comparison to that of Airborne LiDAR?
4. How biomass and carbon stocks are affected by differences in tree height measurements derived from photogrammetry image matching of UAV and field methods.

1.6. Hypothesis or anticipated results

- H0: There is no significant difference in accuracy in DTM generated from 3D point clouds of UAV field in comparison to DTM of LiDAR.
- H1: There is significant difference in accuracy on DTM generated from point clouds of UAV, field height in comparison to DTM of LiDAR.
- H0: There is no significant difference between the accuracy of estimating trees height using UAV, field height in comparison to LiDAR.
- H1: There is significant difference between the accuracy of estimating trees height derived from UAV, measured from field in comparison to tree height derived from LiDAR.
- H0: There is no significant difference between the amounts of biomass estimated from selected trees from field, UAV in comparison to that of ALS.
- H1: There is significant difference between the amount of biomass estimated from selected trees from field, UAV in comparison to that of ALS
- H0: Biomass and carbon estimation are not affected by differences in tree height obtained from field data, and photogrammetry image matching of UAV.
- H1: Biomass and carbon estimation are affected by differences in tree height obtained from field data, and photogrammetry image matching of UAV

2. STUDY AREA

2.1. Geographic location of the study area

This research was carried out in Ayer Hitam Tropical Forest Reserve which is located in the state of Selangor, Peninsular Malaysia (Figure 2). The study area was selected in order to demonstrate the applicability of the photogrammetry technique in comparison with LiDAR in estimation of biomass and carbon stock in tropical forest. This is because of the fact that many study have been conducted in the temperate forest (Torres-sánchez et al., 2015). Limited researches have been conducted in tropical forest. Additionally, availability of ALS in Ayar Hitam Forest Reserve was important for area consideration. Geographically Ayer Hitam Forest Reserve lies between Latitude of 2°56'N - 3°16'N and Longitude of 101°30'E - 101°46'E. It is 20 km and 45 km away from University Putra Malaysia (UPM), and from the city of Kuala Lumpur respectively (Hasmadi et al., 2008). According to Nurul-Shida et al., (2014), Ayare Hitam Forest Reserve is among three left lowland dipterocarps tropical forest reserve in Klang valley. It is currently surrounded by residential buildings and modern infrastructures which make it isolated and hinder ecological connectivity with another forest. Since 1996 the forest has been given to the faculty of forest by Selangor state government. Initially, Ayare Hitam Forest Reserve was logged. The main reason was encroaching forest area for other development activities such as building residential areas, new township, factories highways, agriculture activities and over exploitation of forest resources for social economic development projects (Nurul-Shida et al., 2014; Hanum, 1999). Ayare Hitam Forest Reserve was logged-over forest, however, now is yet to attained its restoration state. It is the only lowland forest reserve found in Selangor state so far, at the beginning the forest area was 4270.7 ha in 1906, however, the remaining forest is 1248 ha which has 6 administrative compartments (Nurul-Shida et al., 2014).

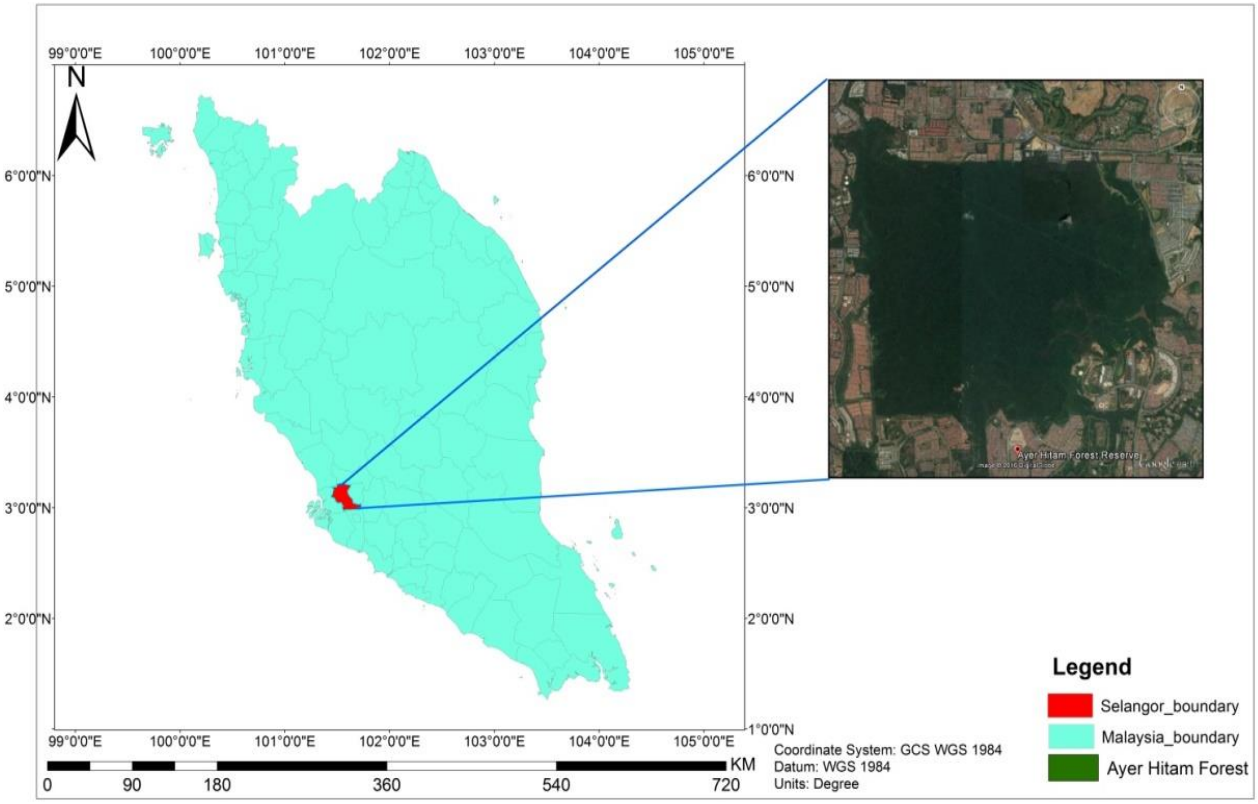


Figure 2: Study area

2.1.1. Climate and Topography

Ayare Hitam Forest Reserve is undulated with alluvium and colluvium soil structured derived from metamorphic and sedimentary rock with a sandy, clay loam soil texture (Hanum, 1999). The reserves consist of approximately 430 species. Generally, the terrain is moderate steep with slope range from 10% to 20% (Hasmadi et al., 2008). The mean yearly temperature is 25.3^{0}C with minimum and maximum temperatures are 22.9^0 and 27.7 ^{0}C respectively (Hanum, 1999).

2.1.2. Dataset Acquired

In this study, three main datasets were acquired, which include UAV, Airborne LiDAR and biometric datasets. The UAV data were acquired by using Phantom 4 DJ (Figure 3), after placing ground control points. The acquired UAV stereo images were used to generate photogrammetric products such as digital surface model, digital terrain model and ortho-mosaic images. The available airborne Lidar Dataset was also used to generate height canopy model from subtraction of DTM from DSM. The biometric dataset was collected by using field equipment such as diameter tape, Leica DISTO 510, global position system and measuring tape.



Figure 3: Phantom4 DJI UAV/Drone

Source: http://www.drone-world.com/phantom-4-vs-phantom-3/

3.1.6. Field equipment

In this study, numbers of field equipment were used for data acquisition. There were two approaches which were used to collect data, direct and indirect approach. Direct approach (Figure 4) involved actual measuring of forest parameters (biometric data collection), which include measuring tree height, DBH at 1.3 m from the ground and recording trees positions. On the other hand, indirect approach (remote sensing technique) involved taking stereo pictures using UAV Phantom 4 DJI was flue to capture stereo images indicates instruments (Appendix 3) and software (Appendix 4) used and their corresponding functions.

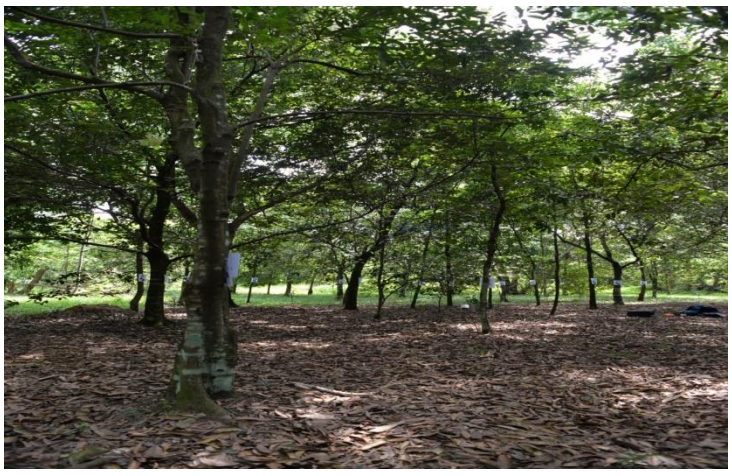


Figure 4: Placing tags before tree measurements

3. METHODS

This study consists of four parts (Figure 5)

1. UAV data acquisition and processing
2. LiDAR data processing
3. Field data collection and process
4. Comparing results and sensitivity analysis

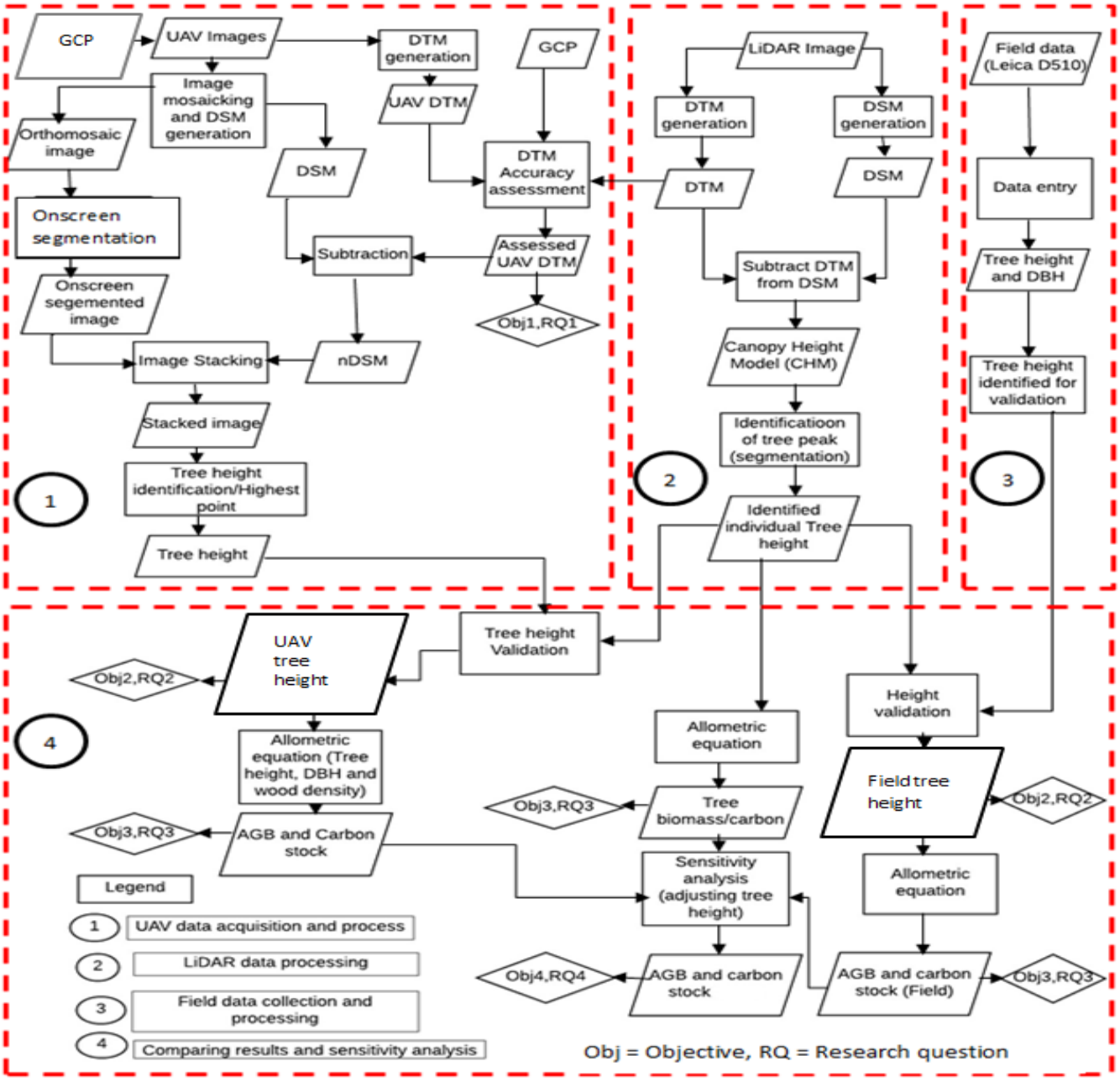


Figure 5: Methods simplified in the flowchart

3.1. UAV data acquisition and processing

3.1.1. UAV Flight Planning

The UAV dataset used in this study consists of the imagery acquired in six areas in Ayare Hitam Forest Reserve. The flight areas were identified based on the availability of open space for placing ground control points and the time the UAV can be airborne in relation to the battery capacity. The Pix4D (capture and Pix4D Ctrl DJI) smartphone based software was used for preparation of UAV flight plan. For all six flights, the following parameters (Table 1) were used.

Table 1: Parameter used for UAV data collection

Parameter	Value
Speed	Moderate
Angle	90 (Nadir)
Overlap	80%
Side Overlap	60%
Altitude Area 1 till 4 and 6	80 m
Altitude area 5	90 m (to avoid collision with surrounding buildings)

Higher overlaps provide more matching points which are very important in selecting tie points for 3D reconstruction. For this reason, the UAV images were recorded with 80% forward overlap and 60% side lap, to allow proper 3D reconstruction and compensate for aircraft instability (Colomina & Molina, 2014). The UAV settings proposed by Torres-sánchez et al. (2015), viz forward overlap of 90% and side lap of 60%, pertained to a situation where the UAV would hold at every picture taken.

This "stop at every picture" approach was criticized in the study done by Rosnell & Honkavaara, (2014) arguing that slowing down and accelerating at every image taken negatively affects flying time/energy use efficiency and increases platform instability. For this reason, they applied the interval model approach, where the UAV was programmed such that the camera shoots the picture a certain interval without the UAV stopping. The interval approach was adopted for this study. Flight altitude of the UAV platform depends on the height of the objects (trees in this case), and it should be at least 50m higher. Figure 6 shows the UAV flight planning areas and UAV settings.

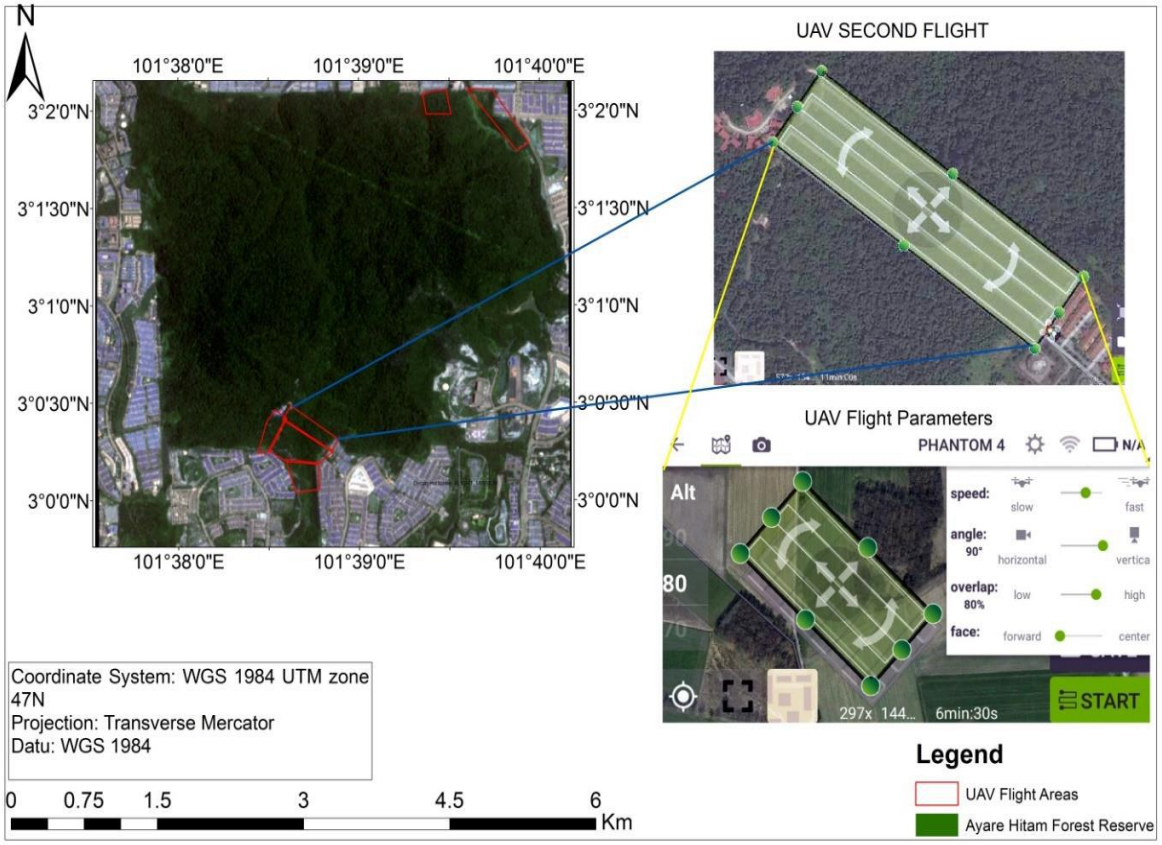


Figure 6: UAV flight mission and parameters set in the study area.

3.1.2. Ground Control Points (GCP)

A Ground Control Point (GCP) is a marking on the ground where x, y and z were measured with high precision using Differential Global Position System (DGPS). Accurate GCP are required for the geometric correction of the UAV images. According to Gerke & Przybilla (2016) because of the weight of the UAV and cost limitations, sensors of UAV's cameras have relatively low quality when compared to professional sensor mounted in the airborne systems, so in order to obtain high accuracy for the final results GCP must be used. Gerke & Przybilla (2016) reported that when ground control points were used in the bundle adjustments (Figure 8) the errors were reduced by the factor of 3 and reduce image deformation. Also in a study done by Nocerino et al. (2013) the image resulted after orientation was deformed and the deformation was corrected by introducing three (3) GCPs in the bundle adjustment.

In this study UAV flight areas were identified in such a way that all areas have had enough open spaces at its corner point for placing ground control. Nocerino et al. (2013) reported that before started flying UAV GCPs were well distributed in the area of interest. In this study, ground control points were marked on the ground using white and black spray paint to provide good contrast and ensure visibility in the UAV images when it was flying at 80 m altitude (Figure 7). The GCP were marked in every corner of the identified flight areas, four points were marked in each flight. The minimum of three (3) is recommended for provision of positioning, scale and orientation of the image in relation to the real object. Then ground control points were recorded by using differential GPS.



Figure 7: Marking ground control point for the DGPS measurements

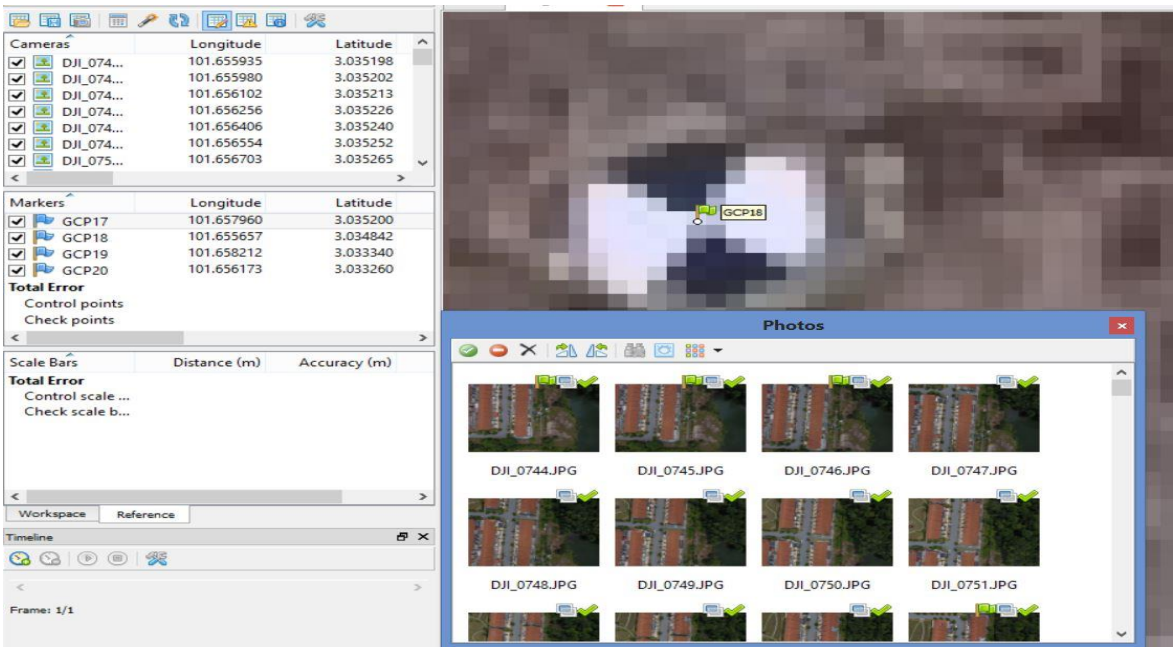


Figure 8: Adding of ground control points in the UAV images

3.1.3. Pre-processing of UAV dataset

Photogrammetry products such as ortho-mosaic images, DSM and DTM generation have been produced by various commercial algorithms and software. These software included Pix4D, MATCH-T version 5.4.1 and Multi Image Matches for Auto Correlation Methods (MICMAC) (Seul et al., 2015; Lisein et al., 2014; Debella-Gilo, 2016). However, in this study UAV stereo images were processed by using Agisoft PhotoScan Professional for generation of photogrammetric products, the same software was used in the study done by Torres-sánchez et al. (2015) due to its efficiency on vegetation point clouds generation (Dandois & Ellis, 2013). Prior to the process of the image processing images taken during take-off and landing were removed (Dandois & Ellis, 2013). Processing of images withPhotoScan consists of the following steps (Torres-sánchez et al., 2015; Verhoeven, 2011):

- loading photos into PhotoScan, inspecting uploaded images, removing unnecessary images,
- aligning photos,
- building dense point cloud,
- building DSM,
- building, ortho mosaic
- building DTM

3.1.4. Loading UAV stereo images into photoscan

UAV photos were loaded (Figure 9) in the Agisoft PhotoScan Professional. This process involved inspection of loaded images, all photos which were not calibrated and aligned were removed (Dandois & Ellis, 2013).

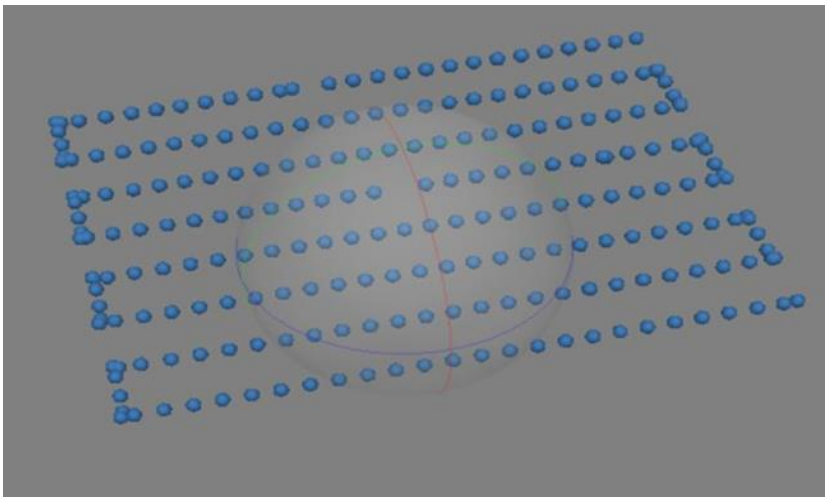


Figure 9: Example of UAV images uploaded in the Agisoft PhotoScan Professional

3.1.5. Aligning photos

In this step, the software finds the camera position and orientation of each UAV photo and builds up a sparse point clouds model. This procedure is guided by accuracy and pair pre-selection. In this study, high accuracy was used since it helps to achieve a more accurate camera position estimate by working with photo of the original size. When the alignment was done (Figure 10), for optimization of the project, Ground Control Points (GCPs) recorded by differential GPS were added in the image within bundle block adjustment (Figure 8) in order to enhance geo-referencing and spatial accuracy of the image (Gerke & Przybilla, 2016).

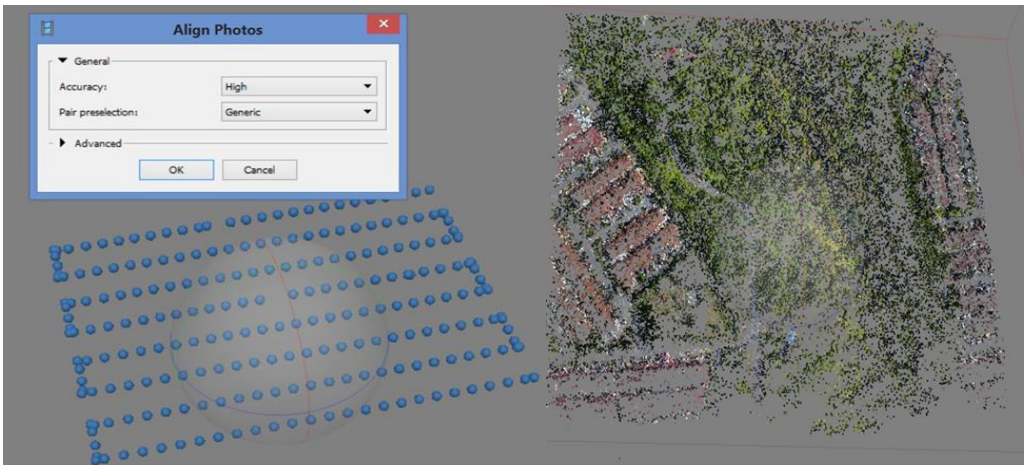


Figure 10: Photoalignment and sparse point clouds

3.1.6. Building dense point cloud

The building of dense point clouds (Figure 11) allows calculation of depth information, which is required for the generation of ortho-mosaic images, DSM and DTM. In order to achieve the best possible geometric accuracy the "high quality" setting of the software was applied.

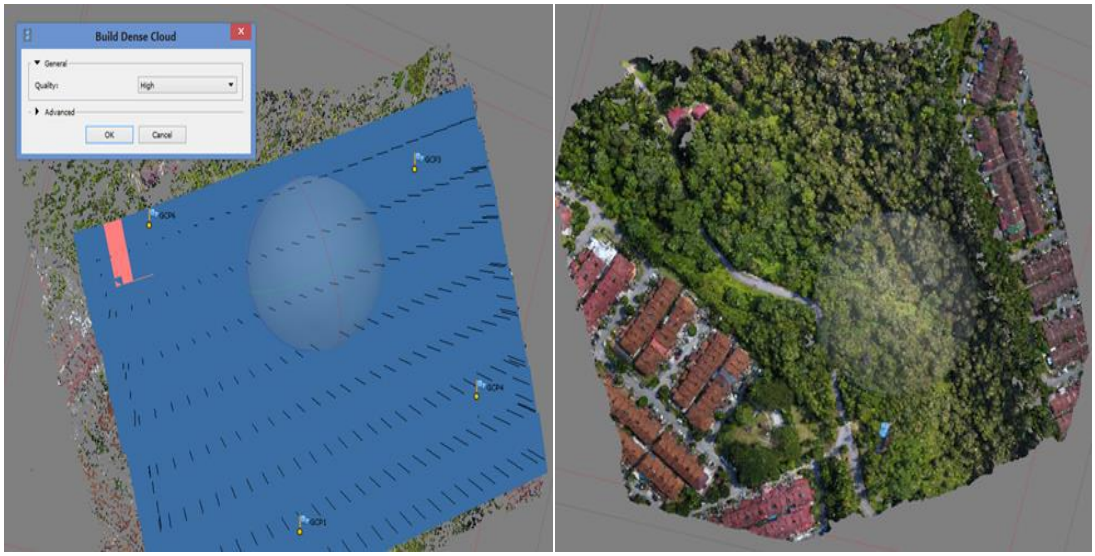


Figure 11: Dense point clouds reconstructing parameter and Dense Point Clouds

3.1.7. Building DSM, Orthomosaic, and DTM

After building the dense point clouds and 3D polygonal model the software can generate a Digital Surface Model (DSM), Orthomosaic image and Digital Terrain Model (DTM) (Figure 12 a,b&c). A DSM represents a surface model as a regular grid of height values. DSM can be rasterized from a dense point cloud, a sparse point cloud. A software enables to perform DSM based point, distance, area, volume measurements as well as generate cross -sections for a part of the scene selected by the user. The building up of ortho-mosaic image was important because mosaic image was used in onscreen segmentation process and matching of individual trees. This was possible because the ortho mosaicked image had very high resolution.

AGISOFT software allows for the automatic generation of a digital terrain model (DTM). In this process, dense point clouds were classified into two classes viz "ground" and "the rest". The technique of identifying ground points from 3D point clouds is often referred to as ground filtering or bare-earth extraction (Wang et al., 2009).



Figure 12: DSM (a), Orthomosaic (b) and DTM (c) for first flight

3.1.8. UAV and ALS Segmentation process

The available Airborne LiDAR CHM and mosaicked image were segmented by using eCognition software, using multi-resolution segmentation option in order to generate image at any chosen resolution. The process involves image partitioning in more or less homogeneous areas representing an individual tree canopy based on a rule set using parameters such as shape and compactness. The rule set was developed for small subset of the whole image and was later applied to the whole study area. Segmentation was done in order to delineate the crown of individual trees. Individual tree identification was important because it was used for matching field, ALS and UAV estimated tree height data which were used to compare calculations of biomass and carbon stock. On screen digitization was used to assess the accuracy of segmentation done in the eCognition (Equation 1 to 3) (Clinton et al., 2014).

Equation 1: Over segmentation equation model

$$Over\ segmentation_{ij} = 1 - \frac{area\ (Xi \cap Yj)}{area\ (Xi)} \quad \ldots\ldots\ldots\ldots\ldots\ldots 1$$

Equation 2: Under segmentation equation model

$$Under\ segmentation_{ij} = 1 - \frac{area\ (Xi \cap Yj)}{area\ (Yj)} \quad \ldots\ldots\ldots\ldots\ldots\ldots 2$$

Where;
xi Reference object manually segment the crown (On screen digitized objects)
yj Corresponding segmented object by eCognition

Equation 3: Measure of goodness

$$D = \sqrt{\frac{over\ segmenation^2 + under\ segmenation^2}{2}} \quad \ldots\ldots\ldots\ldots 3$$

Where;
D is closeness of fit or segmentation goodness
The value of under segmentation and over segmentation lies within the range of 0 to 1, where 0 value for both under and over segmentation means perfect segmentation, that is the training object is matching the segments (Clinton et al., 2014). The segmentation goodness or closeness of fit (D) is a measure of error in segmentation (equation 3). The D is in [0,1] whereas D value equals to 0 means perfect segmentation.

3.1.9. Tree crown onscreen-segmentation using CHM of UAV

Furthermore, the output of segmented UAV mosaicked image was obtained in form of shape file and was uploaded in the ArcMap 10.3.1. The segmented shape file, field circular plot, recorded center plot and individual tree location was later overlaid on the UAV CHM. The maximal elevation was used to identify tree top after segmentation and onscreen segmentation (Figure 13) of CHM was conducted. Tree height estimated from UAV was used to model tree height from the field.

Tree crowns were delineated by hand by a photo interpreter, and metrics were computed on this crown area. The best model, using only one metric, was selected using the best subset regression procedure. Its performance was presented in terms of RMSE (residual mean square error) and model fit coefficient (R^2) (Lisein et al., 2014).

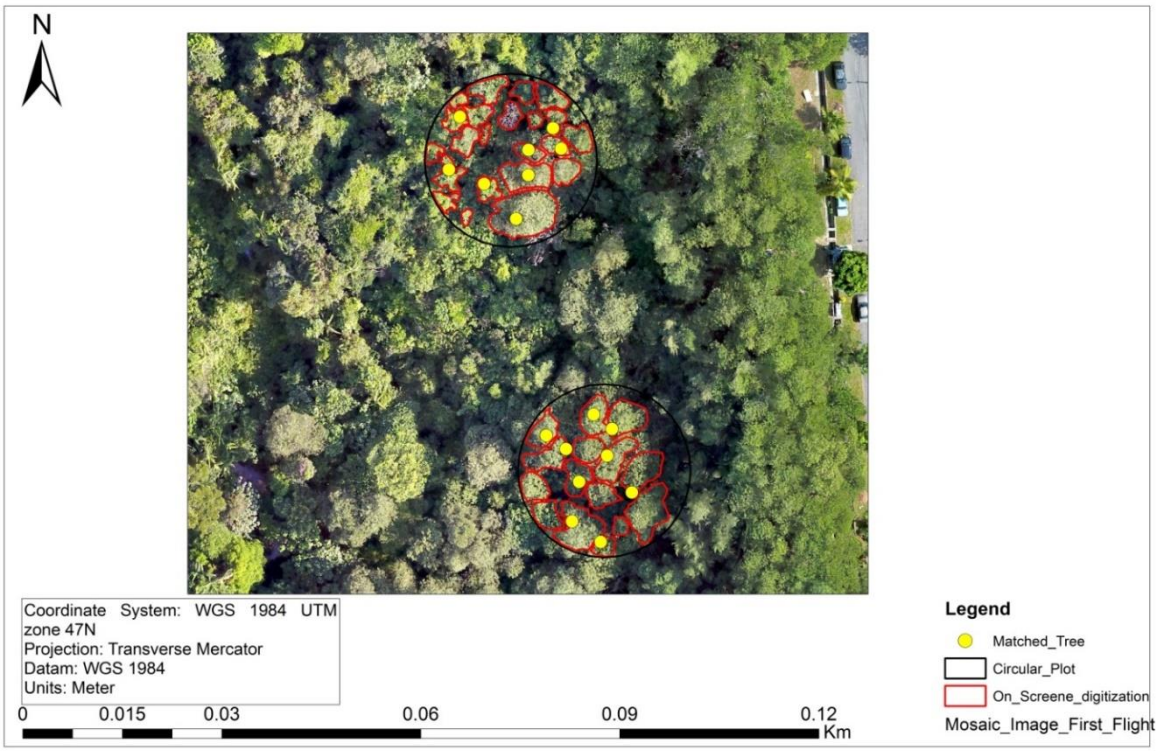


Figure 13: UAV CHM on screen segmentation

3.1.10. Tree height Extraction

Canopy Height Model (CHM) of 3D photogrammetric point cloud of UAV was derived by subtracting DTM from DSM (Figure 14 a&b). Then identification of tree peak was done by overlaying the onscreen segmented ortho mosaic image then tree height was generated using ArcMap 10.3.1.

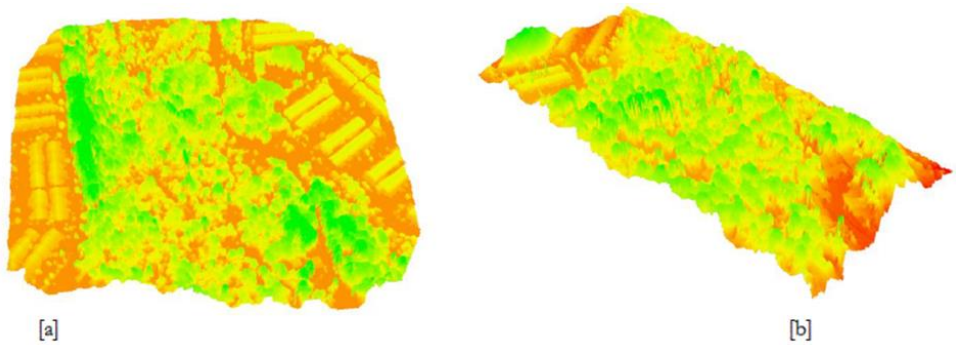


Figure 14: UAV CHM for first and second flight

3.2. LiDAR data processing

Airborne LiDAR dataset was given by University Putra Malaysia (UPM), DSM and DTM collected and utilized in this study. Canopy Height Modal (CHM) was derived by subtracting DTM from DSM. These products were processed by last year students. The CHM were later segmented to obtain the crown of the tree which was important in tree matching.

3.2.1. Segmentation

Prior to actual segmentation (Figure 15) of the Airborne LiDAR image on the whole study area, rule set where established in eCognition software base on the trial and error approach until the best parameters were obtained see the detailed explanation 3.1.8.

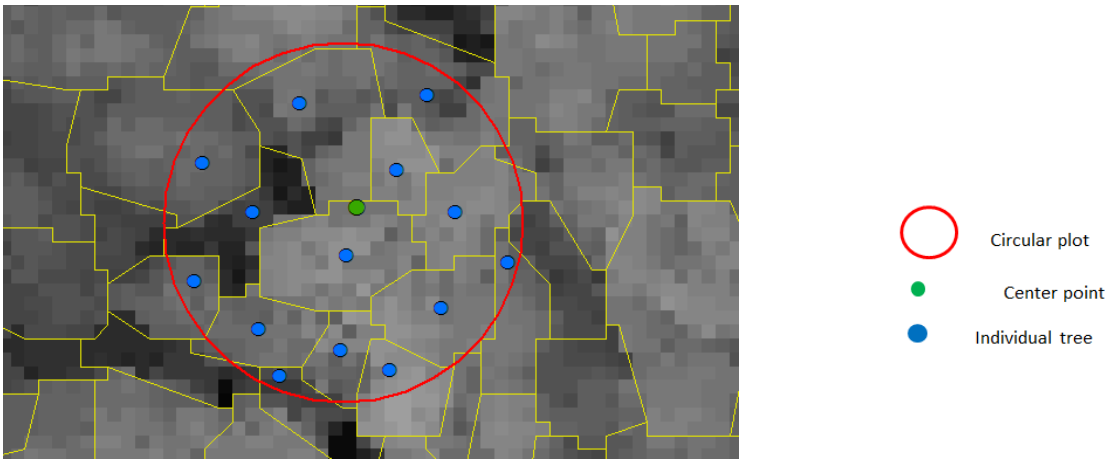


Figure 15: LiDAR data segmentation

3.2.2. Extraction of tree height and CPA

Furthermore, the segmented Airborne LiDAR CHM was in form of shape file and was uploaded in the ArcMap 10.3.1. The segmented shape file, field circular plot, recorded center plot and individual tree location was later overlaid on the CHM (Figure 16). The maximum elevation was used to identify tree height. Tree height derived by airborne LiDAR was later used to model field measured tree height and UAV estimated tree height.

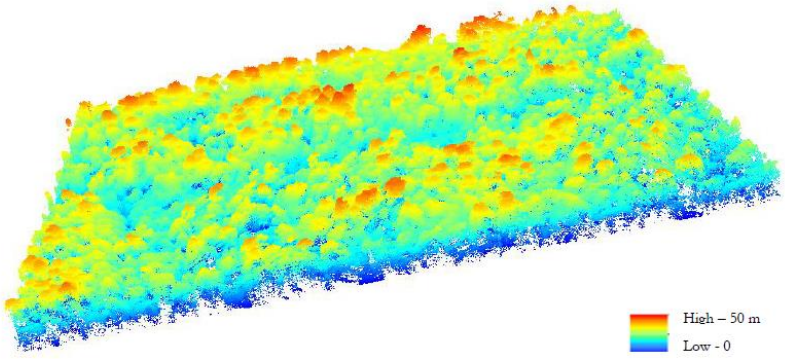


Figure 16: Airborne LiDAR-derived CHM

3.3. Field data collection

3.3.1. Pre-field work

A number of activities were carried out before the field work of this study, which includes:

- Testing of equipment (Appendix 2)
- Design field recorded sheets (appendix 1)
- Upload sentinel image in the locust for navigation

3.3.2. Plot size

In this study, the circular plot (Figure 17) of 0.05 ha (500 m²) which is equivalent to radius of 12.62 m was adopted (Gobakken & Naesset, 2008). In the study done by Ruizet et al. (2014) revealed that increasing the plot size beyond 500–600 m² would not significantly improve the results. However, it significantly increase the number of trees to be measured in each plot, therefore, cost-effective plot size is considered to be near 500–600 m². Alder & Synnott (1992) insisted that in practice circular plot is difficult to demarcate if larger than 0.1 ha. In the area where there is slope, adjustments in terms of slope correction must be done.

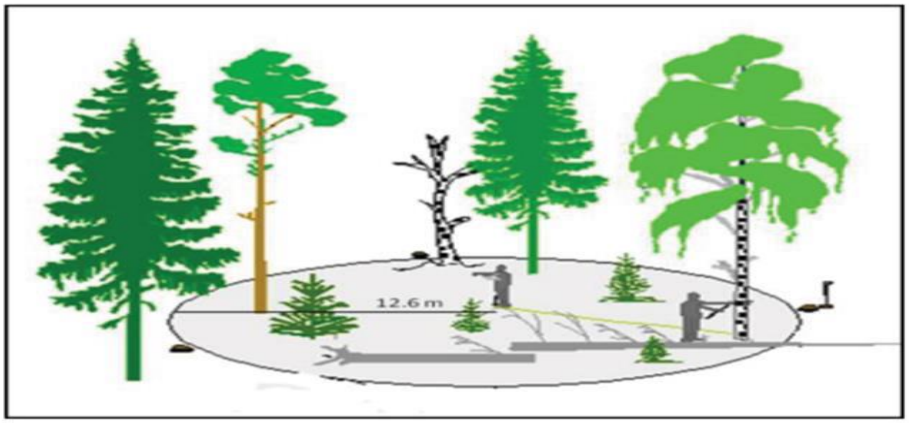


Figure 17: Plot delineation

Source:(Asmare, 2013)

3.3.3. Sampling design

Purposive sampling was a statistical strategy which was employed to establish sample plots in Ayer Hitam Forest Reserve. It is also known as judgmental sampling which falls under non-probability technique where the sampling design is achieved based on the judgment of the researcher depending on the actual environment of the area to be researched. This sampling designed was done by taking into consideration the elevation of the forest as well as flight plan set for collecting UAV dataset. The flight areas for flying UAV were selected in such a way that every corner of the flight area was visible for placing ground control points.

3.3.4. Biometric data collection (Field data collection)

Prior to the fieldwork, a data sheet was designed to secure consistency in data collection (Appendix 1). Biometric data (DBH, tree height) coordinate of individual tree and dominant tree height were recorded by using diameter tape, global position system, and Leica DISTO. Trees with a DBH less than 10 cm was excluded (Brown, 2002).

3.3.4.1. Diameter at Breast Height

In this study, all trees which had DBH greater or equal to 10 cm were recorded, these trees were considered to have significant contribution in biomass and carbon stock of the forest. Brown (2002) reported that tree with DBH less than 10 cm have insignificant contribution in the biomass carbon of a forest and therefore they normally not measured. This was also supported by Talbot et al. (2014) and Molto et al. (2013) who stated that trees whose diameter were greater than 10 cm were measured at 130 cm. In case of buttress, stems were measured above the buttress and DBH was recorded. For folk trees, if the folk is above 1.3m was considered as one tree while if the folk is below 1.3m it was regarded as two trees (Figure 18).



Figure 18: Buttress and folk tree

3.3.4.2. Tree Height

In this study tree heights were measured by using Leica DISTO D510, all trees were measured within distance of 10 m, however, it was still difficult to find the peak of each individual tree. This was attributed to occlusion of the crown of the trees and therefore made the individual trees measurement a big challenge.

3.4. Comparing results and sensitivity analysis

3.4.1. Statistical analysis

In this study a number of statistical analyses were carried out using SPSS and R package. Descriptive statistics, regression analysis, correlation, single factor ANOVA and t-tests were conducted to analyses the comparison of UAV and airborne LiDAR DTM, DBH, tree height, AGB, and carbon stock.

Mainly regression analysis was run to assess the relationship in tree height estimated by ALS, UAV and that measured by the field. Also, the biomass/carbon stocks generated by ALS, UAV and field measurements were analyzed using regression analysis. The single factor ANOVA test was used to assess the variation of the means of ALS, UAV and field. While t-tests were carried out in order to assess whether means of tree height of UAV, filed and ALS differ significantly.

In this study airborne LiDAR was used to validate UAV and field tree heights. In the study done by (Wallace et al. (2014) and Sadadi (2016), ALS tree height was used to validate tree height. Airborne LiDAR was used to model UAV and field data, root mean square error (RMSE) was used to assess the deviation of dependent variable along the line of fit (Equation 4).

Equation 4: RMSE computation

$$\text{RMSE} = \sqrt{\sum_{i=1}^{n} \frac{(Y_i - Y'_i)^2}{n}}$$

Where;
RMSE; Root Mean Square Error

yi ; Measured variable of dependent variable
Ŷi ; Predicted variable of independent variable
n; Number of observations counted

3.4.2. Above ground biomass

In order to avoid repetitive destructive sampling, allometric equations are widely used and accepted for AGB and carbon stock assessment (Gibbs et al., 2007; Chave, 2005; José et al., 2012). Literature provides different allometric equations depending on forest type (Kenzo et al., 2009). In this study, the equation developed by Chave et al. (2014) was used since it was applied in a wide range in tropical rain forests (Equation 5)

Equation 5: Allometric equation for above ground biomass

AGB= 0.0673*[(***ρ***D^2 H)]^ (0.976)

Where AGB refers to the above ground tree biomass (kg); ***ρ*** is oven dry wood green volume in g/cm3 obtained from global wood density Kenzo et al., (2009), while D represent DBH (cm) and H represent tree height (m).

3.4.3. Carbon stock

Carbon stock of each individual tree was calculated from the AGB value obtained in the previous step, based on the relationship that carbon comprises of approximately 50% of total forest biomass (Houghton, 2005). A conversion factor was used to obtain the estimated carbon stock (Equation 6) for each individual tree measured by ALS, UAV and from field data. In this study, the value of 0.47 was be used as recommended by IPCC guideline.

Equation 6: Carbon stock estimation

C = B x CF

Where C is Carbon stock (Mg), B representing the biomass and CF is the fraction of the carbon in the biomass (0.47)

4. RESULTS

4.1. UAV Digital Terrain Model (DTM) Generation

A digital terrain model is a topographic model of the bare earth surface. In photogrammetry DTM is obtained after filtering DSM. In this study photogrammetric DTM was generated from the total of 1,975 photos using Agisoft Photoscan Professional. A number of software such as Pix4D, compute tree and Global Mapper have been used in photogrammetric DTM generation as well. The total of six photogrammetric DTMs was generated from six flights and the summary of the features of DTMs is shown in Table 2.

Table 2: Summary of photogrammetry features of the generated of all flight DTM

Parameters	UAV 1st Flight	UAV 2nd Flight	UAV 3rd Flight	UAV 4th Flight	UAV 5th Flight	UAV 6th Flight
Images (UAV Photos)	234.00	215.00	140.00	638.00	557.00	191.00
Flying Altitude [m]	105.00	95.20	90.10	95.60	94.30	96.70
GSD cm/pixel	3.72	3.52	3.13	3.53	3.40	3.45
Area [ha]	16.30	17.90	14.30	35.90	37.30	10.50
Tie Points	231,288.00	169,952.00	117,701.00	573,027.00	932,147.00	73,713.00
RMSE of Pixel	0.42	0.29	0.40	0.44	0.43	0.40
Dense Pont Clouds	59,428,561.00	50,000,139.00	49,665,199.00	34,301,028.00	131,068,441.00	49,665,199.00
Focal Length [mm]	3.61	3.61	3.61	3.61	3.61	3.61
Resolution	7.45	7.04	6.27	14.10	6.79	6.90
Point density [Point/m2]	180.00	202.00	254.00	50.10	217.00	210.00
Effective overlap	3.75	2.93	2.97	3.18	3.24	3.15

4.2. Comparison of ALS and photogrammetric image matching DTM'S

Comparison of Airborne LiDAR and Photogrammetric image matching DTM was fundamental objective narrated in this subsection because it has its effect on tree height and consequently on the biomass and carbon stock. The available ALS DTM was considered to be more accurate and therefore was used to assess the accuracy of photogrammetric generated DTM. White et al. (2013) reported that main advantage of ALS data is the ability to generate a detailed DTM under the forest canopy. In addition to that Hyyppä et al. (2016) and Hyyppä et al. (2000) reported that the quality of the Airborne LiDAR DTM derived depend on point cloud density and nature of the target. Furthermore, the study suggested that forest canopy and understory vegetation cover are major factors that affect the accuracy of laser DTMs because it hinders more point clouds to hit the ground (Hyyppä et al., 2016). Baltsavias (1999) reported that in the experiment conducted by NASA where very large laser footprint (10 – 30 m) attained the output in dense tropical forest with ground obstruction of 95%. In the study done by Reutebuch et al. (2003) accuracy assessment of DTM derived by ALS was done and the results revealed that the average error in elevation was 0.22 m, with errors increasing with increasing vegetation cover.

4.2.1. Comparison of ALS and photogrammetric image matching DTM'S using GCP recorded by DGPS

The comparison between photogrammetric image matching and ALS DTM was done by using GCP coordinates (x, y, z) which were collected by differential GPS. The derived photogrammetric image matching and ALS and available Airborne LiDAR DTM height (altitude z) values were regressed against Z-value (altitude) of DGCP in which coefficient of determination (R^2) and correlation coefficient used for validation of DTM was computed and evaluated. The accuracy of the DGCP was 2 cm and the accuracy assessment of photogrammetric image matching and ALS DTM was done and assessed using RMSE and RMSE %. The summary of the comparison was shown in Table 3 and Table 4. While the relationship of DTM height was indicated in Figure 19 and Figure 20.

Table 3: Accuracy assessment of ALS DTM using GCP collected by DGPS

Statistics	
Correlation	0.995
R Square	0.991
Adjusted R Square	0.990
RMSE [m]	1.250
RMSE [%]	2.752
Observations	15

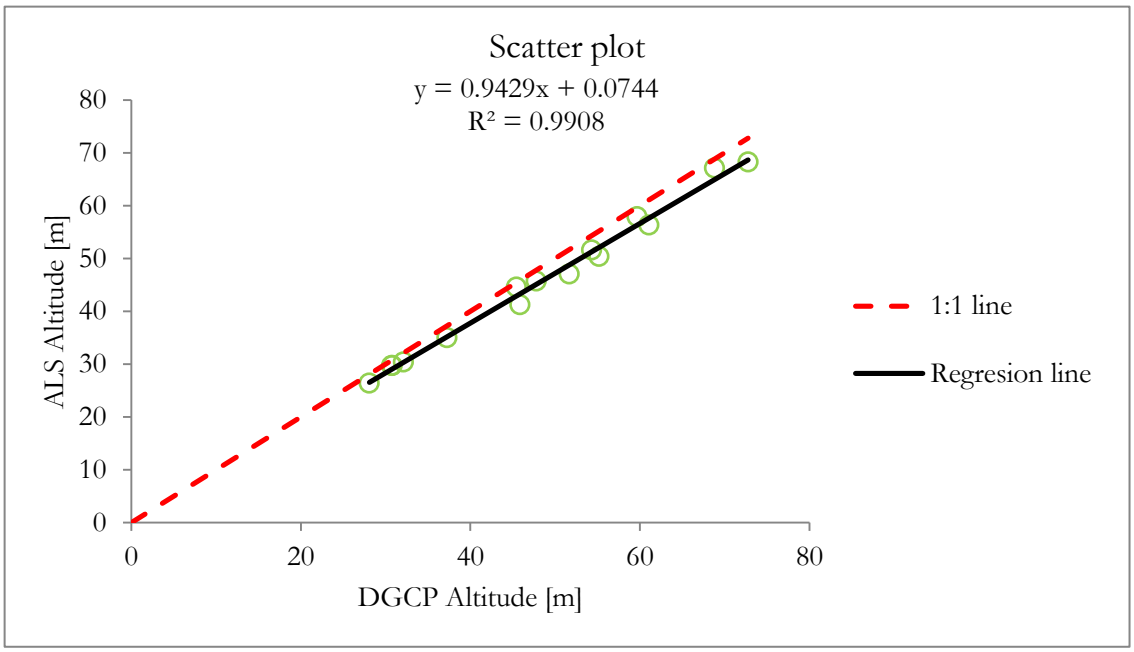


Figure 19: Relationship between ALS DTM and DGCP height

Table 4: Accuracy assessment of UAV DTM using GCP collected by DGPS

Statistics	
Correlation	0.982
R Square	0.964
Adjusted R Square	0.961
RMSE [m]	3.843
RMSE [%]	7.956
Observations	15

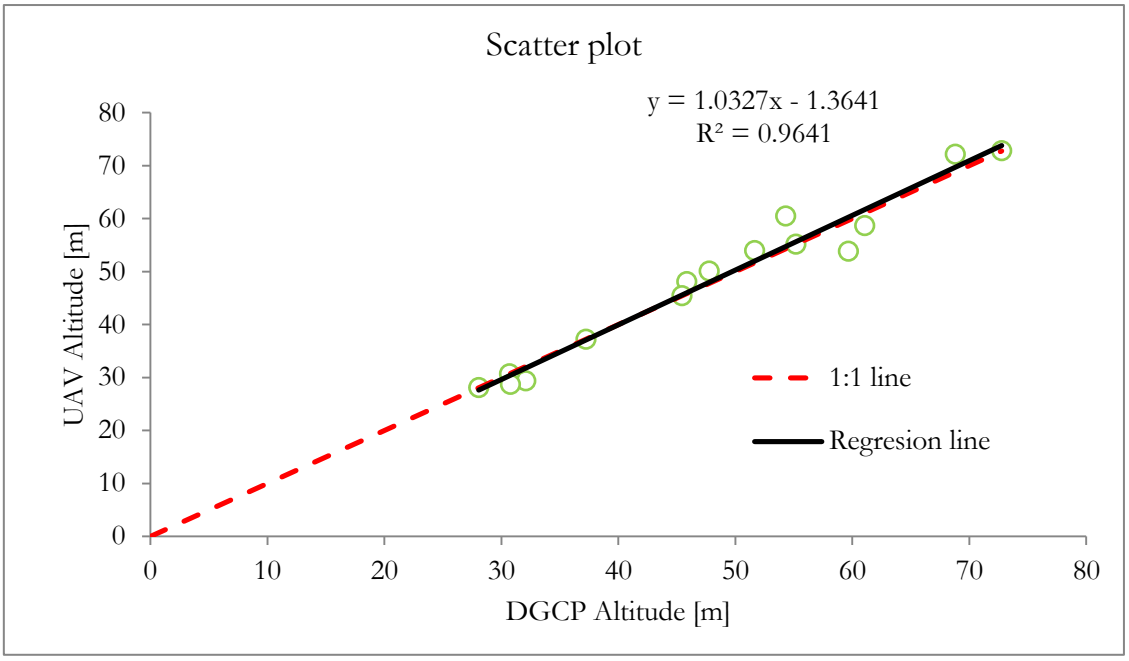


Figure 20: Relationship between UAV DTM and DGCP height

4.2.2. Comparison of photogrammetric image matching and ALS DTM using their height

In this subsection, ALS and photogrammetric image matching DTM height were compared by subtracting the photogrammetric image matching DTMs from ALS DTM. Initially, the image was ensured to be co-registered and the pixels of ALS and UAV DTM were perfect matched (Figure 21 and 22). Using Arc-Map 10.3.1, the centroid DTMs altitude value of all UAV flights and ALS pixels were extracted. The coefficient of determination (R^2), RMSE, RMSE% and t-test (appendix 5) were carried out the results were summarized in Table 5.

Table 5: Summary for comparison of ALS and UAV DTMs height extracted from centroid pixel value for all flights

Statistics	First flight	Second flight	Third flight	Fourth flight	Fifth flight	Sixth flight
R Square	0.86894248	0.836744555	0.85083091	0.967932423	0.805431836	0.13555312
Standard Error [m]	3.08689497	6.16479045	3.11186022	2.529179418	4.054891602	6.32015192
RMSE [m]	3.08686378	6.691111328	3.11182884	2.529164036	4.054874307	6.32006225
RMSE%	7.42040129	13.09324179	7.69921775	6.52083478	10.11266321	9.63156323
Pixels Counts	97821	98767	98306	160912	227412	70484

Furthermore, the study compared estimated tree height from UAV and measured tree height from ALS (Table 6). The results indicated that the coefficient of determination ranges from 0.53 to 0.82. The accuracy was done through RMSE and RMSE %. The calculated RMSE ranges from ±0.31 to ±1.49 m while the computed RMSE % range from 1.57% to 8.34%.

Table 6: Summary of comparison of ALS and UAV tree height extracted from all flights

	First flight		Second flight		Third flight		Fourth flight		Fifth flight		Sixth flight	
Statistics	ALS	UAV	ALS	UAV	ALS	UAV	ALS	UAV	ALS	UAV	ALS	UAV
Mean	18.33	16.75	19.02	17.60	17.35	16.16	19.46	17.85	19.73	19.52	21.91	21.26
Standard Error	0.39	0.36	0.28	0.25	0.44	0.46	0.39	0.40	0.71	0.86	0.79	0.72
Standard Deviation	2.61	2.44	3.33	2.93	3.73	3.84	3.25	3.39	2.76	3.34	5.33	4.81
Minimum	13.00	12.24	12.00	10.40	11.00	10.16	12.00	12.77	16.00	15.56	14.00	13.21
Maximum	26.00	24.72	28.00	28.31	29.00	27.92	30.00	28.39	27.00	26.82	35.00	35.70
R Square	0.53	0.53	0.82	0.82	0.77	0.77	0.75	0.75	0.59	0.59	0.82	0.82
Standard Error [m]	1.68	1.68	1.25	1.25	1.85	1.85	1.72	1.72	2.23	2.23	2.08	2.08
RMSE [m]		1.33		1.28		1.14		1.49		0.31		0.82
RMSE%		7.93		7.26		7.06		8.34		1.57		3.85
Biomass [Mg]	23.05	21.43	76.88	70.91	26.05	24.07	35.5029	33.1818	9.81487	9.79683	30.87	29.61
Carbon stock [Mg]	10.832	10.07	36.13	33.33	12.242	11.313	16.6864	15.5954	4.61299	4.60451	14.509	13.91
Number of trees	45	45	141	141	71	71	71	71	15	15	45	45

The study went further and compares the amount of biomass and carbon stock in each flight by considering the error made in the UAV DTM. The results revealed that the biomass was ranging from 9.2 to 72.06 Mg and corresponding carbon stocks were ranging from 4.32 to 33.87 Mg. In each flight, biomass and carbon stock derived from UAV was compared with ALS derived biomass and carbon stock. Biomass losses were ranging from 0.02 to 5.6 Mg in all flight, while carbon stock loss was ranging from 0.01 to 0.87 Mg. The summary of the results is shown in Table 7.

Table 7: Summary for comparison of ALS and UAV biomass and carbon stock extracted from all flights

	First flight		Second flight		Third flight		Fourth flight		Fifth flight		Sixth flight	
Statistics	ALS	UAV	ALS	UAV	ALS	UAV	ALS	UAV	ALS	UAV	ALS	UAV
R Square	0.87	0.87	0.84	0.84	0.85	0.85	0.97	0.97	0.81	0.81	0.14	0.14
Standard Error [m]	3.09	3.09		6.16	3.11	3.11	2.53	2.53	4.05	4.05	6.32	6.32
RMSE in UAV DTMs [m]		3.09		6.69	3.11	3.11		2.53		4.05		6.32
RMSE% in UAV DTM		7.42		13.09	7.70	7.70		6.52		10.11		9.63
Pixel count	97821	97821	98767	98767	98306	98306	160912	160912	227412	227412	70484	70484
Mean tree height [m]	18.33	16.75	19.02	17.60	17.35	16.16	19.46	17.85	19.73	19.52	21.91	21.26
R Square	0.53	0.53	0.82	0.82	0.77	0.77	0.75	0.75	0.59	0.59	0.82	0.82
Standard Error [m]	1.68	1.68	1.25	1.25	1.85	1.85	1.72	1.72	2.23	2.23	2.08	2.08
RMSE in UAV height [m]		1.33		1.28		1.14		1.49		0.31		0.82
RMSE in UAV height [%]		7.93		7.26		7.06		8.34		1.57		3.85
Biomass [Mg]	21.60	20.08	72.06	66.46	24.41	22.56	33.28	31.10	9.20	9.18	28.93	27.75
Biomass loss [Mg]		1.52		5.60		1.85		2.18		0.02		1.18
Carbon stock [Mg]	10.15	9.44	33.87	31.24	11.47	10.60	15.64	14.62	4.32	4.32	13.60	13.04
Carbon stock loss [Mg]		0.71		2.63		0.87		1.02		0.01		0.56
Number of trees	45	45	141	141	71	71	71	71	15	15	45	45

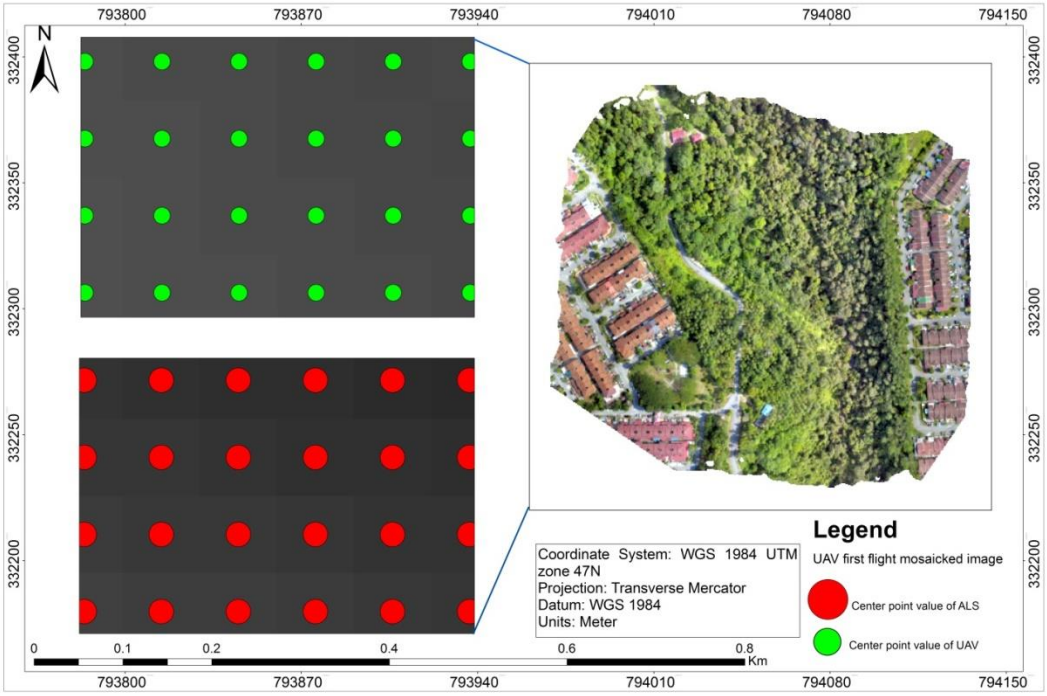


Figure 21: Comparison of UAV from ALS DTM height based on the centroid pixel value (DTM height).

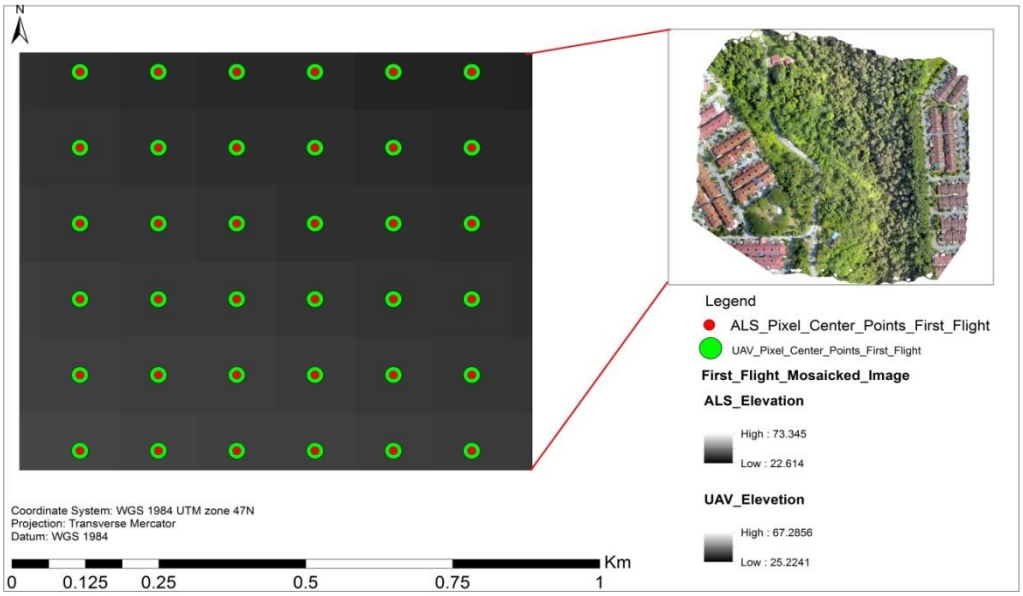


Figure 22: Comparison of UAV from ALS DTM height based on perfect height match.

4.3. Comparison of DTM's in relatively close altitude

This subsection provided more emphasis on the comparison of the ALS and UAV DTMs by considering areas where there was small difference in altitude between ALS and photogrammetric image matching generated DTM. In this area, a total number of 93 trees were selected and the results indicated that the mean tree height measured by airborne LiDAR was 18.69 m with standard deviation of 3.35 m. While,

mean of UAV estimated trees height was 17.93 m with standard deviation of 3.51m. The detailed summary statistics of the tree height estimated by UAV and Airborne LiDAR was shown in Table 8.

Table 8: Descriptive statistics of the ALS and UAV measured tree height in the area where DTMs have slightly difference.

Statistics	Airborne Lidar measured tree height	UAV tree height
Mean [m]	18.68817204	17.93397849
Standard Deviation [m]	3.345920601	3.508488198
Minimum [m]	12	11.54
Maximum [m]	30	28.39
Count	93	93

Furthermore, the relationship between Airborne Lidar and photogrammetric image matching DTM were established in order to assess the influence of photogrammetric image matching error in tree height estimation. This was done by comparing tree height measured by ALS and tree height estimated by photogrammetric image matching at a point where photogrammetric image matching DTM was close in height (RMSE = ±0.19 m and RMSE% = 0.5%) to Airborne LiDAR DTM. At this point, 93 trees were used to evaluate the effect of differences in tree height. The relationship was explained by correlation coefficient and coefficient of determination which was 0.89 and 0.799 respectively. The RMSE of the tree height to UAV estimated tree height was 1.56 m and 8.7%. The summary of the relationship and comparison of the estimated tree height based on the area where photogrammetric image matching and Airborne LiDAR DTM had small difference was indicated in the Table 9 and Figure 23.

Table 9: Comparison of UAV and ALS tree height where UAV and ALS DTMs have slight difference in height

Statistics	ALS and UAV close altitude	ALS and UAV tree height
Correlation Coefficient	0.995785479	0.894274068
R Square	0.99158872	0.799726108
Adjusted R Square	0.991496288	0.797525296
Standard Error [m]	1.008903101	1.505570224
Root Mean Square Error [m]	0.190367513	1.561653393
RMSE%	0.539068939	8.707791154
Observation	93	93

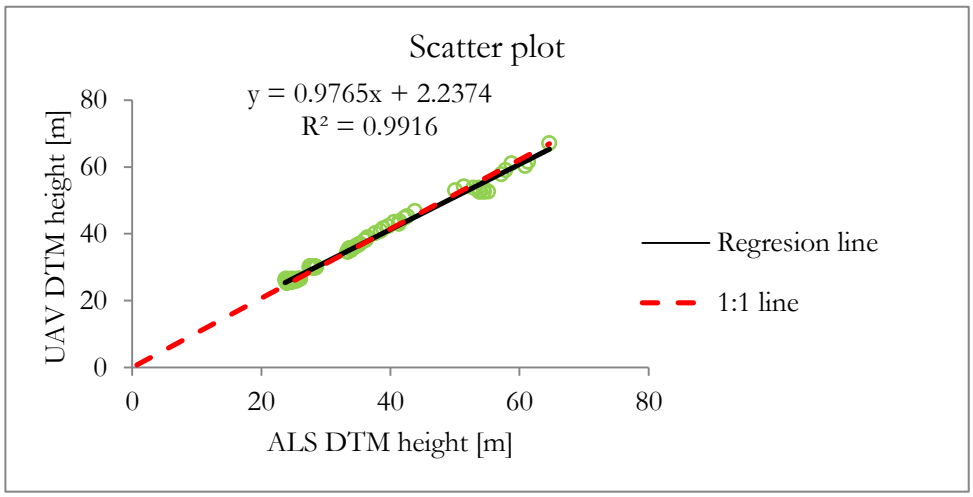


Figure 23: Relationship between ALS DTM height and UAV DTM height

The t-test assuming equal variance was done to compare the mean of the DTM height (altitude) of ALS and photogrammetric image matching. The results revealed that at ($p< 0.05$) there was no significant difference between height of ALS DTM and UAV (Appendix 5). Likewise, in the same area t-test results revealed that at ($p< 0.05$) there were no significant difference in the mean of tree height measured by ALS and that estimated by UAV (Appendix 6) in the point where UAV DTMs had RMSE and RMSE % of RMSE = ±0.19 m and RMSE% = 0.5 respectively.

4.4. Biometric data

In this study, tree height and DBH were the mainly collected as biometric data. Additionally, XY coordinate was also recorded, descriptive statistic and normality test was carried out. The following section narrates the detail of descriptive statistic as calculated by R package of statistical analysis.

4.4.1. Diameter at Breast Height (DBH)

Diameter at breast height was collected in 27 plots, a total of 787 trees were recorded while total of 388 trees were matched between ALS, UAV and field. The descriptive statistic on DBH was carried out using R packed for statistical analysis. The mean tree DBH of 24.70 cm was recorded (Table 10). Additionally the minimum and maximum tree DBH of 10 cm and 75.6 cm were recorded respectively. The standard deviation of the 12.16 cm which shows the spread of the variable from the mean was noted. The summary of the descriptive statistics is shown in Table 10.

Table 10: Descriptive statistics of DBH height

DESCRIPTIVE	
Mean DBH [cm]	24.69832474
Standard Deviation [cm]	12.15035557
Minimum DBH [cm]	10
Maximum DBH [cm]	75.6
Total number of matched trees	388

4.4.2. Normality test of the Diameter at Breast Height (DBH)

The normality test (Table 11) indicated that the DBH data were not normally distributed this can be visualized on histogram by assessing mean and median line (Figure 24). The mean DBH moved rightward which skewed the graph in the positive side. This is because the data collection started at 10cm DBH and higher.

Table 11: DBH normality test

Normality test	
Mean DBH [cm]	24.69832474
Median DBH [cm]	21.8
Mode DBH [cm]	22
Total number of matched trees	388

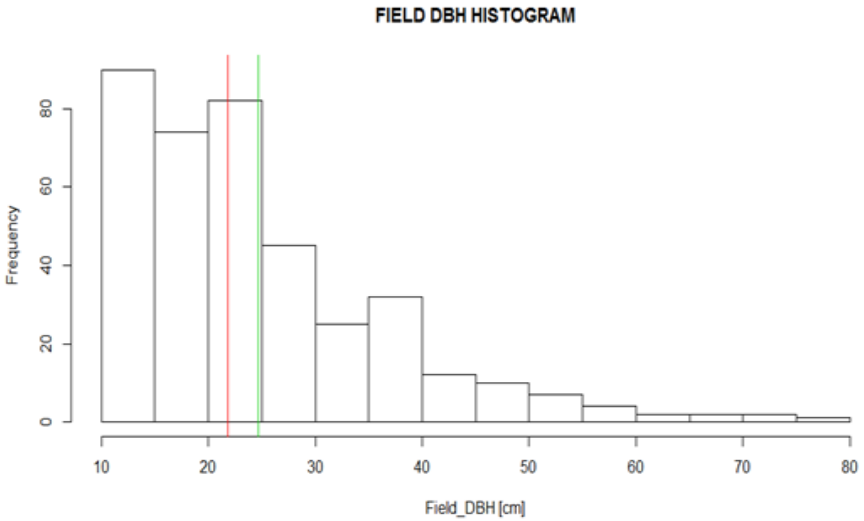


Figure 24: Histogram showing positive skewness of the DBH

4.5. Accuracy assessment for airborne LiDAR CHM

The segmented Airborne LiDAR image was done in eCognition software while on-screen digitized segment was conducted in ArcMap 10.3.1. The areas of each segment were computed and later segmented and digitized CHM was spatially intersected. Over-segmentation and under-segmentation were computed. The value obtained for over segmentation was 0.24 and for under segmentation was 0.3. According to Clinton et al., (2014) over segmentation and under-segmentation range from 0 to 1, where 0 means perfect segmentation, that is the training is perfect match with the segments. The RMS which commonly known as closeness of fit or segmentation goodness (D) was computed. The D value of 0.27 or 73% matched was obtained. The 73% accuracy was accepted for delineation of the crown of individual tree which was later used for matching with UAV and field recorded trees. The summary of the matched trees for all tree approaches is shown in Table 12.

Table 12: Summary statistics for matched trees

	Measured ALS height [m]					Estimated UAV height [m]				Measured Field height [m]			
Plot	Mean	Dev	Min	Max	Counts	Mean	Dev	Min	Max	Mean	Dev	Min	Max
1	16.60	1.30	13.00	18.00	15	16.39	2.28	12.74	20.08	16.02	2.91	12.40	24.00
2	20.82	4.58	17.00	30.00	11	19.02	4.61	15.49	28.39	18.36	7.30	12.00	33.00
3	20.56	2.90	16.00	27.00	16	19.06	3.18	12.77	25.17	19.19	4.89	12.50	30.50
4	20.93	3.41	14.00	27.00	15	19.16	2.65	14.63	23.98	18.72	4.30	13.70	27.75
5	19.74	2.42	16.00	25.00	23	17.86	1.99	14.09	21.56	17.28	3.58	12.60	25.50
6	19.08	3.53	13.00	24.00	12	17.61	3.16	12.28	22.34	18.09	4.18	12.76	25.60
7	20.70	4.01	14.00	28.00	20	19.49	4.02	12.68	28.31	18.50	5.10	12.60	31.90
8	16.25	2.47	12.00	21.00	20	16.04	2.73	11.54	22.74	15.06	2.50	11.90	20.10
9	18.19	5.39	13.00	29.00	16	16.84	4.58	11.49	25.59	17.47	5.54	12.21	28.70
10	18.56	4.12	11.00	29.00	18	18.30	4.30	11.63	27.92	18.31	5.13	12.00	29.20
11	20.83	3.43	18.00	27.00	6	19.68	4.33	15.74	26.82	15.98	4.38	12.10	24.20
12	19.25	2.12	16.00	22.00	8	19.76	2.79	15.56	22.88	17.75	4.72	12.19	25.23
13	16.59	1.97	13.00	21.00	17	13.39	0.40	10.16	16.63	14.99	2.69	12.20	21.30
14	18.80	3.45	12.00	26.00	15	17.78	4.20	13.56	26.39	15.83	3.53	12.10	22.40
15	21.80	4.05	16.00	27.00	10	19.77	3.52	13.21	24.85	18.29	3.38	11.90	23.40
16	23.20	6.71	14.00	33.00	10	21.78	5.54	16.23	31.85	17.73	6.42	12.20	32.00
17	20.70	3.59	16.00	26.00	10	21.22	2.84	17.51	26.71	16.47	3.79	12.20	21.60
18	21.93	6.26	14.00	35.00	15	21.92	6.12	13.77	35.70	17.75	4.45	12.20	27.20
19	18.05	2.16	15.00	22.00	21	16.73	2.22	22.04	15.90	15.90	3.05	12.90	25.40
20	17.59	3.08	13.00	24.00	17	16.66	2.55	12.00	21.02	15.55	2.88	12.20	22.60
21	18.35	2.87	12.00	25.00	20	17.14	2.91	10.40	23.74	15.96	3.15	12.10	23.50
22	17.76	2.55	13.00	25.00	21	16.17	2.14	13.81	22.51	15.55	2.55	11.90	22.40
23	21.17	2.17	19.00	26.00	12	18.29	2.58	10.28	24.72	15.83	4.76	12.30	30.30
24	20.38	2.62	17.00	24.00	8	16.92	1.77	14.43	19.20	16.15	2.62	12.60	20.60
25	17.85	3.65	13.00	26.00	13	16.67	2.27	13.01	21.37	16.09	4.28	12.60	25.70
26	19.22	1.39	21.00	26.00	9	17.56	1.68	15.32	20.37	13.29	1.34	11.90	15.40
27	16.63	2.13	13.00	19.00	8	14.34	1.16	12.24	15.75	13.50	1.22	12.20	15.50

4.6. Accuracy of assessing tree height measurement

Three different approaches were used to estimate trees height. These approaches included: actual measuring tree height in the field using Leica DISTO D510, estimating tree height from UAV and Airborne Lidar. After matched trees, trees heights were validated by using regression analysis and RMSE. The validation of tree height was done based on 388 matched trees from field tree height, ALS and UAV. UAV and field tree height was validated based on the Airborne LiDAR tree height. This is because ALS height was considered to be more accurate in estimating upper canopy trees.

The descriptive statistics was carried out between Airborne LiDAR and UAV estimated tree height, the mean was computed to assess the average tree height estimated by both approaches. The mean estimated tree height of Airborne Lidar and UAV were 19.08 m and 17.78 m respectively. The spread of the estimated tree height values of Airborne Lidar and UAV around the mean were 3.78 m and 3.7 m respectively. The matched minimum tree height recorded by Airborne LiDAR was 11 m while for field measurement was 10.16 m. The result shows that the maximum tree height measured in the field is 35.70

m which was a bit higher than that recorded by Airborne LiDAR (35 m). The summary of the descriptive statistics are shown in Table 13.

Table 13: Descriptive statistics for Lidar and UAV tree height

Statistics	Airborne LiDAR Estimated Tree Height [m]	UAV Estimated Tree Height [m]
Mean	19.07989691	17.78212556
Standard Deviation	3.781678666	3.703073032
Minimum	11	10.15921021
Maximum	35	35.70339203
Count	388	388

In this study, the total number of 388 matched trees was used to assess the relationship between Airborne Lidar and UAV estimated tree height. The model of fit was developed. Airborne Lidar and UAV derived tree height was considered to be independent and dependent variable respectively. Then Airborne Lidar was used to predict photogrammetry image matching estimated tree height. The coefficient of determination (R^2) of 0.785, standard error of 1.72 and RMSE of ±1.71 m was obtained (Table 14). The model indicated that when the independent variable was zero (0 m) the dependent variable was 1. 22 m (intercept). In addition to that the linear equation showed that the regression coefficient (slope) for Airborne LiDAR was 0.8678 m. This coefficient indicated that for every additional 1 meter in Airborne LiDAR estimated tree height we expect photogrammetry image matching of UAV estimated height to increase by the average of 0.8678 m (Figure 25).

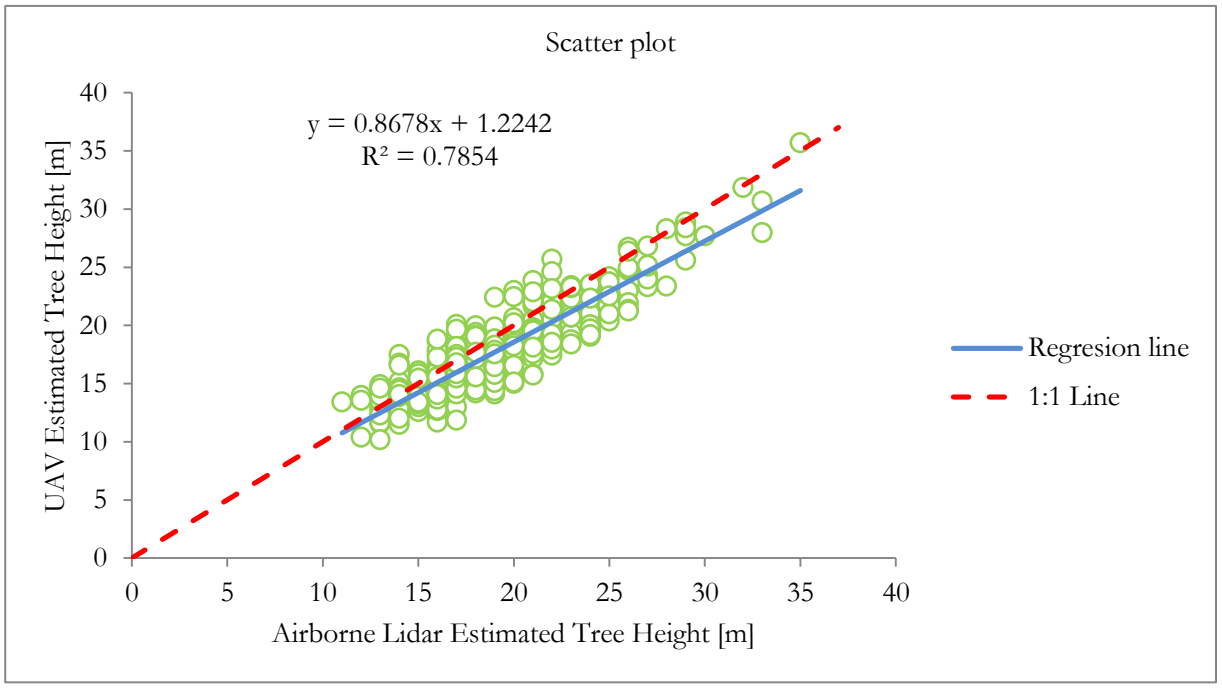


Figure 25: Scatter plot of the relationship between UAV and Airborne LiDAR

Table 14: Relationship between ALS height and UAV estimated tree height

Summary of fit	
Correlation Coefficient	0.886242067
R Square	0.785425001
Adjusted R Square	0.784869107
Standard Error [m]	1.717566921
Root Mean Square Error (RMSE) [m]	1.390869978
Observations	388

4.6.1. Relationship between estimated UAV and field measured tree height

The descriptive statistics were done to assess the matched trees between UAV and field measured trees. The average UAV estimated tree height and actual field measurements were 17.78 m and 16.68 respectively. UAV recorded a minimum tree height of 10.16 m while the minimum tree height recorded by field was 11.9 m (Table 15). The relationship between UAV estimated tree height and measured field were established using coefficient of determination (R^2). The coefficient of determination (R^2) shows that 63.26% of variability measured tree height in Airborne LiDAR was explained by UAV estimated tree height. The correlation coefficient and RMSE was 0.795 and ±2.52 m respectively. The summary is shown in Table 16 and (Figure 26) indicated the relationship between UAV and field tree height.

Table 15: Descriptive statistics for UAV and field height

	UAV Estimated Tree Height [m]	Field Measured Tree Height [m]
Mean	17.78212556	16.68435567
Standard Deviation	3.703073032	4.157636273
Minimum	10.15921021	11.9
Maximum	35.70339203	33
Count	388	388

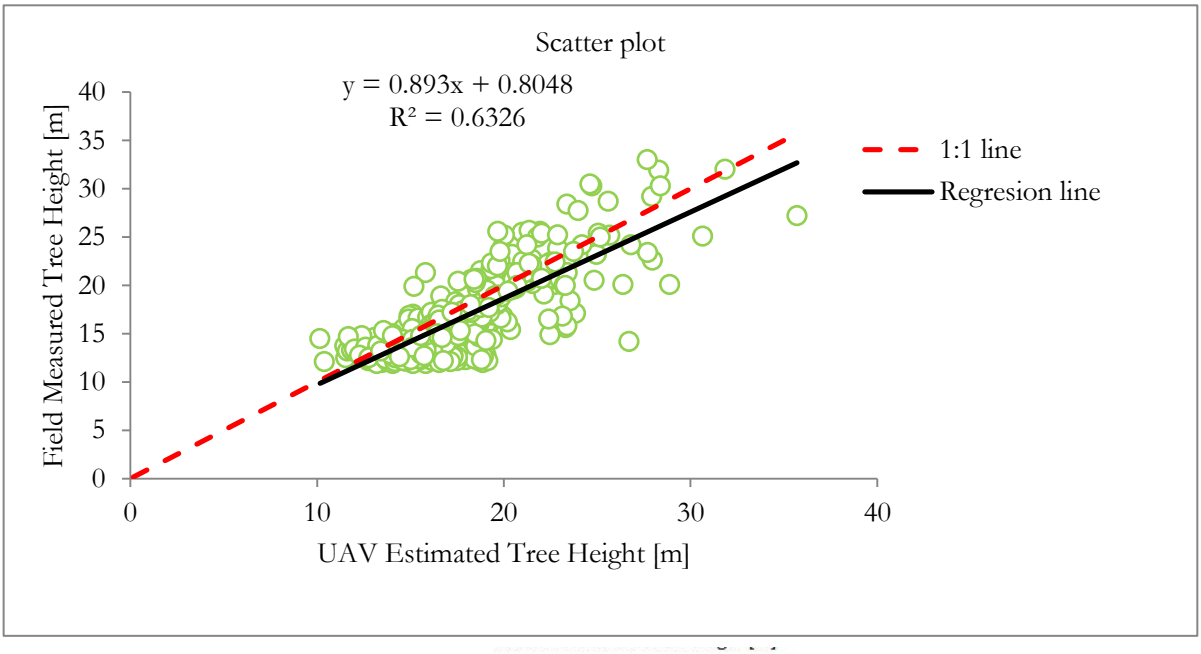


Figure 26: Scatter plot of the relationship between field height and UAV tree height

Table 16: Relationship between UAV height and Field height

Summary of fit	
Correlation Coefficient	0.795372145
R Square	0.632616849
Adjusted R Square	0.63166508
Standard Error [m]	2.523294494
Root Mean Square Error (RMSE) [m]	1.167025904
Observations	388

4.6.2. Accuracy of field measured tree height

The average Airborne LiDAR estimated tree height and actual field measurements were 19.08 m and 16.68 respectively. Airborne LiDAR recorded a minimum of tree height of 11 m while the minimum tree height recorded by field was 11.9 m. The spread of the height for Airborne LiDAR was 3.78 m while in field measured height was 4.16 m. The summary of descriptive statistics was shown in Table 17.

The relationship between Airborne LiDAR estimated tree height and measured field height were established and the relationship which was validated using coefficient of determination (R^2). The coefficient of determination (R^2) shows that 62.43% of variability in measured tree height was explained by ALS estimated tree height. The correlation coefficient and RMSE was 0.790 and ±2.55 m respectively. The summary is shown in Table 18. Figure 27 showing the relationship between Airborne LiDAR and field tree height.

Table 17: Descriptive statistics for ALS and field height

Statistics	Airborne Lidar Estimated Tree Height [m]	Field Measured Tree Height [m]
Mean	19.07989691	16.68435567
Standard Deviation	3.781678666	4.157636273
Minimum	11	11.9
Maximum	35	33
Count	388	388

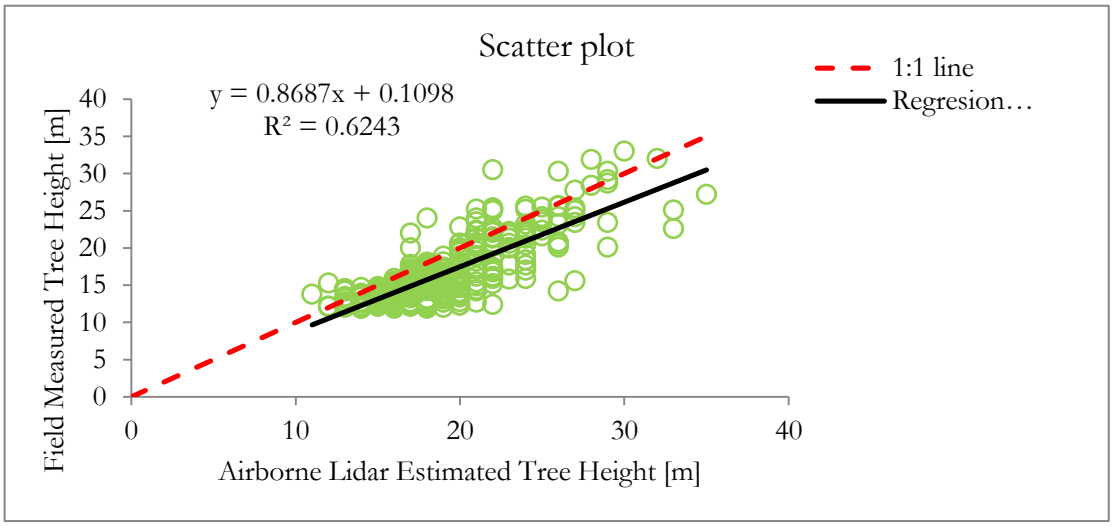


Figure 27: Scatter plot of the relationship between ALS height and Field height

Table 18: Relationship between ALS height and Field height

Summary of fit	
Correlation Coefficient	0.790138011
R Square	0.624318076
Adjusted R Square	0.623344806
Standard Error [m]	2.551634543
Root Mean Square Error (RMSE) [m]	2.45
Observations	388

4.7. Assessing tree height measurement differences (ALS, UAV and Field)

The difference between means tree height measured from field, UAV and Airborne Lidar were tested by using statistical analysis. One way analysis of variance (ANOVA) was carried out to determine whether there were any statistically significant differences between the means of three independent groups that is field tree height, UAV and ALS estimated height (Davis, 2002). The conducted ANOVA test can be seen in Appendix 7 which shows that F calculated was higher than F critical, therefore the tested null hypothesis was rejected. This means that there was significant difference between the means. However, the test did not specify which mean differ from which. So to understand more the variation between the means of the measured tree height from the field and estimated tree height from UAV and Airborne LiDAR, t-test was done and explained in the next section.

4.7.1. Tree height differences between Airborne Lidar and UAV

In order to understand more about the variation in estimated tree height by Airborne Lidar and UAV the means t-test was conducted. Prior to the t-test, F-test was done in order to determine which specific t-test could be applied. F test was used to tests whether means have equal variation. F test results indicated that the F calculated was less than the F critical. Therefore null hypothesis was accepted, that is there was no significant variation between the mean of estimated tree height from Airborne Lidar and UAV. The summary of the F test is shown in Appendix 8.

Furthermore, the normality test using Shapiro-Wilk test was done in order to reveal whether the data were normally distributed. The same test was done in the study done by (Shapiro & Wilk, 1965). In this study the result shows that the mean and median are close to each other, however, the value of the mean was slightly higher than median, this indicated that data were less skewed in the positive side. Since real data are seldom perfect symmetrical, therefore in this case the data were assumed to be normally distributed. Figure 31a&b shows the normality test of the ALS and UAV estimated tree height as done in R package for statistical analysis.

Following F-test, t-test assuming equal variance was conducted to see whether there is a significant difference between the mean of the tree estimated by Airborne LiDAR and UAV. The results show that there was significant difference at ($p < 0.05$) that is t statistic (4.83) was greater than t critical (1.65) therefore the tested null hypothesis was rejected. The summary of the t statistics is as shown in the (Appendix 9).

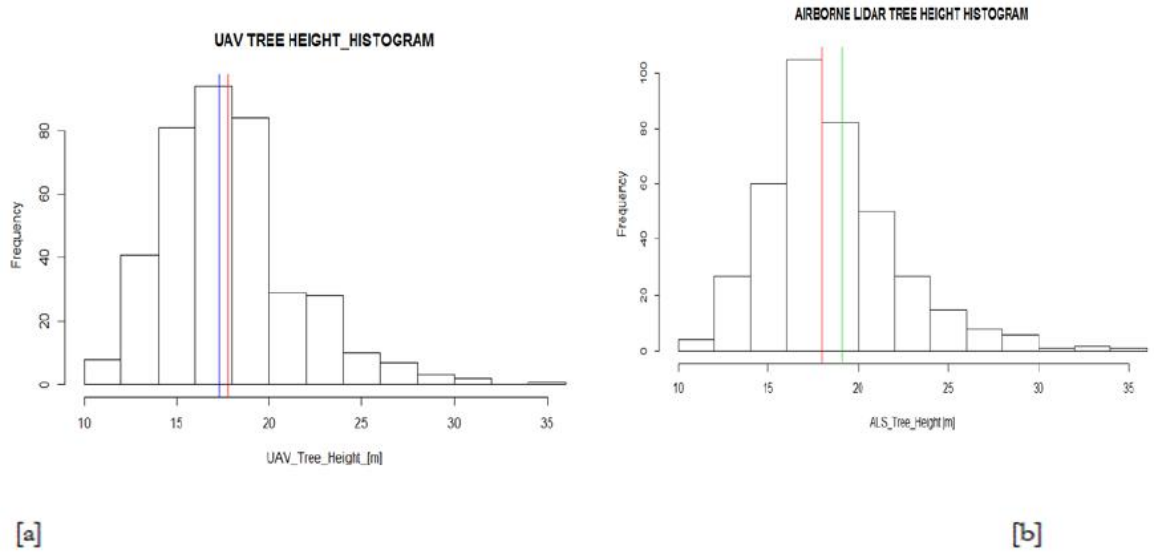


Figure 31: (a&b) Show the normality test of ALS and UAV

4.7.2. Differences between measured tree height and UAV estimated tree height

Before t-test was done, F test was carried out to reveal whether there is significant difference between the mean of tree height estimated by UAV and that of field height. The results of the test indicated that there was no significant difference between the means. Thus null hypothesis was accepted. The summary of the results is indicated in the (Appendix 10). The t-test assuming equal variance was used to test whether there is significant difference between the mean of tree height estimated by UAV and that of field height. The results in the (Appendix 11) show that there is significant difference ($p < 0.05$) between the mean of the tree height measured from the field and that from the UAV.

4.7.3. Differences between field and Airborne LiDAR measured tree height

F-test was conducted to determine whether there is significant difference between the mean of tree height estimated by Airborne LiDAR and that of field height. The results of the test indicated that there were no significant difference between the means, so null hypotheses was not rejected while the alternative hypothesis was un-accepted. The summary of the results are shown in Appendix 12. The t-test assuming equal variance was used to test whether there is significant difference between the mean of tree height estimated by Airborne Lidar and that of field height. The results are shown in Appendix 13 which indicate that there is a significant difference ($p < 0.05$) between the mean of the tree height measured from the field and that from the Airborne Lidar.

4.8. Biomass estimation

The amount of biomass of individual tree was calculated by using allometric question. Tree height estimated from photogrammetric point clouds of UAV, ALS, and field measured height, DBH and wood density was used as input in the allometric equation for AGB computation. The summary of descriptive statistics (Table 19) and relationship in regression line (Appendix 14 & 16), t-test (Appendix 15 &17) and accuracy of field and UAV biomass are shown in Table 20 and 21.

Table 19: Descriptive statistics for ALS, UAV and Field biomass

Statistics	ALS Biomass	UAV Biomass	Field Biomass
Mean Biomass [Mg]	0.488365779	0.456530248	0.445806688
Standard Deviation	0.631030645	0.593642199	0.61919538
Minimum	0.04339033	0.044276364	0.040129629
Maximum	4.243148145	3.881050837	4.733283954
Total Biomass [Mg]	189.4859223	177.1337361	172.972995
Observations (Total Trees)	388	388	388

Table 20: Relationship and accuracy of UAV computed biomass

Statistics	
Correlation	0.994455197
R Square	0.988941139
Standard Error	0.06250889
RMSE [Mg]	0.062347613
RMSE%	13.65684164
Observations	388

Table 21: Relationship and accuracy of field computed biomass

Statistics	
Correlation	0.984822411
R Square	0.969875181
Standard Error	0.107609785
RMSE [Mg]	0.107332097
RMSE%	24.07592803
Observations	388

4.9. Carbon Stock estimation

The amount of carbon stock of individual tree was computed based on the calculated biomass, the descriptive statistics indicated that in the total matched trees of 388 the average mean biomass of ALS, UAV and field tree height was 0.218, 0.204 and 0.199 Mg respectively. ALS recorded the standard deviation of 0.29 Mg, UAV of 0.27 Mg and field of 0.28 Mg. The total carbon stock generated was 84.95 Mg for ALS, 79.29 Mg for UAV and 77.47 Mg for field measured tree height. The summary of descriptive statistics is shown in Table 22 and relationship regression line (Appendix 18 & 19) and accuracy of the field and UAV carbon stock are shown in Table 23 and 24.

.

Table 22: Summary of ALS, UAV and field carbon stock

Statistics	ALS Carbon Stock	UAV Carbon Stock	Field Carbon Stock
Mean Carbon Stock [Mg]	0.229531916	0.214569216	0.209529143
Standard Deviation	0.296584403	0.279011833	0.291021829
Minimum	0.020393455	0.020809891	0.018860925
Maximum	1.994279628	1.824093893	2.224643459
Total Carbon Stock [Mg]	89.05838348	83.25285599	81.29730763
Observations (Total Trees)	388	388	388

Table 23: Summary of relationship and accuracy of UAV computed carbon stock

Statistics	
R Square	0.969875181
Standard Error	0.050576599
RMSE	0.029303393
RMSE%	13.65684853
Observations	388

Table 24: Relationship and accuracy of field computed carbon stock

Statistics	
R Square	0.969875181
Standard Error	0.050576599
RMSE	0.051644377
RMSE%	24.64782525
Observations	388

4.10. Sensitivity analysis

The sensitivity analysis was conducted to assess the effect of differences of the tree height on the biomass and carbon stock. The approaches which were used to estimate trees height was assessed to realize how differences in tree height measurements affected AGB estimation. In actual field work measuring trees height were associated with challenges due to topographical complexity, complexity of canopy structure and human blunders in tree height measurement. Therefore, potential differences in trees height measurements affect the AGB and carbon stock.

4.10.1. Effect of differences of field measured tree height on biomass and carbon stock.

The relationship between tree height estimated by Airborne LiDAR and field measurement indicated that coefficient of determination (R^2) was 0.62. The model developed was used to compute RMSE, when computation was done RMSE of ±2.55 m was obtained. The obtained RMSE indicated that the average deviation of the measured trees height was approximately 3 m from the line of fit. Thus, the obtained RMSE was used as a basis to assess the effect of differences of trees height measurements on AGB. This was done by adjusting the height of the trees based on the potential RMSE obtained and see how was affecting the AGB and carbon stock estimation. To reveal the effect of differences of trees height measurements in the AGB and carbon stock, a scatter plot of random selected thirty (30) trees were

plotted by adjusting the value of tree height in the range of -3 m to +3 m due to RMSE of ±2.55 m (Table 25 and Figure 28).

Table 25: Effect of differences of measured field tree height on biomass estimation

Statistics	RMSE[-3]	RMSE[-2]	RMSE[-1]	RMSE[0]	RMSE[+1]	RMSE[+2]	RMSE[+3]
Mean biomass [Mg]	0.39	0.42	0.44	0.47	0.50	0.52	0.55
Standard Deviation	0.53	0.56	0.59	0.61	0.64	0.67	0.69
Minimum biomass [Mg]	0.03	0.03	0.04	0.04	0.04	0.05	0.05
Maximum biomass [Mg]	2.60	2.72	2.83	2.95	3.06	3.18	3.29
Total biomass [Mg]	11.68	12.49	13.29	14.10	14.90	15.71	16.51
Selected trees	30	30	30	30	30	30	30

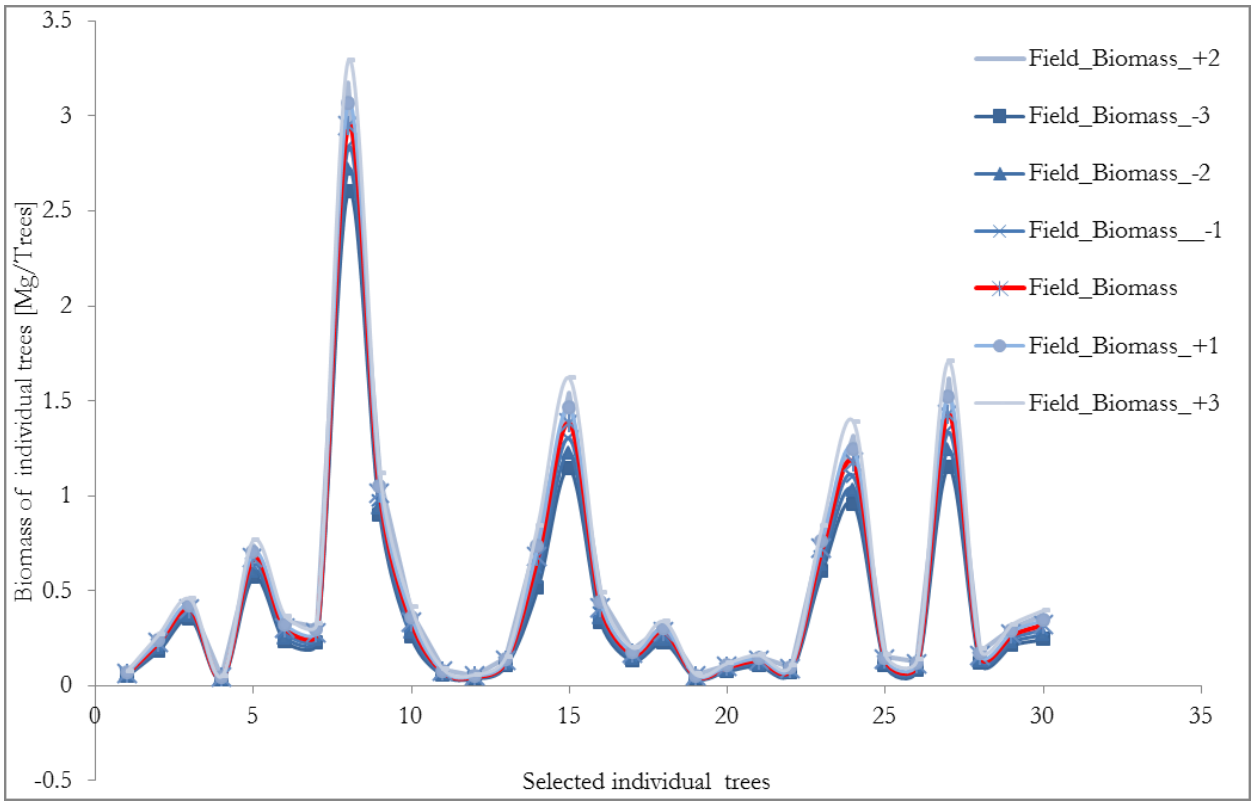


Figure 28: Effect of differences of field measured tree height on AGB estimation

In addition to that, since there is a direct proportional relationship between biomass and carbon stock the study went further and assess the impact of differences of tree height in estimation of carbon stock. Furthermore, since the accuracy assessment of the Airborne LiDAR and field measured tree height revealed that the RMSE was ±2.55 which were approximated to ±3 m. Then trees height was adjusted in the range of -3 to +3 m when carbon stock was computed. The descriptive summary is shown in Table 26.

Table 26: Effect of differences of trees height measurements on estimation of carbon stock estimation

Statistics	RMSE[-3]	RMSE[-2]	RMSE[-1]	RMSE[0]	RMSE[+1]	RMSE[+2]	RMSE[+3]
Mean carbon stock[Mg]	0.18	0.20	0.21	0.22	0.23	0.25	0.26
Standard Deviation	0.25	0.26	0.28	0.29	0.30	0.31	0.33
Minimum carbon stock	0.01	0.02	0.02	0.02	0.02	0.02	0.02
Maximum carbon stock	1.22	1.28	1.33	1.39	1.44	1.49	1.55
Total carbon stock[Mg]	5.49	5.87	6.25	6.63	7.00	7.38	7.76
Selected trees	30	30	30	30	30	30	30

Furthermore, the differences which were associated with measurements of trees height in the tropical rain forest resulted into over or under estimation of biomass and carbon stock. From the obtained total biomass and carbon stock, differences in biomass and carbon stock was calculated (Table 27) and presented in the bar chart (Figure 29) for differences in biomass and (Figure 30) for differences in carbon stock.

Table 27: Effect of differences of field height measurement on AGB and carbon stock estimation

Statistics	RMSE[-3]	RMSE[-2]	RMSE[-1]	RMSE[0]	RMSE[+1]	RMSE[+2]	RMSE[+3]
Total biomass [Mg]	11.68	12.49	13.29	14.10	14.90	15.71	16.51
Change in biomass[Mg]	-2.42	-1.61	-0.80	0.00	0.80	1.61	2.41
Total carbon stock[Mg]	5.49	5.87	6.25	6.63	7.00	7.38	7.76
Change in carbon stock[Mg]	-1.14	-0.76	-0.38	0.00	0.38	0.75	1.13
Selected trees	30	30	30	30	30	30	30

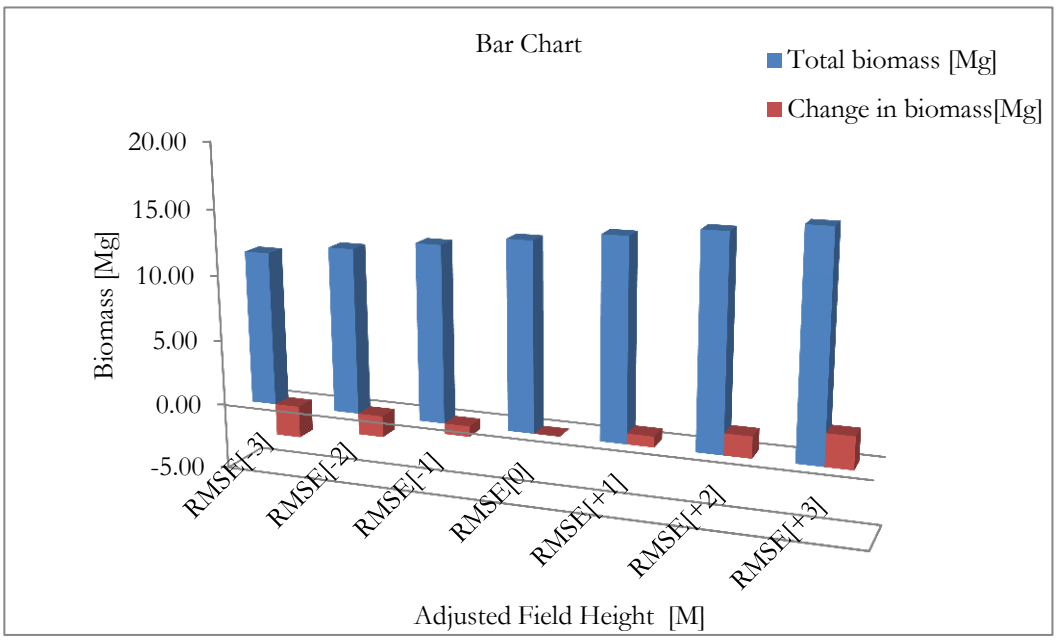


Figure 29: Bar chart indicating the effect of differences of field tree height measurements on AGB estimation

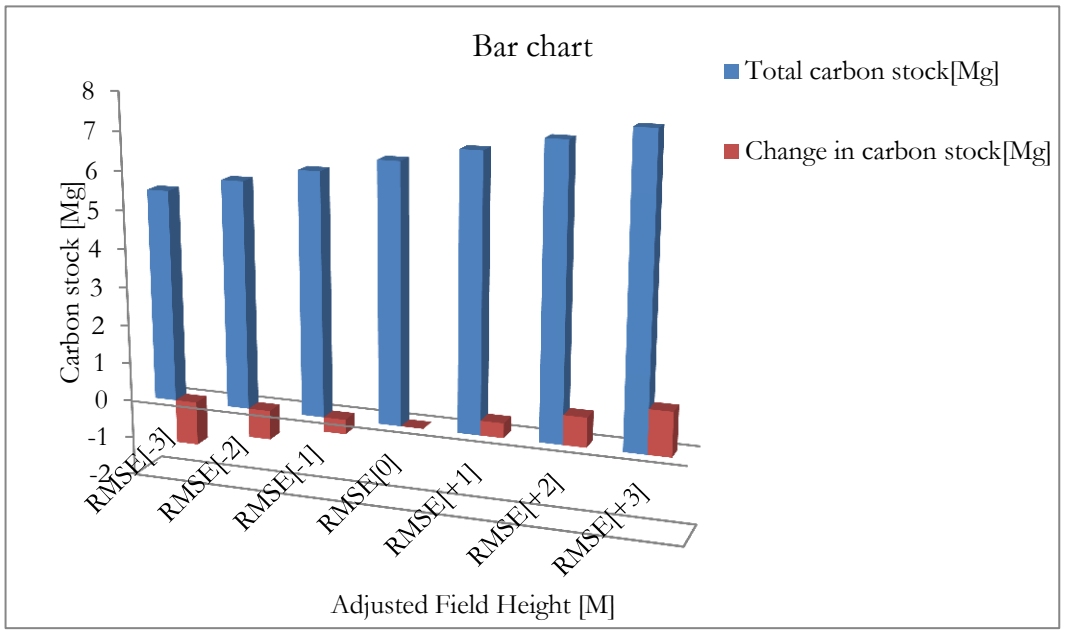


Figure 30: Bar chart indicating the effect of differences of field trees height measurements on carbon stock

4.10.2. Effect of differences of UAV estimated tree height measurements on biomass and carbon stock

The relationship between trees height measured by Airborne Lidar and UAV estimated tree height indicated that coefficient of determination (R^2) was 0.78. Then, the generated equation model was used to calculate RMSE and RMSE% for accuracy assessment. The RMSE of ±1.7 m (RMSE %9.63) m was obtained, which showed that the average distance from the line of fit in the estimated trees height was 1.7 m. The obtained RMSE was used to assess the impact of differences of the trees height estimated from UAV on the AGB and carbon stock estimation by adjusting the height of the tree based on the potential RMSE obtained and see how it was affecting the AGB and carbon stock estimation. To reveal the effect of differences of trees height measurements estimated from UAV on the AGB and carbon stock estimation. The summary of descriptive statistics (Table 28, Figure 31) and scatter plot (Figure 32) for selected thirty (30) trees were plotted by adjusting the value of tree height estimated from UAV in the range of -1.7 m to +1.7 m due to RMSE of ±1.7 m.

Table 28: Effect of differences of UAV estimated trees height on biomass estimation

Statistics	RMSE[-1.7]	RMSE[0]	RMSE[+1.7]
Mean biomass [Mg]	0.55	0.59	0.64
Standard Deviation	0.70	0.74	0.79
Minimum biomass [Mg]	0.06	0.06	0.07
Maximum biomass [Mg]	3.39	3.58	3.78
Total biomass [Mg]	16.38	17.74	19.10
Selected trees	30	30	30

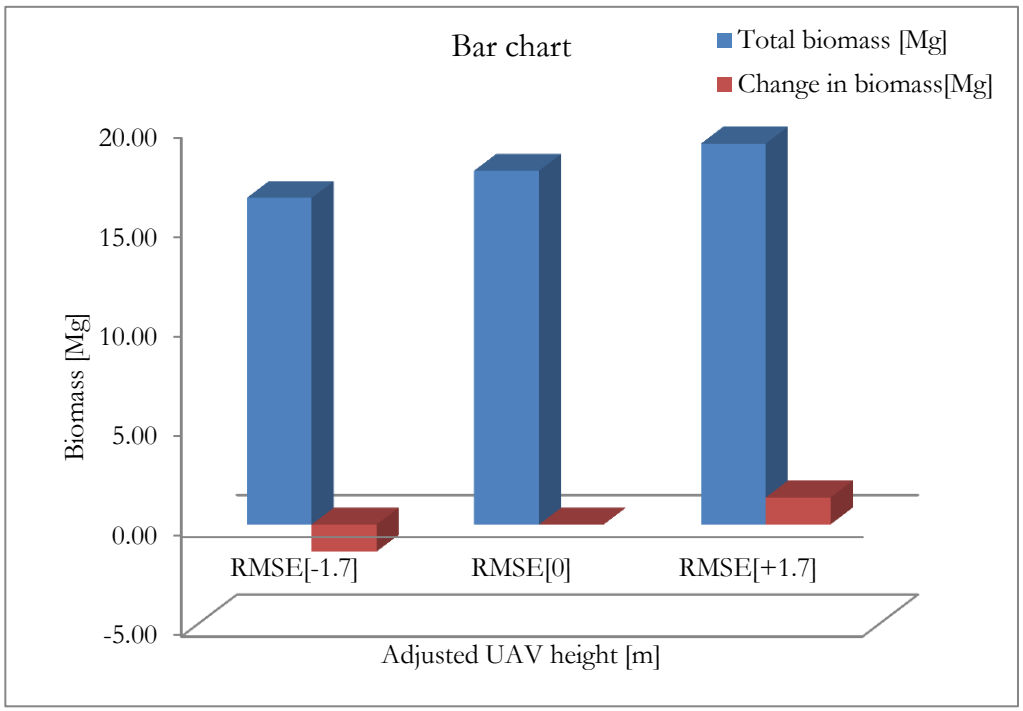


Figure 31: Bar chart indicating effect of differences of UAV tree height measurements on biomass estimation

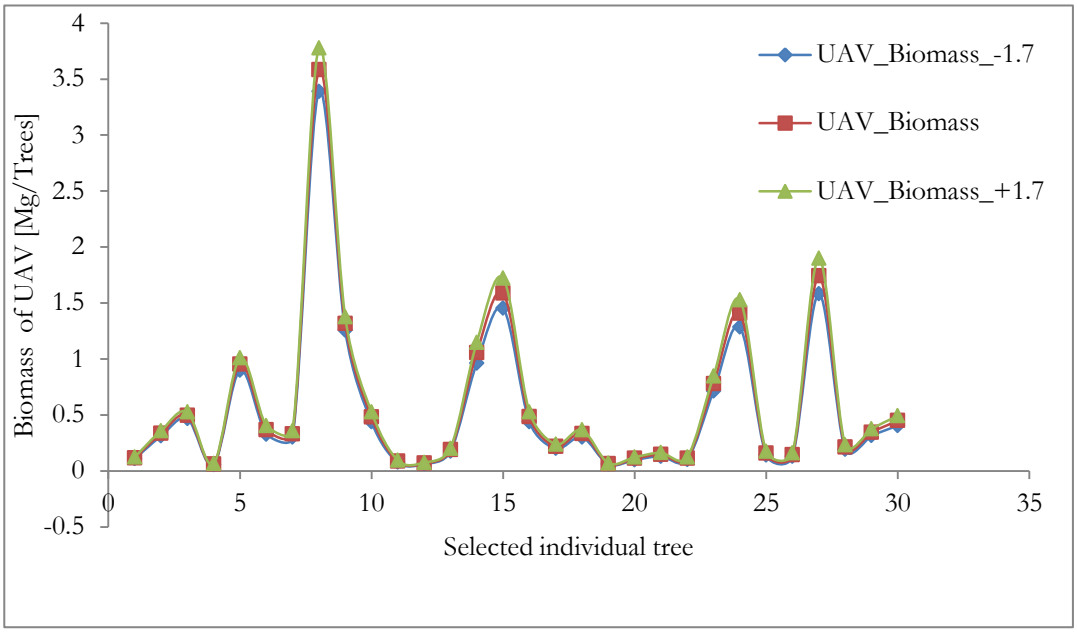


Figure 32: Sensitivity analysis of AGB to tree height adjusted based on the RMSE

Since the accuracy assessment of tree height estimated by Airborne LiDAR and 3D point cloud of photogrammetric image matching revealed that the RMSE was ±1.7 m. Therefore, tree height was adjusted in the range of -1.7 to +1.7 m when carbon stock was computed and the descriptive summary is shown in Table 29.

Table 29: Effect of differences of UAV estimated tree height on estimation of carbon stock

Statistics	RMSE[-1.7]	RMSE[0]	RMSE[+1.7]
Mean carbon stock[Mg]	0.26	0.28	0.30
Standard Deviation	0.33	0.35	0.37
Minimum carbon stock	0.03	0.03	0.03
Maximum carbon stock	1.59	1.68	1.78
Total carbon stock[Mg]	7.70	8.34	8.98
Selected trees	30		30

Furthermore, RMSE which was attributed to differences in measurements of tree height in the complex rain forest resulted into over or under estimation of biomass and carbon stock. The biomass and carbon stock was calculated (Table 30 and Figure 33).

Table 30: Change in biomass and carbon stock due to field measurement error

Statistics	RMSE[-1.7]	RMSE[0]	RMSE[+1.7]
Total biomass [Mg]	16.38	17.74	19.10
Change in biomass[Mg]	-1.36	0.00	1.36
Total carbon stock[Mg]	7.70	8.34	8.98
Change in carbon stock[Mg]	-0.64	0.00	0.64
Selected trees	30	30	30

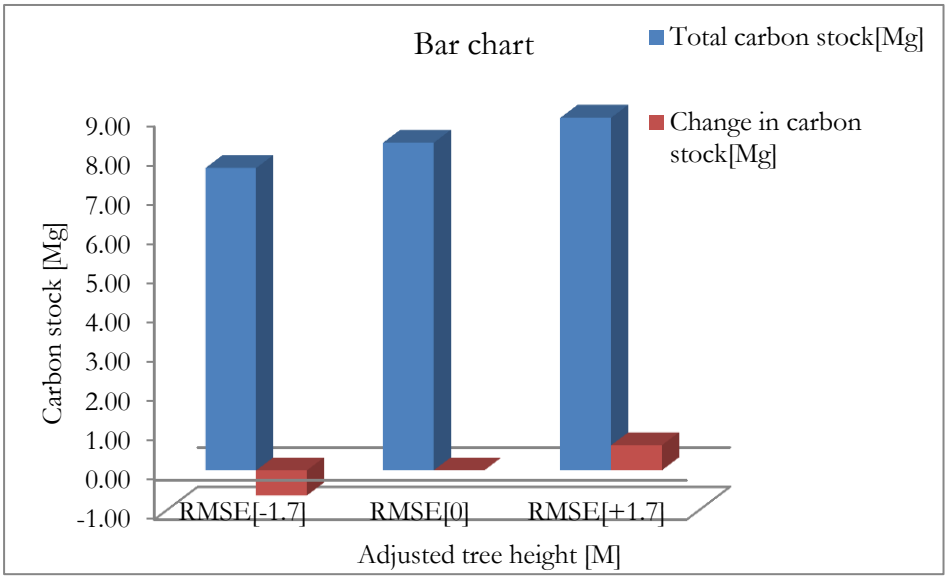


Figure 33: Bar chart indicating effect of error in tree height on carbon stock

On the other hand, when UAV estimated trees height was regressed with DGPS height (z – value) the coefficient of determination R^2 obtained was 0.96 and RMSE ±3.8 m. Therefore the measurements of UAV estimated trees height were adjusted in the range of – 4 m to +4 m as shown in figure 34.

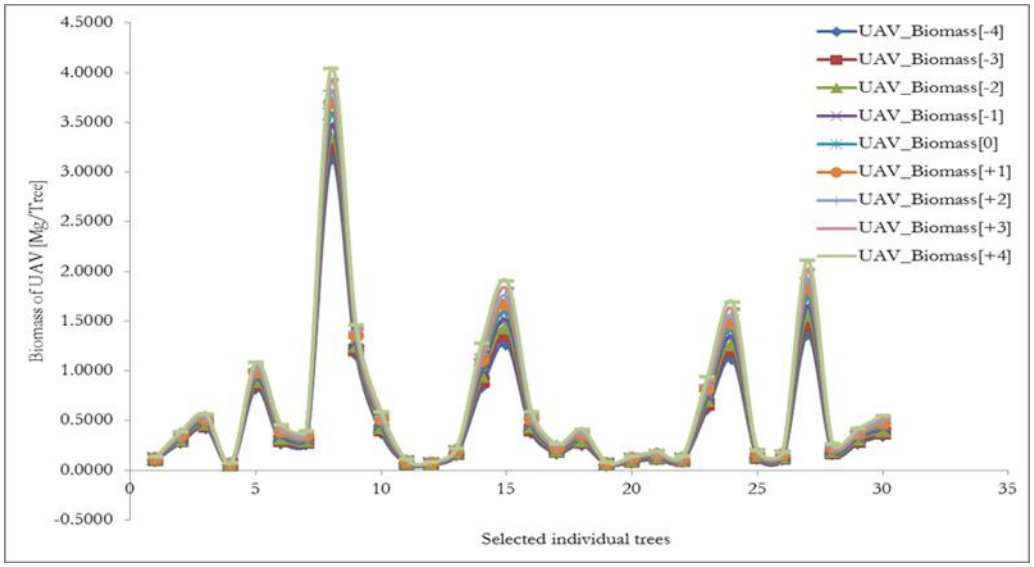


Figure 34: The effect of differences of UAV estimated trees height on AGB

Additionally, the thirty (30) selected trees were used to assess the effect of differences of trees height measurements on AGB. The effect of differences of trees height of both approaches (UAV, field and ALS) were assessed. The scatter plot revealed the differences in amount of AGB resulted by effect of differences of tree height measurements. The sensitivity analysis line shows that the amount of AGB was influenced by differences in tree height. Figure 35 shows how measured tree height and estimated tree height by UAV affected biomass estimation. The line graph shows that, Airborne Lidar estimated biomass higher than UAV and field. On the other hand UAV estimate biomass relatively higher than field measurement. The field seemed to under estimate biomass when compared to all.

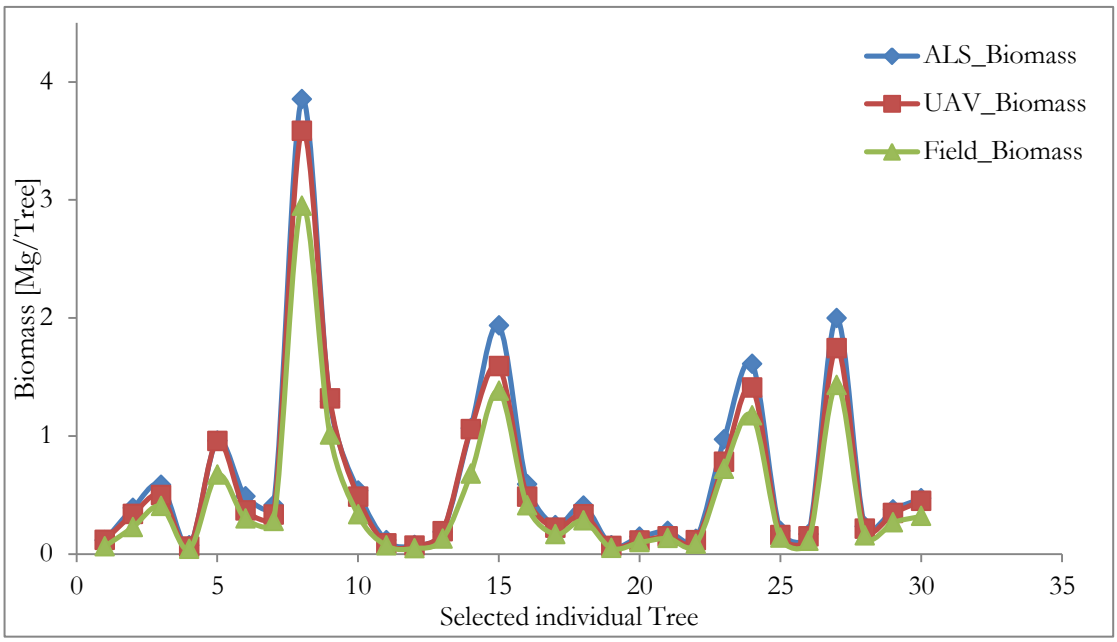


Figure 35: Effects of differences of tree height measurement in ALS, UAV and field on biomass estimation.

5. DISCUSSION

5.1. Accuracy of UAV DTM

In this study data from six flights UAV photogrammetric DTMs were derived. Absolute orientation was successful for a total of 1,975 out of 1,980 stereo photos collected by Phantom4 DJI were used. Five images were discarded because their orientation appeared to be wrong. The flight altitude used for all flight were 80 m except flight five which was 90 m, the side overlap was 60 to 70 % and the images were taken at nadir in a continuous mode where photos were taken at the interval. These parameters were important to be considered in data processing since they influence the quality of the generated photogrammetric DTM. In a study by Lisein et al. (2014) using unmanned aerial system (UAS) revealed that the photos collected had high overlap (60-70) which provide accurately model the canopy structure at high spatial and temporal resolution. The important of image overlap was emphasized in the study by Colomina & Molina, (2014).

According to Torres-sánchez et al. (2015) the 60% overlap configured in flight mission was higher enough to be applied in 3D reconstruction of the object. In this study the point clouds per m^2 generated were 180, 202, 254, 50.1, 217 and 210 for the first, second, third, fourth, fifth and sixth flight respectively. Higher overlaps provide more matching points which are important in developing 3D reconstruction of the object. The ground Sampling Distance (GSD) was ranging from 3.13 to 3.72 cm/pixel and RMSE of the pixel of the DTM generated in the six flights was ±0.42, ±0.29, ±0.4, ±0.44, ±0.43 and ±0.40 respectively. A number of studies were based on the accuracy report generated by the software to justify the uses of DTM in photogrammetry image matching. Wallace et al., (2014) reported the mean difference of 0.09 m between photogrammetry DTM and ALS DTM in their entire study area. The large difference was more pronounced in the area where there were close canopy with mean difference of 0.12 m. The difference in the results was attributed to the fact that their study was conducted in the patches of Eucalyptus forest where image could see the ground unlike this study which was conducted in a tropical dense forest.

Furthermore, the accuracy of the UAV and ALS DTM was assessed by using the ground control point which was collected by using differential GPS. The results revealed that the coefficient of determination (R^2) was 0.96 and RMSE was ±3.84 m with RMSE % of 7.96 for DTM of UAV while Airborne LiDAR had RMSE of ±1.25 (2.75%).

On the other hand the DTM height of Airborne LiDAR was used to model, validate and evaluate the accuracy of photogrammetry DTM. During the process photogrammetry DTM was subtracted from Airborne LiDAR thereafter R^2, RMSE, and RMSE% was computed. Strong relationship was found in the flights one up to five (R^2 was 0.93, 0.91, 0.92, 0.98, 0.90 for the first, second, third, fourth and fifth). However, flight six seems to have weak relationship. RMSE for first, second, third, fourth, fifth and sixth were ±3. 09 m, ±6.69 m, ±3.11 m, ±2.53 m, ±4.05 m and ±6.32 m respectively. Flight two and six were more dense area, therefore few points cloud reached the ground and therefore the DTM generated overestimated the height. This contributed to the big difference in DTM height compared to other flight. However, t-test at $p<0.05$ (Appendix 5) showed that there was no statistically significant difference between the UAV and ALS DTM.

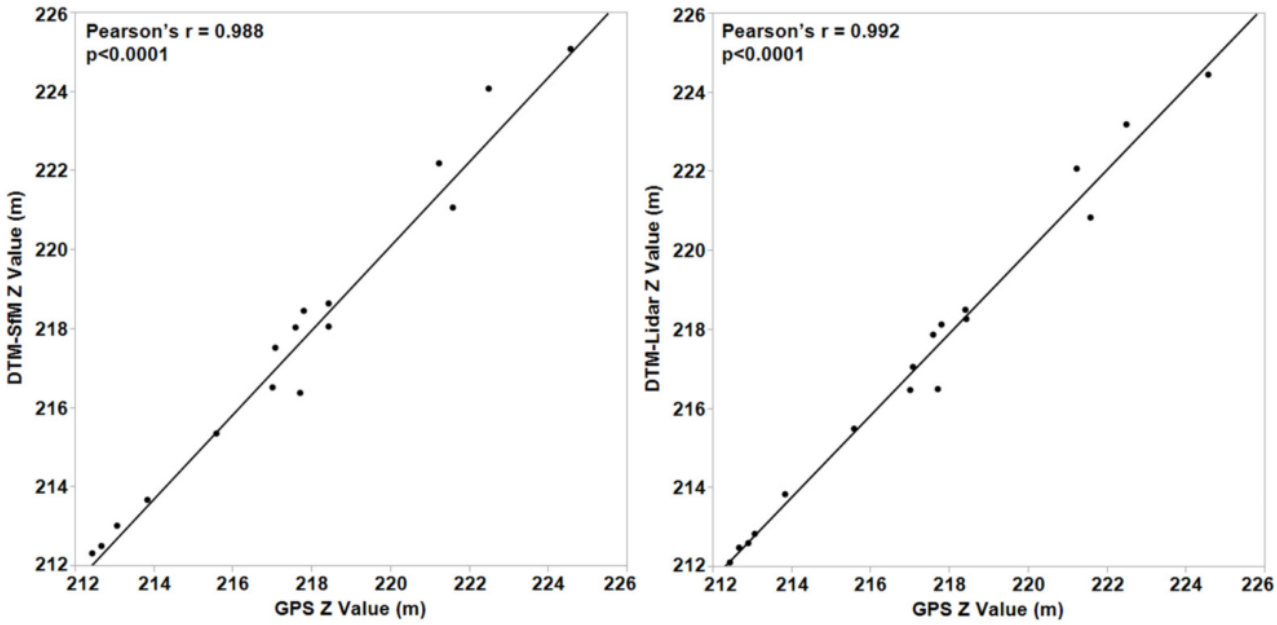
Similar study was conducted by Jensen & Mathews (2016) in which photogrammetry DTM (DTM_{SfM}) was compared by Airborne LiDAR (DTM_{Lidar}) using GPS surveyed center points which revealed that DTM_{SfM} underestimated mean height by – 0.31 m (st.dev.=0.73 m) while DTM_{Lidar} overestimate by 0.08 m (st.dev

0.49 m) (Table 31 and Figure 36). The difference in the results was attributed to the difference in classification algorithms.

Table 31: Comparison of photogrammetry and ALS DTM using GPS surveyed

Comparison Metrics (n = 17)	GPS-DTM_{SfM}	GPS-DTM_{lidar}
Mean difference [m]	-0.31	0.08
Standard deviation of difference [m]	0.73	0.49
Median difference [m]	0.1	0.08
Minimum difference [m]	-0.59	-0.85
Maximum difference [m]	1.29	1.17

Source: (Jensen & Mathews, 2016)



Source: (Jensen & Mathews, 2016).

Figure 36: Scatterplots showing the relationship between GPS surveyed plot center points against DTM_{SfM} (left) and DTM_{lidar} (right).

On the other hand, the accuracy assessment of photogrammetry DTM using ALS DTM as reference was evaluated in the study conducted by (Debella-Gilo, 2016). Initially, photogrammetry DTM was interpolated by using national DTM (DTED10) thereafter RMSE was used to evaluate the quality of newly interpolated (Table 32) photogrammetry DTM (Debella-Gilo, 2016). The results of this study (flight 1, 3,4 and 5) were comparable with the results which were obtained in site 4 by Debella-Gilo (2016) because they all had dense forest. While on other sites, the RMSE was low compared to that obtained in this study. The reason could be due to the fact that site 1 to 3 was bare soil to low vegetation. Unlike this study which was dense forest which create less point clouds were recorded on the ground and therefore generate more error.

Table 32: The error variables of the DTMs interpolated by the five different methods for the four test sites

Interpolation method	Error variable [m]	Site 1	Site 2	Site 3	Site 4
	Mean error	0.1	-0.1	0.5	-0.5
	Standard error	0.7	1.2	0.7	2.3
	Median Absolute Deviation	0.5	0.7	0.7	1.1
Inverse Distance Weighted	RMSE	0.7	1.2	0.9	2.4
	Mean error	0.0	-0.3	0.5	-0.5
	Standard error	0.6	1.5	0.7	2.1
	Median Absolute Deviation	0.5	0.7	0.7	1.1
Natural Neighbour	RMSE	0.6	1.5	0.8	2.2
	Mean error	0.0	-0.2	0.4	-0.6
	Standard error	0.7	1.4	1.3	2.4
	Median Absolute Deviation	0.5	0.9	1.0	1.3
Regularized Spline	RMSE	0.7	1.4	1.4	2.5
	Mean error	0.0	-0.3	0.5	-0.6
	Standard error	0.6	1.5	1.2	2.4
	Median Absolute Deviation	0.5	0.8	0.9	1.2
TriangleBased Piece-Wise Cubic	RMSE	0.6	1.5	1.2	2.5
	Mean error	0.0	-0.1	0.5	-0.5
	Standard error	0.5	1	0.7	2.1
	Median Absolute Deviation	0.5	0.7	0.6	1
ANUDEM	RMSE	0.5	1	0.8	2.1
DTED10	RMSE	3	2.2	1.1	4
Reduction in RMSE from that of DTED	RMSE (%)	83	55	27	47

Source: (Debella-Gilo, 2016)

Where the site 1 was a bare area with a slope varying gradually from flat to steep, site 2 was a steep area partly covered by dense vegetation, site 3 was a built up urban area and its surroundings and site 4 was an area with a complex topography including steep and undulating terrain, dense forests and open areas (Debella-Gilo, 2016).

Furthermore, the comparison of the photogrammetry and Airborne LiDAR DTM was done using the height generated at the center of the pixel (1mx1m) resolution for both UAV and ALS. The results indicated that RMSE for all flights range from ±2.53 m to ±6.32 m, the RMSE% range from 6.6 to 13.09 and R^2 range from 0.14 to 0.97. The reasons for the differences were because of the fact that point clouds generated in UAV photos was not able to image the ground (Figure 37) and therefore miss the terrain information. Normally the photogrammetry DTM is made by filtering it from DSM. The generation of the final DTM was performed using the mean and median values of classified ground hits where the missing surface heights were interpolated using the nearby heights and the Delaunay algorithm (Hyyppä et al., 2000). A similar approach of assessing the accuracy of photogrammetry DTM by subtracting from Airborne LiDAR was done by Jensen & Mathews (2016), where it was revealed that DTM_{SfM} was ±0.5 m to ±1.0 m of the Airborne LiDAR DTM. The RMSE was less than the RMSE reported in this study because the point centers were recorded to cover the variety of canopy cover characteristics ranging from open to dense forest, which was contrasting with this study which took place in the dense forest of Ayare Hitam Forest Reserve. Similar approach was used in the study of Naumann et al., (2013) to assess the accuracy of photogrammetry DSM to DSM generated by TLS.



Source: (Lisein et al., 2014)
Figure 37: Comparison of Airborne LiDAR and photogrammetry points cloud.

The study went further and assess the accuracy of the UAV DTM by estimating tree height in the area were Airborne LiDAR and UAV photogrammetry DTM had nearly the same height RMSE of 0.19 m (0.53%) and R^2 of 0.99. In this research it was revealed that RMSE of estimating tree height in UAV DTM was reduced to 1.56 m (8.7%) with R^2 of 0.80. At this point, the RMSE (±1.56 m) was comparable to RMSE of ±1.5 m which were reported by (Jensen & Mathews, 2016). The reason for similarity was due to the fact that at these points UAV was able to image the ground..

5.2. Tree height estimation using Leica DISTO

In this study tree height was measured using Leica DISTO 510, the instrument uses laser technology to measure tree height. The equipment itself has high accuracy, however measuring tree height in the complex tropical forest which has dense canopy lead to introduction of error because of occlusion of tree branches, which makes it difficult to see tree top (Figure 38). This challenge was also revealed by Chave (2005), Rahman et al. (2015) and Dassot et al. (2011) who reported challenges on accurate measuring of tree height due to complexity of close forest. Williams et al. (1994) insisted that measuring of tall trees was more difficult in the closed forest because the top of the tree was blocked by the tree branches which lead to the visibility impaired of the peak of the tree. Hunter et al. (2013) and Larjavaara et al. (2013) stated that measuring of tree height in the tropical forest face some challenges. However, using of laser became more useful in measuring of tree heights from direct under the canopy. They went further and insisted that there must be some direct and unblocked path to ensure visibility impaired to the top of the tree in order for the measurement to be taken.

Ayare Hitam Forest Reserve is the forest which attained its restoration condition. Thus measuring tree height in this kind of the forest was tricky. Some trees are very tall and the ecosystem is composed of dense understory. Chopping of the understory trees was inevitable. This was important because it helped to remove some shrubs which act as occlusion and hence limit visibility of the top of the trees. This approach was also supported in the study done by Rahman et al. (2015) who reported that tradition based techniques of measuring tree height needed chopping of part of trees in order to gather as accurate measurement as possible. The analysis of measuring tree height using Leica DISTO 510 yield RMSE of ±2.55 m when was validated by tree height estimated by Airborne Lidar. The error was due to the fact that it was difficult to see and measure tree top because of slope and occlusion of the branches. The influence of slope and multi-layered canopies structure on the accuracy of measuring tree height was also observed by (Balenovi et at., 2015; Hollaus et al., 2007). Furthermore, Hunter et al. (2013) insisted that they

recognize five sources of uncertainty that contributed to the precision of field height measurements which were offset between measured distance and crown top position, tree-top occlusion, ground slope, obstacles for distance measurements, and clinometer error.

In this study, the percentage of field measured height variation explained by linear model was 62%, RMSE of ±2.55 m and RMSE% of 15.25. These results are relatively comparable with the results obtained by Sadadi (2016) who worked in the same study area who got the coefficient of determination of 0.61 and RMSE of ±4.2 m. Likewise, Priscilla (2016) who got the coefficient of determination of 0.59 and RMSE of ±3.4 m. The RMSE of ±2.55 m (15.25%) was slightly lower than the RMSE reported by (Priscilla, 2016) and Sadadi (2016). This might be attributed to fact that the Airborne LiDAR dataset was collected in year 2013 while the field measurement was collected in September and October 2016. The potential reduction of RMSE was due to the increment of the tree height attributed by the growth during time difference. This result is in contrary to the results of Hunter et al. (2013) which revealed that there was no significant difference (paired t-test p = 0.34) in mean height of field heights of emergent trees measured at Tapa-jos Km 67 site and Airborne LiDAR estimated tree with a one-year inter-sample period. Wallace et al. (2014) reported the R^2 of 0.84 and RMSE of 0.9 m. The RMSE is less than the error reported in this study because their study was done in the open forest unlike this study which took place in tropical rain forest.

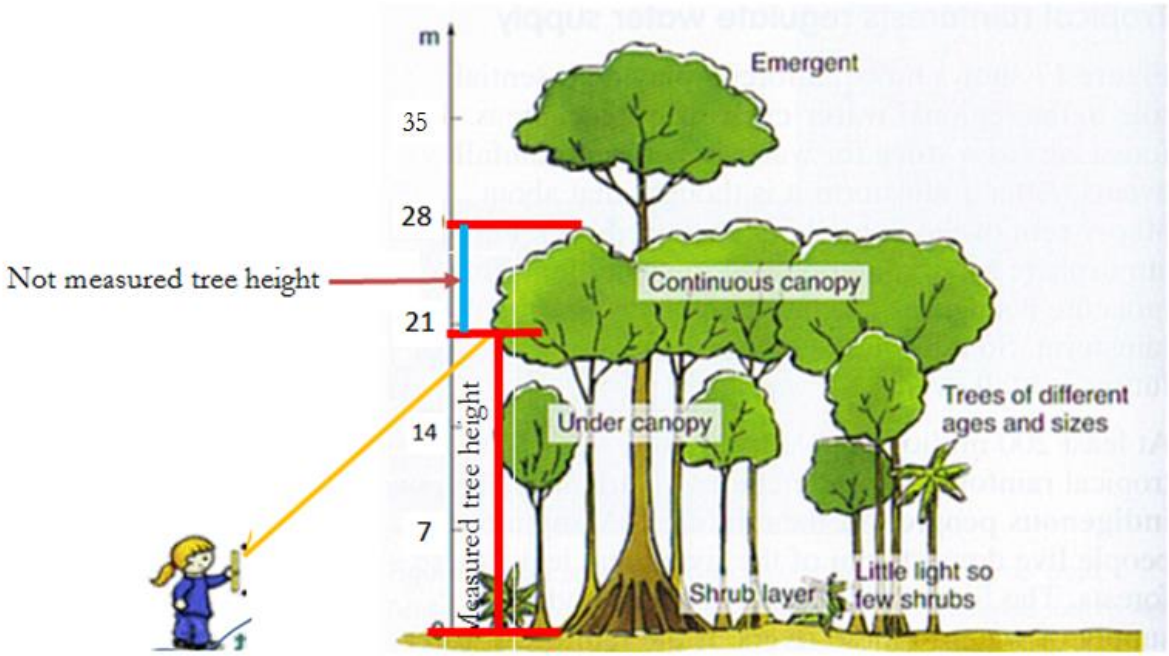
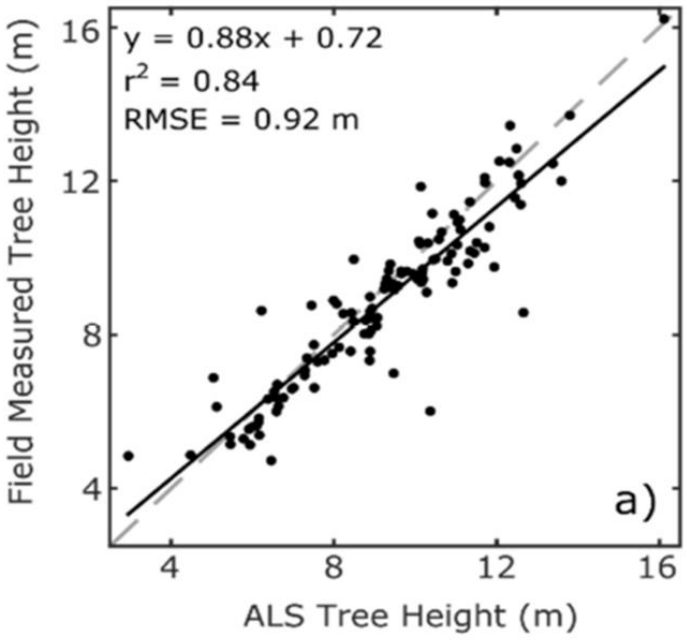


Figure 38: Effect of occlusion in tree height measurements
Source (modified): http://www.acegeography.com/eco---key-services.html

When ANOVA test (Appendix 7) was carried out, results revealed that there was variation in the mean of the tree height measurements derived from ALS, UAV and field. Furthermore, t-test (Appendix 13) revealed that at $p<0.05$ there was statistically significant difference between height of the tree derived from ALS and field measured tree height. Wallace et al. (2014) presented their results in which, R^2 was 0.84 and RMSE was 0.92 (Figure 39). The coefficient of determination (R^2) was higher than R^2 obtained in this study because their study was carried out in the open forest unlike our study which measurements

took place in the close tropical forest. They recorded RMSE of ±0.92, which is less than ±2.52 m obtained in our study.



Source: (Wallace et al., 2014)

Figure 39: Relationship between ALS and field tree height

5.3. UAV tree height estimation

In total, 388 trees were estimated by photogrammetry measurements. The mean tree height estimated was 17.78 with the standard deviation of ±3.7 m and trees height was ranging from 10.16 m to 35.7 m minimum and maximum respectively. Then, photogrammetry measured tree height was validated using ALS. Thus when UAV tree height was regressed with ALS derived tree height, R^2 of 0.78 was obtained. This indicated that the variation in tree height estimated by UAV was explained by ALS tree height by 78%. This implies that there was strong relationship between height derived from ALS and that of UAV.

The accuracy assessment of UAV tree height was evaluated by using tree height derived from ALS and the RMSE of ±1.7 m (RMSE=9.6%) was obtained. This study is comparable to the study conducted by Wallace et al. (2014) in Australia native forest stand in which in their study 112 trees out of 136 measured trees which had spatial detailed on the upper canopy where captured by UAV. The study revealed that when photogrammetry tree height was regressed against field measured tree height showed R^2 of 0.63 and RMSE was ±1.30 m (Figure 40). The small difference existed was attributed to the difference in the complexity of the forest.

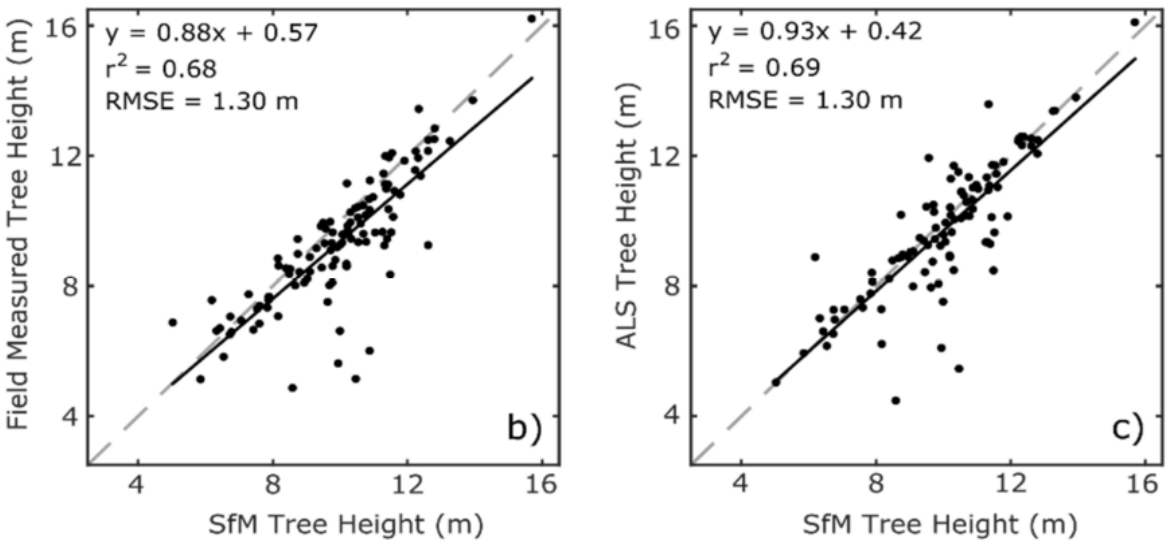


Figure 40: The relationship between SfM against field measured tree (left) and ALS tree height (right)
Source: (Wallace et al., 2014)

On the other hand this study was comparable to the study done in Maryland USA by Dandois & Ellis (2013) which stated that accuracy of field tree height and photogrammetry measured tree height had coefficient of determination ranging from 0.63 to 0.84 with 155 points/m² while in his study the point cloud density was ranging from 50 to 254 points/m².

This result is comparable with the results obtained by Lisein et al. (2014) done in a mix of uneven-aged broadleaved stands with a predominance of Oaks (*Quercus robur* and *Quercus petraea*) and some even-aged coniferous stands where tree height ranged from 10.5 to 29.4 m, with an average of 22.3 m. The error was attributed to the fact that point clouds of UAV could not penetrate to the ground. This result is comparable to the study done by Balenovi et al. (2015) in temperate forest where they reported that RMSE and RMSE % range from ±0.31 to ±5.27 m and 10 to 28.5% respectively for sub-compartment 16a, 17a, 17b, 18a, 18b, 20a, 20b, 20c. Likewise in the study done by Lisein et al. (2014) revealed that regression model performed quite well, it predicted individual trees height with an RMSE of 4.7% (±1.04 m, R² of 0.91) based on photo-CHM (Table 33), the RMSE was less than that obtained in this study because they studied temperate forest (more point clouds at the ground because forest was opened). Unlike this study which was done in tropical rain forest.

Table 33: Comparison of individual tree height models (n = 86) based on photo-CHM and LiDAR-CHM metrics.

CHM	R² Adjusted	RMSE [m]	RMSE %
Photo-CHM	0.91	1.04	4.7
LiDAR-CHM	0.94	0.83	3.7

Source: Lisein et al. (2014)

Additionally, in the study conducted by Zarco-Tejada et al. (2014) field height was regressed against UAV derived tree height and the coefficient of determination (R^2) was 0.86 and R^2 = 0.81 for study area 1 and 2 respectively, in that study the accuracy assessment was done using relative root mean square error and the calculated relative root mean square error was 10.8% and 13.3% for study 1 and 2 respectively. These results are comparable with RMSE% of 9.6 obtained in this study. On the other hand RMSE of ±1.5 m was reported in the study done by Jensen & Mathews (2016), the RMSE was comparable to this study.

Furthermore, when t-test (Appendix 8) was conducted at $p<0.05$ the results revealed that there was statistically significant difference between the height derived from the UAV and that of ALS.

5.4. Tree height derived from Airborne LiDAR

Tree height measured from Airborne LiDAR was derived from Airborne LiDAR CHM. The LiDAR CHM was generated when DTM was subtracted from DSM. Segmentation was undergone to delineate the crown of the trees, and then upper canopy trees were matched for comparison. The approach of comparing tree height which is visible by both Airborne LiDAR and field was also done by Hunter et al., (2013) where emergent trees were compared with Airborne LiDAR. Segmentation of LiDAR CHM was done in order to delineate the crown of the individual tree for matching of the trees. The D value of 0.27 (73%) was obtained. The 73% accuracy was accepted for delineation of the crown of the individual tree which was later used for matching with UAV and field recorded trees.

Airborne LiDAR estimated tree height was used to validate field measured tree height and UAV estimated tree height by plotting them in the scatter plot for validation. The variability in the field tree height was explained by airborne LiDAR by R^2 of 0.62 while the accuracy was assessed by RMSE of ± 2.55 m and RMSE% of 15.25 respectively. These results revealed that measured tree height was underestimated by 0.25 m on average. This result is comparable to study of Sadadi (2016) where he reported the coefficient of determination of 61% and RMSE and RMSE% of ± 4.2 m and 21.44% respectively. The t-test at ($p<0.05$) revealed that there was statistically significant difference between the height derived from Airborne LiDAR and tree height measured by Leica DISTO-510. However in the study done by Hyyppä et al. (2000) the coefficient of determination was higher ($R^2=0.969$) with RMSE of ±0.98 (Figure 42). The difference in the results might be attributed to the fact that their study was done in temperate forest where Laser point clouds hit the ground and therefore the DTM produced had higher accuracy. Additionally, R^2 of 0.78 and RMSE of 1.7 m were obtained when UAV derived height was validated by ALS estimated tree height.

5.5. Estimation of above ground biomass

The above ground biomass of the measured tree height, estimated tree height of UAV was computed and compared with that of Airborne LiDAR. The equation used to compute AGB was developed by Chave et al. (2014), the equation utilizes DBH, average wood density as suggested by Reyes et al. (1992) and tree height as input parameters. This is because of the fact that using the local equation of Yamakura et al. (1986) and Kenzo et al. (2009)which utilize only DBH as input in allometric equation to calculate AGB yield low value. Additionally Gibbs et al. (2007) suggested that the uses of local and regional allometric equations are not appropriate. However, the uses of generic equations is suitable because the development of trees were based on large number of trees (Gibbs et al., 2007; Chave et al., 2014). Extensive studies have been done to assess the accuracy of estimating tree height which provided superior results in forest (Wallace et al., 2014; Popescu, 2007).

In this study the accuracy assessment of the biomass of UAV and field measurements was done by using AGB computed from ALS. When AGB computed from UAV validated by AGB of ALS the results revealed that coefficient of determination ($R^2=0.99$), RMSE was 0.06 Mg and RMSE% was 13% (Appendix 14). The R^2 indicated that, 99% of AGB of UAV was explained by ALS. Also RMSE of 13% Mg showed average error of predicting AGB in UAV. On the other hand the validation of field biomass revealed that R^2, RMSE and RMSE% was 0.96, 107 Mg and 24% respectively. The coefficient of determination (R^2) indicated that 96% of variability in estimating of AGB of field was explained by ALS estimated AGB. The average error of modeling of AGB of the field was 24%. For the total of 388 matched trees, the total amount of biomass computed from ALS was 189.49 Mg, 177.13 Mg for UAV and

172.97 Mg for measured tree height. This result is comparable to the results of Sadadi (2016) which reported the AGB of ALS, TLS and field were 179.85 Mg, 170.86 Mg and 146.33 Mg respectively for 312 total trees. Furthermore t-test (Appendix 15 and 17) indicated that at $p<0.05$ there was no significant difference in biomass estimated by ALS and that of field and UAV.

5.6. Carbon stock estimation

The computation of carbon stock was based on the amount of biomass which was calculated. The carbon stock is approximated to 50% of the biomass in the tree. The mean carbon stock for tree derived from Airborne LiDAR was 0.229 Mg, 0.215 Mg for UAV and 0.209 for measured tree height. This implies that there was loss in carbon stock. This result is comparable to the study done by Sadadi, (2016) who reported 0.27 Mg , 0.26 Mg and 0.22 Mg for LiDAR, TLS and Field respectively. However, most of the study reported the carbon stock for the whole study area.

5.7. Sensitivity Analysis of tree height measured error to the biomass and carbon stock estimation

This subsection provides a discussion on the effect of differences of trees height measurements on the biomass and carbon stock estimation. The approaches employed in measurement of trees height (UAV and field) have its effect on accuracy of estimating biomass and carbon stock (Figure 41). The assessment of the effect of differences of trees height derived from Leica DISTO 510 and UAV was validated by Airborne LiDAR. The validation between tree height measured from the field and that of Airborne LiDAR revealed that the RMSE was ±2.55 m and RMSE% of 15.25 and R^2 of 0.62. Additionally, tree height which was measured by Airborne LiDAR was regressed against UAV estimated tree height. The results revealed that the R^2 of 0.78, RMSE of ±1.7 m and RMSE% of 9.63. The RMSE recorded by UAV was less than the one obtained by field because UAV were able to capture well the top of the tree unlike field measurements which tree peak was obscured by branches. Then the actual measurements of the tree height from ALS, UAV and field were used to compute biomass and carbon stock. The equation used include mean wood density Reyes et al. (1992), DBH and tree height (Chave et al., 2014).

Then, tree height was adjusted based on RMSE obtained when UAV and field tree height was validated by ALS measured tree height. When UAV estimated tree height was regressed by LiDAR derived trees height RMSE obtained was ±2.55 m, which was estimated to RMSE of ±3 m. Therefore measured field tree height was adjusted from -3 m to +3 m. This was conducted in order to assess its effect on biomass and carbon stock estimation. On the other hand, since the RMSE of ±1.7 m was obtained when UAV estimated tree height was regressed against ALS measured tree height. Therefore, tree height was adjusted by ±1.7 m for 30 selected trees. The results revealed that the differences in tree height affect the amount of biomass and carbon stock. The result of this study is comparable with the results of (Sadadi, 2016) where the RMSE of the measured tree height obtained was ±4.2 m while for TLS RMSE was ±1.5 m. The RMSE of the field measured tree height was higher than UAV estimated tree height because UAV had capability to see the trees at the top which enhance trees height measurements. Unlike in the field measurement where occlusion was possible due to intermingling of canopy of the trees and visibility impaired of the trees top in tropical rain forest. Furthermore, the results revealed that AGB was sensitive to the change in tree height, since when tree height was adjusted, AGB was underestimated or overestimated from the original AGB. This indicated how AGB was influenced by the change in tree height.

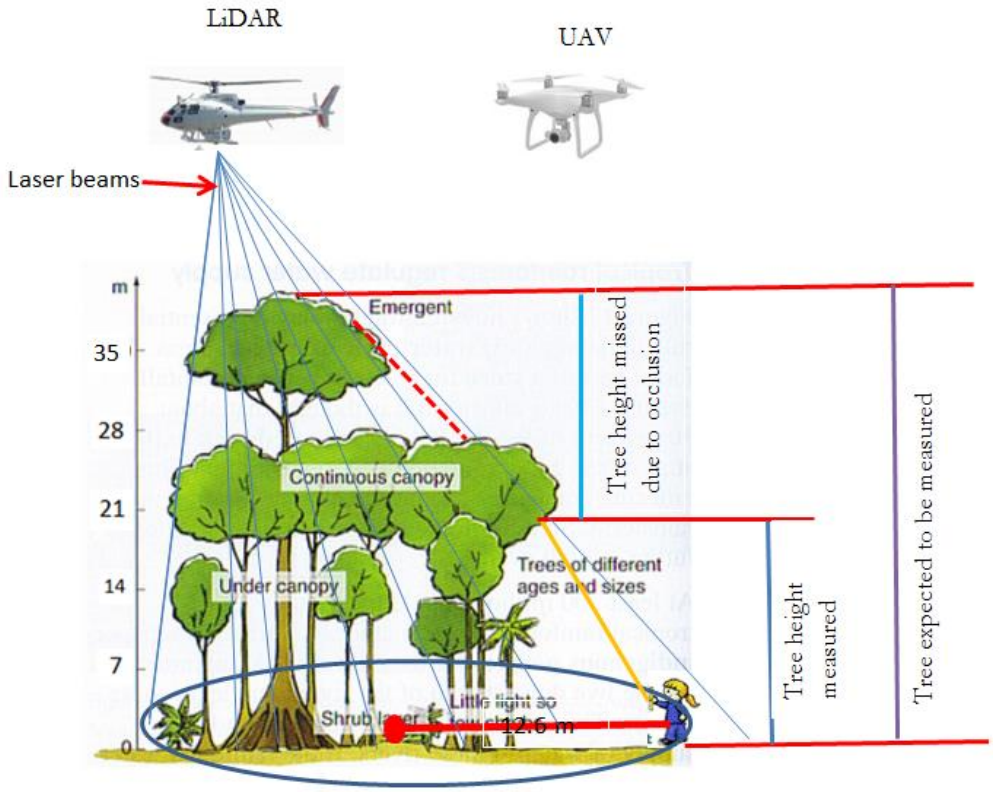


Figure 41: LiDAR, UAV and field measurements

Source (modified): http://www.acegeography.com/eco---key-services.html

5.8. Limitation of the study

- Ayare Hitam Forest Reserve is the tropical rain forest which is intact, the areas for placing mark for GCP was very challenging. Only few spot were available for putting the mark. Chopping of some part of the forest was necessary in order to place the mark for GCP.

- Navigating in the forest was challenging, regardless the fact that locust map was used. Therefore, indigenous knowledge was important for identifying routes towards potential areas for data collection.

- Data processing consumed time, generation of point clouds which was essential for the ortho-mosaic image. DSM and DTM generation needed knowledge and skill on photogrammetry.

- Flying UAV requires understanding of aviation regulation.

6. CONCLUSION AND RECOMMENDATION

6.1. Conclusion

The Photogrammetry image matching algorithms were able to generate DTM from UAV dataset which was used in developing CHM for tree height estimation. Initially, the generated photogrammetry and ALS DTM were assessed by comparing with the altitude (z) recorded by differential GPS. The assessment of the UAV DTM was important since it effects the estimation of tree height and consequently biomass and carbon stock. The assessment of the UAV DTM using GCP recorded by GPS revealed the RMSE of ±3.84 m (7.76%, R^2 0.96) while RMSE of Airborne LiDAR DTM was ±1.25 m (2.75%, R^2 = 0.99). The results showed that the UAVgenerated DTM was less accurate by (RMSE of ±2.59 m) compared to ALS generated DTM. When UAV DTM was later validated by using ALS DTM height at each flight the results indicated that RMSE for all flights range from ±2.53 m to ±6.32 m, with RMSE% range from 6.6 to 13.09 and R^2 range from 0.14 to 0.97.

Additionally, when accuracy of UAV DTM was assessed in the areas where it had small different in height with DTM of ALS (RMSE of ±0.19 m 0.53%) and r of 0.99 and R^2 of 0.99, in this area it was revealed that RMSE of estimating tree height in UAV DTM showed 1.56 m (8.7%) with r of 0.89 and R^2 of 0.80. This result is different compared to RMSE of ±1.7 m and RMSE 9.63%, R^2 of 0.78 which was obtained in the accuracy assessment of the tree height estimated from UAV when validated by ALS in the entire study area of this research. The increase in error in the UAV DTM was attributed to the fact that its point clouds could not manage to hit the ground due to the closeness of the forest, availability of understory vegetation and error during the reconstruction and calibration of consumer grade GPS. In contrast, ALS point clouds were able to penetrate in the forest and provide information about the terrain of the forest and hence its DTM was more accurate than that of the UAV.

The results obtained (RMSE = 1.7 m , R^2 = 0.78) which are promising to advice forest managers to potentially consider utilization of photogrammetry DTM to derived tree height and consequently use it for the assessment of biomass and carbon stock since the cost of using UAV and the data collection is substantially lower than using ALS for data collection. The following are the answers to the research questions of this study:

What is the accuracy of DTM derived from 3D photogrammetric point clouds of UAV in comparison to DTM of LiDAR?
When the photogrammetry and ALS DTM was assessed by using GCP recorded by differential GPS, it was revealed that the accuracy of ALS DTM was 97.25% (R^2=0.99, RMSE=±1.25 m, RMSE%= 2.) while the accuracy of photogrammetry DTM was 92.25% (R^2=0.96, RMSE=±3.84 m, RMSE%=7.96). The accuracy of the photogrammetry DTM was less than ALS because of the error generated due by consumer grade GPS mounted in the UAV. Then, when ALS DTM generated height was used to assess the accuracy of photogrammetry DTM the accuracy dropped to 91.3% in the area where DTM of ALS was close in height compared to the DTM generated by UAV images. Furthermore, the assessment was done by comparing the tree height in the area where ALS and UAV DTM had small differences. The results revealed that tree height was estimated by accuracy of 99.47% (RMSE=±1.56 m, RMSE%=8.7 and R^2=0.80). The t-test revealed that there was no statistically significant difference between the DTM of ALS and that of UAV and therefore the null hypoesthesia was accepted and alternative hypoesthesia was rejected.

What is the difference in the accuracy of tree height estimated from UAV and field data in reference to the Airborne LiDAR?

In this study, since ALS were able to generate CHM which is more accurate than photogrammetry DTM of UAV, which was attributed to the capacity of the pulses of ALS to penetrate down to the ground. Thus the tree height estimated from UAV data and field measured tree were regressed with ALS derived tree height for validation and accuracy assessment. When tree height derived from photogrammetry matching of UAV was regressed against ALS measured tree height the coefficient of determination (R^2) obtained was 0.78 and tree height derived was accurate by 90.37% (RMSE = ±1.7 m, RMSE%= 9.63), this implies that 90.37% of the tree height derived from UAV data was accurately estimated.

On the other hand when tree height measured by ALS was used to validate tree height measured from the field it was revealed that the accuracy was decreased to 84.75% (RMSE = ±2.55 m, RMSE% = 14.15) this was contributed to the fact that Leica DISTO 510 was underestimating tree height by the average of 2.55 m because of occlusion which hindered the observer to measure tree height. In both cases, the ANOVA revealed that there was variation in the means of tree height derived from the CHM of ALS, UAV and measured tree height. Following up the ANOVA test the t-test found that there was a significant difference in the means of the tree height derived from ALS, UAV and measured trees from field. Therefore, in both cases, null hypothesis was rejected and the alternative hypothesis was accepted.

What is the difference in amount of biomass from sampled trees which derived from estimation height and DBH parameter of field measurements and UAV in comparison to that of Airborne LiDAR?

The results revealed that the amount of AGB estimated by the ALS was 189.49 Mg of AGB derived from Airborne LiDAR. On the other hand, the AGB of estimated UAV total matched sampled trees were 177.13 Mg for UAV while the AGB which was estimated by field was 172.97 Mg. This implies that UAV and field approaches underestimated biomass and carbon stock. Furthermore t-test revealed that there was no significant difference in the means of the AGB and carbon stock derived from ALS, UAV and field measured trees. Therefore, in both cases, null hypothesis was accepted and the alternative hypothesis was rejected.

How biomass and carbon stocks are affected by differences in tree height measurements derived from photogrammetry image matching of UAV and field methods.

Since three approaches were used to estimate biomass and carbon stock, ALS approach was considered to be more accurate in estimating AGB because it was able to see the trees at the top and had accurate DTM. Tree height estimated by photogrammetry image matching point clouds and tree height measured from the field were adjusted based on RMSE obtained when validated by ALS derived height. The results revealed that biomass was sensitive to the differences in tree height measurements.

6.2. Recommendation

More GCP should be taken in each flight, the minimum of eight coordinates points should be taken per flight, then minimum of four coordinates should be used as a GCP while the remaining coordinate points should be used as a checkpoint, this is important in assessing the accuracy of the data.

The UAV photos acquired in the flight area should be tested immediately after removed in the USB device to test whether they have maximum overlap base on the parameters set during data acquisition. This is important for ensuring data quality.

Further study should involve collecting more samples using DGPS in order to assess more the effect of tree measured height from the field and estimated tree height derived from the photogrammetry image matching of point clouds on biomass and carbon stock estimation.

Since the point clouds of UAV cannot penetrate to the ground, especially in the close forest, further study can be done by integrating DSM of UAV and DTM of ALS to estimate AGB and carbon stock.

More study should be done on modeling of CHM of UAV to derive DBH consequently biomass and carbon stock.

LIST OF REFERENCES

Alder, D., & Synnott, T. J. (1992). *Permanent sample technique for mixed tropical forest*. London, England: Oxford Forestry Institute, University of Oxford.

Andersen, H., Reutebuch, S. E., & Mcgaughey, R. J. (2006). A rigorous assessment of tree height measurements obtained using airborne lidar and conventional field methods. *Canadian Journal of Remote Sensing*, *32*(5), 355–366. http://doi.org/10.5589/m06-030

Angelsen, A. (2009). *Realising REDD+:National strategy and policy options*. (M. Brockhaus, M. Kanninen, E. Sills, & W. D. Sunderlin, Eds.). Bogor, Indonesia: CIFOR.

Asmare, M. F. (2013). *Airborne LiDAR data and VHR worldview satellite imagery to support community based forest certification in Chitwan , Airborne LiDAR data and VHR worldview satellite imagery to support community based forest certification in Chitwan , Nepal*. Unpublished MSc theses, Univerisity of Twente Faculty of Geo_Information and Earth Observation(ITC), Enschede, Netherlands. Retrieved from https://www.itc.nl/library/papers_2013/msc/nrm/asmare.pdf

Balenovi, I., Seletkovi, A., Pernar, R., & Jazbec, A. (2015). Estimation of the mean tree height of forest stands by photogrammetric measurement using digital aerial images of high spatial resolution. *Annals of forest Research*, *58*(1), 125–143. http://doi.org/10.15287/afr.2015.300

Baltsavias, E. P. (1999). A comparison between photogrammetry and laser scanning. *ISPRS Journal of Photogrammetry & Remote Sensing*, *54*, 83–94. Retrieved from http://www.sciencedirect.com/science/article/pii/S0924271699000143

Bellard, C., Bertelsmeier, C., Leadley, P., Thuiller, W., & Courchamp, F. (2012). Impacts of climate change on the future of biodiversity. *Ecology Letter*, *15*, 365–377. http://doi.org/10.1111/j.1461-0248.2011.01736.x

Bonan, G. B. (2008). Forests and Climate Change : Climate Benefits of Forests. *Science*, *320*, 1444–1450. http://doi.org/0.1126/science.1155121

Brown, S. (2002). Measuring carbon in forests : current status and future challenges. *Environmental Pollution*, *116*, 363–372. Retrieved from http://www.sciencedirect.com/science/article/pii/S0269749101002123

Chave, J. (2005). *Measuring tree height for tropical forest trees:A field manual*. Toulouse, France. Retrieved from http://www.afritron.net/upload/en/manuals/TreeHeight_english[1].pdf

Chave, J., Rejo-Mechain, M., Burquez, A., Chidumayo, E., Colgan, M. S., Delitti, W. B. C., … Vieilledent, G. (2014). Improved allometric models to estimate the aboveground biomass of tropical trees. *Global Change Biology*, *20*, 3177–3190. http://doi.org/10.1111/gcb.12629

Chhetri, D. B. K., & Fowler, G. W. (1996). Prediction models for estimating total heights of trees from diameter at breast height measurements in Nepal ' s lower temperate broad-leaved forests. *Forest Ecology and Management*, *84*(1-3), 177–186. http://doi.org/10.1016/0378-1127(96)03726-7

Clinton, N., Holt, A., Scarborough, J., Yan, L., & Gong, P. (2014). Accuracy Assessment Measures for Object- based Image Segmentation Goodness Accuracy Assessment Measures for Object-based

Image Segmentation Goodness. *Photogrammetric Engineering and Remote Sensing*, (November). http://doi.org/10.14358/PERS.76.3.289

Colomina, I., & Molina, P. (2014a). ISPRS Journal of Photogrammetry and Remote Sensing Unmanned aerial systems for photogrammetry and remote sensing : A review. *ISPRS Journal of Photogrammetry and Remote Sensing*, *92*, 79–97. http://doi.org/10.1016/j.isprsjprs.2014.02.013

Colomina, I., & Molina, P. (2014b). Unmanned aerial systems for photogrammetry and remote sensing : A review. *ISPRS Journal of Photogrammetry and Remote Sensing*, *92*, 79–97. http://doi.org/10.1016/j.isprsjprs.2014.02.013

Dandois, J. P., & Ellis, E. C. (2013). Remote Sensing of Environment High spatial resolution three-dimensional mapping of vegetation spectral dynamics using computer vision. *Remote Sensing of Environment*, *136*, 259–276. http://doi.org/10.1016/j.rse.2013.04.005

Dassot, M., Constant, T., & Fournier, M. (2011). The use of terrestrial LiDAR technology in forest science : application fields , benefits and challenges. *Annals of Forest Science*, *68*, 959–974. http://doi.org/10.1007/s13595-011-0102-2

Davis, C. S. (2002). *Statistical Methods for the Analysis of Repeated Measurements*. (G. Casella, S. Fienberg, & I. Olkin, Eds.). New York: Springer-Verlag New York, Inc.

Debella-Gilo, M. (2016). Bare-earth extraction and dtm generation from photogrammetric point clouds with a partial use of an existing. *The International Archives of the Photogrammetry, Remote Sensing and Spatial Information Sciences*, *XLI-B3*, 201–206. http://doi.org/10.5194/isprsarchives-XLI-B3-201-2016

Evans, J. S., Hudak, A. T., Faux, R., & Smith, A. M. S. (2009). Discrete Return Lidar in Natural Resources : Recommendations for Project Planning , Data Processing , and Deliverables. *Remote Sensing*, *1*(4), 776–794. http://doi.org/10.3390/rs1040776

Fritz, A., Kattenborn, T., & Koch, B. (2013). UAV-based photogrammetric point clouds - tree stem mapping in open stands in comparison to terrestrial laser scanner point clouds. *International Archives of the Photogrammetry, Remote Sensing and Spatial Information Sciences*, *XL-1/W2, 2*, 4–6. Retrieved from https://pdfs.semanticscholar.org/86ae/6b335ab8134506234d9ebd2c9f37736fd84b.pdf

Gerke, M., & Przybilla, H. (2016). Accuracy Analysis of Photogrammetric UAV Image Blocks : Influence of Onboard RTK-GNSS and Cross Flight Patterns. *Photogrammetrie - Fernerkundung - Geoinformation*, (March). http://doi.org/10.1127/pfg/2016/0284

Getzin, S., Wiegand, K., & Schoning, I. (2012). Assessing biodiversity in forests using very highresolution images and unmanned aerial vehicles. *Methods in Ecology and Evolution*, *3*(2). http://doi.org/10.1111/j.2041-210X.2011.00158.x

Gibbs, H. K., Brown, S., Niles, J. O., & Foley, J. A. (2007). Monitoring and estimating tropical forest carbon stocks : making REDD a reality. *Environmental Research Letters*, *2*(045023), 13. http://doi.org/10.1088/1748-9326/2/4/045023

Gobakken, T., & Naesset, E. (2008). Assessing effects of laser point density, ground sampling intensity, and field sample plot size on biophysical stand properties derived from airborne laser scanner data. *Research, Canadian Journal of Forest*, *38*(5), 1095 – 1109. http://doi.org/10.1139/X07-219

Hanum, F. (1999). Plant Diversity and Conservation Value of Ayer Hitam Forest, Selangor, Peninsular

Malaysia. *Pertanika Journal Of Tropical Agriculture Science*, *22*(2), 73–83. Retrieved from http://psasir.upm.edu.my/3795/1/Plant_Diversity_and_Conservation_Value_of_Ayer_Hitam_Forest,.pdf

Hasmadi, M., Amirin, K., & Hidayah, S. N. (2008). Estimated DEM uncertainty in creating a 3-D of the UPM ' s Ayer Hitam Forest reserve in Selangor , Malaysia. *Malaysian Journal of Society and Space*, *4*, 45–53. Retrieved from http://www.ukm.edu.my/geografia/images/upload/5.2008-hasmadi-english-2.pdf

Henry, M., Picard, N., Trotta, C., Manlay, R. J., Valentini, R., Bernoux, M., & Saint-andré, L. (2011). Estimating Tree Biomass of Sub-Saharan African Forests : a Review of Available Allometric Equations. *Silva fennica*, *45*(3B), 477–569. http://doi.org/10.14214/sf.38

Herold, M., & Schiller, F. (2009). *An assessment of national forest monitoring capabilities in tropical non-Annex I countries : Recommendations for capacity building*. Retrieved from http://bioclimate.net/images/pdf/external/technical/Forest Monitoring National Capacity Needs Assessment 2009.pdf

Hollaus, M., Wagner, W., Maier, B., & Schadauer, K. (2007). Airborne Laser Scanning of Forest Stem Volume in a Mountainous Environment. *Sensors*, *7*(8), 1559 – 1577. http://doi.org/10.3390/s7081559

Holmgren, J., Nilsson, M., & Olsson, H. (2003). Simulating the effects of lidar scanning angle for estimation of mean tree height and canopy closure. *Remote Sensing*, *29*(5), 623–632. http://doi.org/http://dx.doi.org/10.5589/m03-030

Houghton, R. A. (2005). Aboveground Forest Biomass and the Global Carbon Balance. *Global Change Biology*, 945–958. http://doi.org/10.1111/j.1365-2486.2005.00955.x

Hunter, M. O., Keller, M., Victoria, D., & Morton, D. C. (2013). Tree height and tropical forest biomass estimation. *Biogeosciences*, *10*, 8385–8399. http://doi.org/10.5194/bg-10-8385-2013

Hyyppä, J., Hyyppä, H., Leckie, D., Gougeon, F., Yu, X., Maltamo, M., … Maltamo, M. (2016). Review of methods of small - footprint airborne laser scanning for extracting forest inventory data in boreal forests. *International Journal of Remote Sensing ISSN:*, *29*(5), 1366–5901. http://doi.org/10.1080/01431160701736489

Hyyppä, J., Pyysalo, U., Hyyppä, H., & Samberg, A. (2000). Elevation accuracy of laser scanning-derived digital terrain and target models in forest environment. In *EARSeL-SIG-Workshop LiDAR* (pp. 139–147).

IPCC. (2014). *Climate Change: Impacts , Adaptation , and Vulnerability. Part B : Regional Aspects. Working Group II Contribution to the Fifth Assessment Report of the Intergovernmental Panel on Climate Change*. (B. V. R, F. C. B, D. D. J, M. M. D, M. K. J, E. T. Bilir, … W. L.L., Eds.). .)]. Cambridge University Press, Cambridge, United Kingdom and New York, NY, USA.

Jaime Paneque-Gálvez, McCall, M. K., Napoletan, B. M., Wich, S. A., & Koh, L. P. (2014). Small Drones for Community-Based Forest Monitoring: An Assessment of Their Feasibility and Potential in Tropical Areas. *Forests*, *5*, 1481–1507. http://doi.org/10.3390/f5061481

Jensen, J. L. R., & Mathews, A. J. (2016). Assessment of Image-Based Point Cloud Products to Generate a Bare Earth Surface and Estimate Canopy Heights in a Woodland Ecosystem. *Remote Sensing*, *50*(8).

http://doi.org/10.3390/rs8010050

José, A., Lima, N., Suwa, R., Henrique, G., Mello, P. De, Castro, P., … Higuchi, N. (2012). Allometric models for estimating above- and below-ground biomass in Amazonian forests at São Gabriel da Cachoeira in the upper Rio Negro , Brazil. *Forest Ecology and Management*, *277*, 163–172. http://doi.org/10.1016/j.foreco.2012.04.028

Kattenborn, T., Sperlich, M., Bataua, K., & Koch, B. (2014). Automatic single palm tree detection in plantations using uav-based photogrammetric point clouds. *The International Archives of the Photogrammetry, Remote Sensing and Spatial Information Sciences*, *XL-3*, 139–144. http://doi.org/10.5194/isprsarchives-XL-3-139-2014

Kenzo, T., Furutani, R., Hattori, D., Kendawang, J. J., Tanaka, S., Sakurai, K., & Ninomiya, I. (2009). Allometric equations for accurate estimation of above-ground biomass in logged-over tropical rainforests in Sarawak , Malaysia. *Journal of Forest Research*, *14*, 365–372. http://doi.org/10.1007/s10310-009-0149-1

Kenzo, T., Ichie, T., Hattori, D., Itioka, T., Handa, C., Ohkubo, T., … Ninomiya, I. (2009). Development of allometric relationships for accurate estimation of above- and below-ground biomass in tropical secondary forests in Sarawak , Malaysia. *Journal of Tropical Ecology*, *25*, 371–386. http://doi.org/10.1017/S0266467409006129

Koch, B., Heyder, U., & Weinacker, H. (2006). Detection of Individual Tree Crowns in Airborne Lidar Data. *Photogrammetric Engineering & Remote Sensing*, *72*(4), 357–363. http://doi.org/0099-1112/06/7204–0357

Kumar, V. (2012). *Forestry inventory parameters and carbon mapping from Airborne LiDAR*. Unpublished MSc theses, Univerisity of Twente Faculty of Geo_Information and Earth Observation(ITC), Enschede, Netherlands. Retrieved from http://www.itc.nl/library/papers_2012/msc/nrm/vinodkumar.pdf

Lane, D. R., Ready, R. C., Buddemeier, R. W., Martinich, J. A., Shouse, K. C., & Wobus, C. W. (2013). Quantifying and Valuing Potential Climate Change Impacts on Coral Reefs in the United States : Comparison of Two Scenarios. *PLoS One 8, 1–13*, *8*(12). http://doi.org/10.1371/journal.pone.0082579

Larjavaara, M., & Muller-landau, H. C. (2013). Measuring tree height : a quantitative comparison of two common field methods in a moist tropical forest. *Methods inEcology andEvolution*, *4*, 793–801. http://doi.org/10.1111/2041-210X.12071

Leeuwen, M. Van, & Nieuwenhuis, M. (2010). Retrieval of forest structural parameters using LiDAR remote sensing. *Eur J Forest Res*, *129*, 749–770. http://doi.org/10.1007/s10342-010-0381-4

Lindquist, E. J., D'Annunzio, R., Gerrand, A., MacDicken, K., Achard, F., Beuchle, R., … Stibig, H.-J. (2012). *Global forest land-use change 1990–2005* (No. 169). Rome. Retrieved from http://www.fao.org/docrep/017/i3110e/i3110e.pdf

Lisein, J., Pierrot-Deseilligny, M., Bonnet, S., & Lejeune, P. (2014). A Photogrammetric Workflow for the Creation of a Forest Canopy Height Model from Small Unmanned Aerial System Imagery. *Forests*, *4*, 922–944. http://doi.org/10.3390/f4040922

Masek, J. G., Hayes, D. J., Hughes, M. J., Healey, S. P., & Turner, D. P. (2015). Forest Ecology and Management The role of remote sensing in process-scaling studies of managed forest ecosystems q.

Forest Ecology and Management, *355*, 109–123. http://doi.org/10.1016/j.foreco.2015.05.032

Mayr, W. (2011). UAV-MAPPING – A user report. *International Archives of the Photogrammetry, Remote Sensing and Spatial Information Sciences*, *XXXVIII-1/*, 14–16. Retrieved from http://www.int-arch-photogramm-remote-sens-spatial-inf-sci.net/XXXVIII-1-C22/277/2011/isprsarchives-XXXVIII-1-C22-277-2011.pdf

Moberg, F., & Folke, C. (1999). Ecological goods and services of coral reef ecosystems. *Ecological Economics*, *29*(2), 215–233. http://doi.org/10.1016/S0921-8009(99)00009-9

Molto, Q., Rossi, V., & Blanc, L. (2013). Error propagation in biomass estimation in tropical forests. *Methods in Ecology and Evolution*, *4*, 175–183. http://doi.org/10.1111/j.2041-210x.2012.00266.x

Mugasha, W. A., Bollandsås, O. M., & Eid, T. (2016). Relationships between diameter and height of trees in natural tropical forest in Tanzania. *Southern Forests: A Journal of Forest Science ISSN:*, *2620*(May). http://doi.org/10.2989/20702620.2013.824672

Nabuurs, G. J., Putten, B. Van, Knippers, T. S., & Mohren, G. M. J. (2008). Forest Ecology and Management Comparison of uncertainties in carbon sequestration estimates for a tropical and a temperate forest. *Forest Ecology and Management*, *256*, 237–245. http://doi.org/10.1016/j.foreco.2008.04.010

Nations, U. (1998). *Kyoto protocol to the united nations framework convention on climate change*.

Naumann, M., Geist, M., Bill, R., Niemeyer, F., & Detection, C. (2013). Accuracy comparison of digital surface models created by unmanned aerial systems imagery and terrestrial. *International Archives of the Photogrammetry, Remote Sensing and Spatial Information Sciences*, *XL-1/W2*(September), 4–6. Retrieved from http://www.int-arch-photogramm-remote-sens-spatial-inf-sci.net/XL-1-W2/281/2013/isprsarchives-XL-1-W2-281-2013.pdf

Nocerino, E., Menna, F., Remondino, F., & Saleri, R. (2013). Accuracy and block deformation analysis in automatic uav and terrestrial photogrammetry - lesson learnt -. *ISPRS Annals of the Photogrammetry, Remote Sensing and Spatial Information Sciences*, *II-5/W1*(September), 2–6. Retrieved from http://s3.amazonaws.com/academia.edu.documents/34331571/isprsannals-II-5-W1-203-2013.pdf?AWSAccessKeyId=AKIAIWOWYYGZ2Y53UL3A&Expires=1486977309&Signature=uSpgX3VStc06laKy63JAswWPY1c=&response-content-disposition=inline; filename=Accuracy_and_block_deformation_analysis.pdf

Nurul-Shida, Faridah-Hanum, Wan-Razali, & Kamziah. (2014). Community structure of trees in ayer hitam forest researve, puchong, selangor, malaysia. *the malaysian forester*, *77*((1)), 73–86. Retrieved from https://www.researchgate.net/profile/Nurul_Shida_Saari/publication/270106458_Community_structure_of_trees_in_Ayer_Hitam_Forest_Reserve_Puchong_Selangor_Malaysia/links/54a0f2690cf256bf8bae1ecf.pdf

Popescu, S. C. (2007). Estimating biomass of individual pine trees using airborne lidar. *Biomass and Bioenergy*, *31*, 646–655. http://doi.org/10.1016/j.biombioe.2007.06.022

Priscilla, M. T. (2016). *Assessment of above ground biomass with terrestrial lidar using 3D quantitative structure modelling in tropical rain forest of Ayer hitam forest reserve, Malaysia.* Unpublished MSc theses, Univerisity of Twente Faculty of Geo_Information and Earth Observation(ITC), Enschede, Netherlands. Retrieved from http://www.itc.nl/library/papers_2016/msc/nrm/madhibha.pdf

Rahman, M. Z. A., Majid, Z., Bakar, M. A. A., Rasib, A. W., & Kadir, W. H. W. (2015). Individual Tree Measurement in Tropical Environment using Terrestrial Laser Scanning. *Jurnal Teknologi (Science and Engineering)*, *5*, 127–133. Retrieved from www.jurnalteknologi.utm.my

Reutebuch, S. E., Mcgaughey, R. J., Andersen, H., & Carson, W. W. (2003). Accuracy of a high-resolution lidar terrain model under a conifer forest canopy. *Journal of Remote Sensing*, *29*(5), 527–535. http://doi.org/10.5589/m03-022

Reyes, G., Brown, S., Chapman, J., & Lugo, A. E. (1992). Wood Densities of Tropical Trees Species. *Gen. Tech. Rep. SO-89 New Orleans, LA: U.S. Department of Agriculture, Forest Service, Southern Forest Experiment Station*, 15p. Retrieved from https://www.srs.fs.usda.gov/pubs/gtr/gtr_so088.pdf

Ritchie, J. C. (2016). Remote sensing applications to hydrology : airborne laser altimeters Remote sensing applications to hydrology : airborne laser altimeters. *Hydrological Sciences Journal*, *41*(4), 625–636. http://doi.org/10.1080/02626669609491529

Rosnell, T., & Honkavaara, E. (2014). Point Cloud Generation from Aerial Image Data Acquired by a Quadrocopter Type Micro Unmanned Aerial Vehicle and a Digital Still Camera. *Sensors*, 460. http://doi.org/10.3390/s120100453

Ruiz, L. A., Hermosilla, T., Mauro, F., & Godino, M. (2014). Analysis of the Influence of Plot Size and LiDAR Density on Forest Structure Attribute Estimates. *Forests*, *5*, 936–951. http://doi.org/10.3390/f5050936

Sabogal, C., Guariguata, M. R., Broadhead, J., Lescuyer, G., Savilaakso, S., Essoungou, J. N., … Sist. (2013). *Multiple-use forest management in the humid tropics: opportunities and challenges for sustainable forest management.* (No. 173). Rome: Center for International Forestry Research.

Sadadi, O. (2016). *Accuracy of measuring tree height using airborne lidar and terrestrial laser scanner and its effect on estimating forest biomass and carbon stock in Ayer Hitam tropical rain forest reserve , Malaysia*. Unpublished MSc theses, Univerisity of Twente Faculty of Geo_Information and Earth Observation(ITC), Enschede, Netherlands. Retrieved from http://www.itc.nl/library/papers_2016/msc/nrm/ojoatre.pdf

Seul, L. Y., Hien, L. P., Soo, P. J., Hee, L. M., Wook, P. M., & Jee-In, K. (2015). Calculation of Tree Height and Canopy Crown from Drone Images Using Segmentation. *Journal of the Korean Society of Surveying, Geodesy, Photogrammetry and Cartography*, *33*(6), 605–613. http://doi.org/http://dx.doi.org/10.7848/ksgpc.2015.33.6.605

Shapiro, A. S. S., & Wilk, M. B. (1965). An analysis of variance test for normality (complete samples). *Oxford Journals*, *52*(3/4), 591–611. Retrieved from http://www.jstor.org/stable/2333709

Sicking, L. P. (1998). Rangefinder comparison. Retrieved September 8, 2016, from http://www.fs.fed.us/eng/pubs/html/98241307/98241307.html

Solomon, D. S., & Nolet, R. J. (1968). *Reliability of tree-height measurements in northern hardwood stands*. New Hampshire. Retrieved from http://www.nrs.fs.fed.us/pubs/rn/rn_ne86.pdf

Talbot, J., Lewis, S. L., Lopez-gonzalez, G., Brienen, R. J. W., Monteagudo, A., Baker, T. R., … Phillips, O. L. (2014). Forest Ecology and Management Methods to estimate aboveground wood productivity from long-term forest inventory plots. *Forest Ecology and Management*, *320*, 30–38. http://doi.org/10.1016/j.foreco.2014.02.021

Torres-sánchez, J., López-granados, F., Serrano, N., & Arquero, O. (2015). High-Throughput 3-D Monitoring of Agricultural-Tree Plantations with Unmanned Aerial Vehicle (UAV) Technology. *RESEARCH ARTICLE*, 1–20. http://doi.org/10.1371/journal.pone.0130479

Verhoeven, G. (2011). Software Review Taking Computer Vision Aloft ^ Archaeological Three-dimensional Reconstructions from Aerial Photographs with PhotoScan. *Archaeological Prospection*, *73*(January), 67–73. http://doi.org/10.1002/arp

Wallace, L., Lucieer, A., Malenovsky, Z., Turner, D., & Vopenka, P. (2014). Assessment of Forest Structure Using Two UAV Techniques : A Comparison of Airborne Laser Scanning and Structure from Motion (SfM) Point Clouds. *Forests*, 460. http://doi.org/10.3390/f7030062

Wang, C., Menenti, M., Stoll, M., Feola, A., Belluco, E., & Marani, M. (2009). Separation of Ground and Low Vegetation Signatures in LiDAR Measurements of Salt-Marsh Environments. *IEEE Transactions on geoscience and Remote Sensing*, *47*(7), 2014–2023. http://doi.org/10.1109/TGRS.2008.2010490

White, J. C., Wulder, M. A., Vastaranta, M., Coops, N. C., Pitt, D., & Woods, M. (2013). The Utility of Image-Based Point Clouds for Forest Inventory: A Comparison with Airborne Laser Scanning. *Forests*, *4*, 518–536. http://doi.org/10.3390/f4030518

Williams, M. S., Bechtold, W. A., & LaBau, V. J. (1994). Five Instruments for Measuring Tree Height: An Evaluation. *Southern Journal of Applied Forestry*, *18*(2), 76–82(7). Retrieved from http://www.ingentaconnect.com/content/saf/sjaf/1994/00000018/00000002/art00008

Winjum, J. K., Dixon, R. K., & Schroeder, P. E. (1992). *Estimating the Global Potential of Forest and Agroforest Management Practices to Sequester Carbon*. (A. E. Joe Wisniewski, Lugo, Ed.). Corvallis: Kluwer Academic. Retrieved from http://link.springer.com/chapter/10.1007/978-94-011-2793-6_12

Yamakura, T., Hagihara, A., Sukardjo, S., & Ogawa, H. (1986). Aboveground biomass of tropical rain forest stands in Indonesian Borneo. *Vegetion*, 71–82. http://doi.org/10.1007/BF00045057

Yang, X., & Li, J. (2012). *Advances in Mapping from Remote Sensor Imagery: Techniques and Applications*. (1st Ed, Ed.). CRC Press. Retrieved from http://www.asprs.org/a/publications/pers/2014journals/PERS_December_2014/HTML/files/assets/common/downloads/page0021.pdf

Zarco-Tejada, P. J., Diaz-varela, R., Angileri, V., & Loudjani, P. (2014). Tree height quantification using very high resolution imagery acquired from an unmanned aerial vehicle (UAV) and automatic 3D photo-reconstruction methods. *European Journal of Agronomy*, *55*, 89–99. http://doi.org/10.1016/j.eja.2014.01.004

Zawawi, A. A., Shiba, M., Janatun, N., & Jemali, N. (2015). Accuracy of LiDAR-based tree height estimation and crown recognition in a subtropical evergreen broad-leaved forest in Okinawa , Japan. *Research Article*, *24*(1), 1–11. http://doi.org/10.5424/fs/2015241-05476

Zhang, J., Hu, J., Lian, J., Fan, Z., Ouyang, X., & Ye, W. (2016). Seeing the forest from drones : Testing the potential of lightweight drones as a tool for long-term forest monitoring. *Biological Conservation*, *198*, 60–69. http://doi.org/10.1016/j.biocon.2016.03.027

APPENDICES

Appendix 1: Field Measurement form

DATA COLLECTION SHEET (AYARE HITAM FOREST RESEARVE, MALAYSIA)									
Author:		**Sample: 1**	**Slope (%):**	**Plot radius: 12.6**			**Data: 30-09-20**	**Ayer Hitam, 2016**	
GPS Plot		Latitude: 3.00115	Longitude: 101.64479					Crown diam. (m)	Crown cover (%)
ID	Tree No.	Latitude	Longitude	Species	DBH (cm)	Field height (m)			
1									
2									
3									
4									
5									
6									
7									
8									
9									
10									
11									
12									
13									
14									
15									
16									
17									
18									
19									
20									
21									
22									
23									
24									
25									
26									
27									
28									
29									
30									
31									
32									
33									
34									
35									

Appendix 2: Common LiDAR sensor parameters for natural resource applications

Parameter	Value
Wavelength	1.064 μm
Pulse Repetition Rate (PRF)	50–150 kHz
Returns per pulse	3–4
Pulse width	10 nano-seconds
Beam divergence	10–80 m rad
Scan angle	<15° off-nadir, 30° total look
Scan pattern(s)	Ziz-zag, parallel, elliptical, sinusoidal
GPS frequency	1–2 Hz
INS frequency	50 Hz (200 Hz max)
Operating altitude	100–3,000 m (6,000 m max), average ~2,000 m
Footprint size	0.10–0.30 cm
Pulse Density	> 4 pulse/m2
Accuracy (Vertical/Elevation)	<0.15 m
Delivery format	Binary LiDAR exchange format (LAS)

Source: (Evans et al., 2009)

Appendix 3: List of equipment which was used in field equipment

Equipment	Functions
Phantom 4 DJI	Acquire stereo image(UAV image)
Defferential GPS	Marking ground control points
Tablet	Prepare Flight Mission Plan and navigation
Remote Controller	Control UAV and setting flight parameters
Garmin GPS	Recording position of individual trees
Diameter tape (5 meters)	DBH measurement
Measuring tape (30 meters)	Plot establishment (delineation)
Leica Disto	Tree height measurement

Appendix 4: List of software and its principle function

Software	Function
ArcGIS 10.3.1	All GIS operation
ERDAS image 2015	Image processing
Agisoft Photoscan Professional Pro	UAV data processing
R Studio	Statistical analysis
eCognition	Object Based Image Analysis (OBIA)
MS Office 2010 (Excel)	Data preparation
MS Office 2010 (Word)	Reports and Thesis writing
SPSS	Statistical analysis

LasTool	Airborne Lidar data processing
Microsoft visio	Flow chart creation
Pix4D Capture	Prepare Flight Plan/mission
Locus	Mobile/Tablet image upload/navigation

Appendix 5: t-test to compare height for ALS and UAV DTMs

t-Test:Two-Sample Assuming Equal Variances

	ALS Altitude	UAV Altitude
Mean	33.87312936	35.31413121
Variance	124.476306	119.6989614
Observations	93	93
Pooled Variance	122.0876337	
Hypothesized Mean Difference	0	
df	184	
t Stat	-0.889314098	
P(T<=t) one-tail	0.187497745	
t Critical one-tail	1.653177088	
P(T<=t) two-tail	0.37499549	
t Critical two-tail	1.972940542	

Appendix 6: t-test to compare tree height for ALS and photogrammetric image matching DTMs where DTM had small difference

t-Test:Two-Sample Assuming Equal Variances

	ALS_Hgt_m	UAV_Hgt_m
Mean	18.68817204	17.93397849
Variance	11.19518467	12.30948943
Observations	93	93
Pooled Variance	11.75233705	
Hypothesized Mean Difference	0	
df	184	
t Stat	1.500193123	
P(T<=t) one-tail	0.067639153	
t Critical one-tail	1.653177088	
P(T<=t) two-tail	0.135278307	
t Critical two-tail	1.972940542	

Appendix 7: One way analysis of variance (ANOVA) for field, UAV and ALS tree height

Groups	Count	Sum	Average	Variance		
ALS Height [m]	388	7403	19.07989691	14.30109353		
UAV Height [m]	388	6899.464718	17.78212556	13.71274988		
Field Height [m]	388	6473.53	16.68435567	17.28593938		
ANOVA						
Source of Variation	SS	df	MS	F	P-value	F crit
Between Groups	1115.878561	2	557.9392806	36.9497984	2.22045E-16	3.003475486
Within Groups	17531.01594	1161	15.0999276			
Total	18646.8945	1163				

F> F critical: Decision: There is variation in the mean of the tree measurement

Appendix 8: F test for variance

	Airborne Lidar Tree Height [m]	UAV Tree Height [m]
Mean	19.07989691	17.78212556
Variance	14.30109353	13.71274988
Observations	388	388
df	387	387
F	1.042904862	
P(F<=f) one-tail	0.339827287	
F Critical one-tail	1.182263528	

Appendix 9: t-test for ALS and UAV tree height

	Airborne Lidar Tree Height [m]	UAV Tree Height [m]
Mean	19.07989691	17.78212556
Variance	14.30109353	13.71274988
Observations	388	388
Pooled Variance	14.00692171	
Hypothesized Mean Difference	0	
df	774	
t Stat	4.829783854	
P(T<=t) one-tail	8.23859E-07	
t Critical one-tail	1.646824694	
P(T<=t) two-tail	1.64772E-06	
t Critical two-tail	1.963033651	

*Significant at 95% level of significant

Appendix 10: F test of UAV and field tree height

	UAV Tree Height [m]	Field Tree Height [m]
Mean	17.78212556	16.68435567
Variance	13.71274988	17.28593938
Observations	388	388
df	387	387
F	0.79328925	
P(F<=f) one-tail	0.011491155	
F Critical one-tail	0.845835109	

Appendix 11: t-test for field and UAV tree height

	UAV Tree Height [m]	Field Tree Height [m]
Mean	17.78212556	16.68435567
Variance	13.71274988	17.28593938
Observations	388	388
Pooled Variance	15.49934463	
Hypothesized Mean Difference	0	
df	774	
t Stat	3.883787974	
P(T<=t) one-tail	5.58144E-05	
t Critical one-tail	1.646824694	
P(T<=t) two-tail	0.000111629	
t Critical two-tail	1.963033651	

*Significant at 95% level of significant

Appendix 12:F test for ALS and field tree height

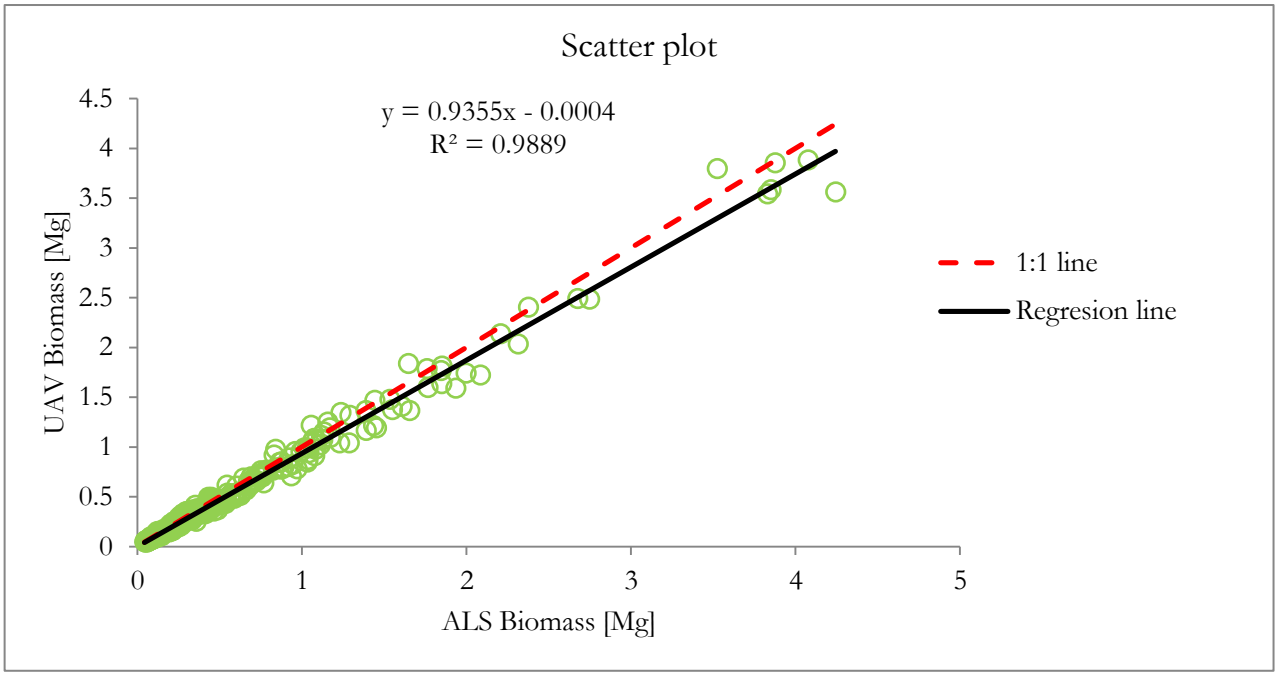
	Airborne Lidar Tree Height [m]	Field Tree Height [m]
Mean	19.07989691	16.68435567
Variance	14.30109353	17.28593938
Observations	388	388
df	387	387
F	0.827325216	
P(F<=f) one-tail	0.031307084	
F Critical one-tail	0.845835109	

Appendix 13: t-test for Airborne Lidar and Field height

	Airborne Lidar Tree Height [m]	Field Tree Height [m]
Mean	19.07989691	16.68435567
Variance	14.30109353	17.28593938
Observations	388	388
Pooled Variance	15.79351645	
Hypothesized Mean Difference	0	
df	774	
t Stat	8.39585825	
P(T<=t) one-tail	1.09718E-16	
t Critical one-tail	1.646824694	
P(T<=t) two-tail	2.19436E-16	
t Critical two-tail	1.963033651	

*Significant at 95% level of significant

Appendix 14: Relationship between ALS and UAV biomass

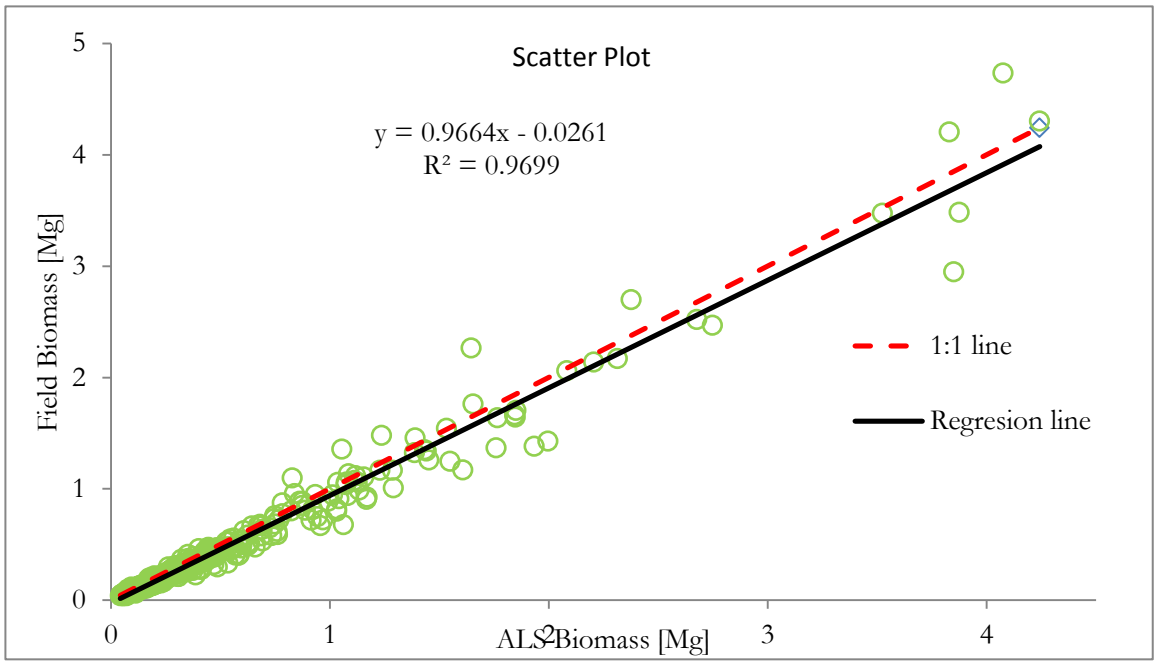


Appendix 15: t-test: for ALS and UAV biomass

	ALS biomass	UAV biomass
Mean	0.465831939	0.434784355
Variance	0.386046353	0.340701463
Observations	388	388
Pooled Variance	0.363373908	
Hypothesized Mean Difference	0	

df	774
t Stat	0.717384196
P(T<=t) one-tail	0.236676755
t Critical one-tail	1.646824694
P(T<=t) two-tail	0.473353509
t Critical two-tail	1.963033651

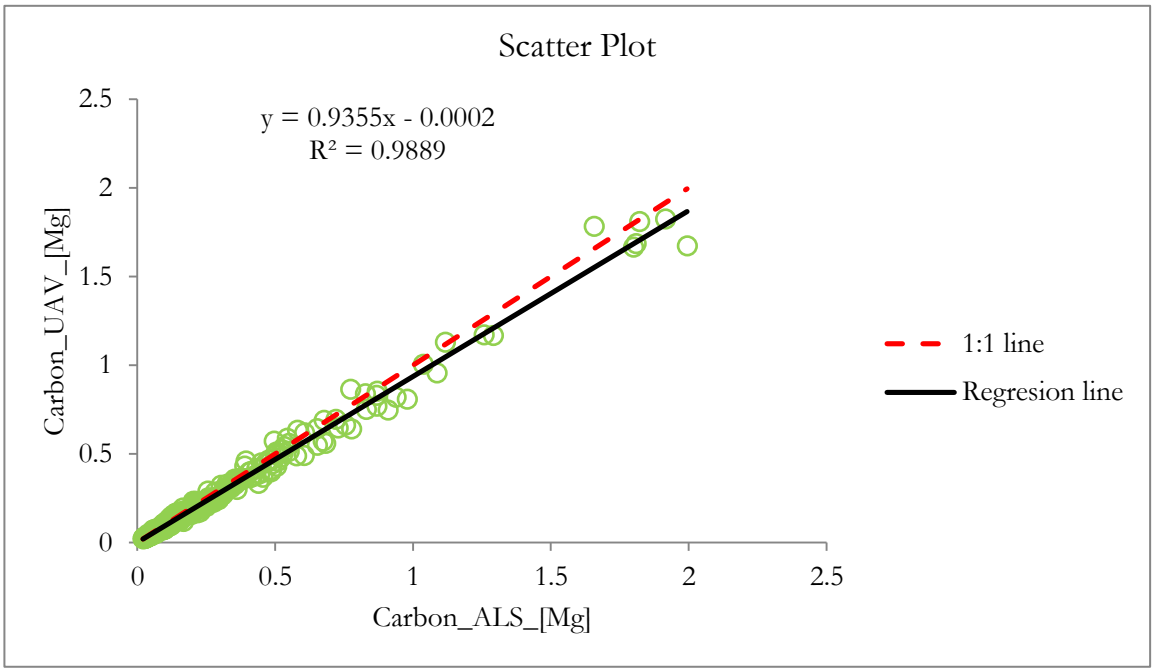
Appendix 16: Relationship between ALS and field biomass



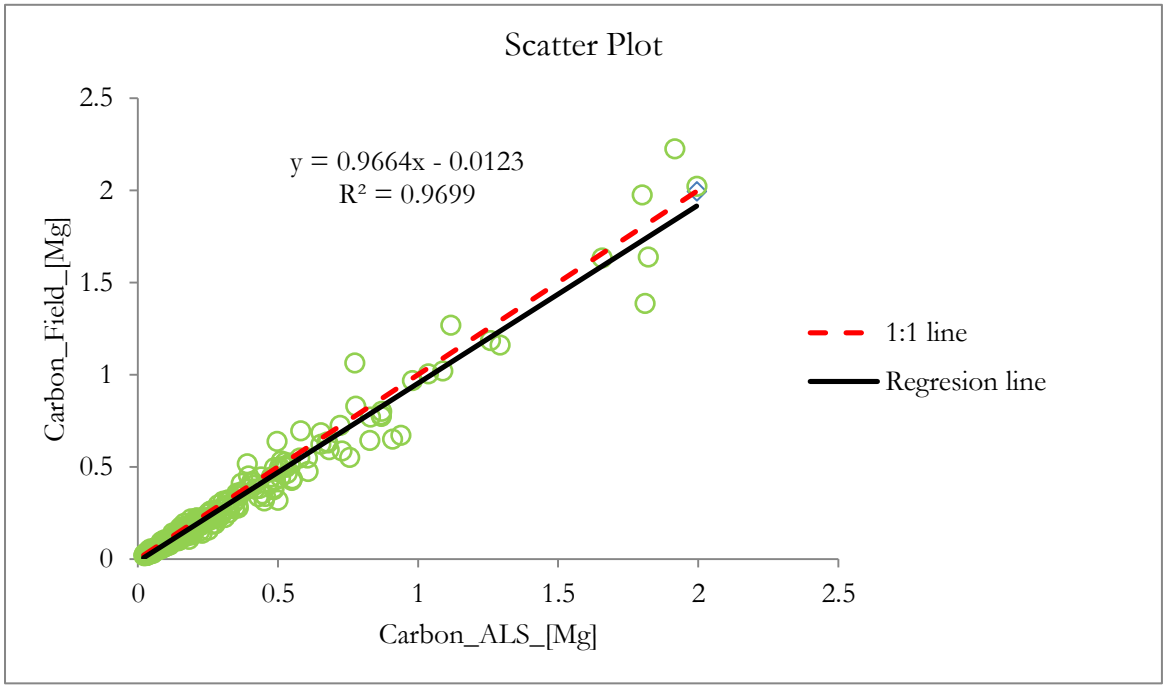
Appendix 17: t-test: for ALS and field biomass

	ALS biomass	Field biomass
Mean	0.465831939	0.424839077
Variance	0.386046353	0.371800108
Observations	388	388
Pooled Variance	0.37892323	
Hypothesized Mean Difference	0	
df	774	
t Stat	0.927541802	
P(T<=t) one-tail	0.17696722	
t Critical one-tail	1.646824694	
P(T<=t) two-tail	0.353934441	
t Critical two-tail	1.963033651	

Appendix 18: Relationship between ALS and field carbon stock



Appendix 19: Relationship between ALS and UAV carbon stock



Appendix 20: Sampled trees with their GPS coordinate of individual tree and DBH and tree height measurement

Plot No.	Tree No.	X	Y	Height ALS [m]	Height UAV [m]	Height Field [m]	Field DBH [m]
1	45	794011.429845	332073.561114	16	15.56	12.90	20.20
1	46	794011.445901	332066.922047	18	19.12	17.30	22.00
1	49	794012.544941	332072.457293	18	19.96	24.00	38.90
1	28	794012.544941	332072.457293	17	20.08	20.00	25.80
1	17	794012.520855	332082.415893	16	12.74	12.40	13.40
1	25	794008.076527	332080.192109	13	13.35	13.50	11.50
1	7	793993.604363	332084.583177	17	16.33	15.10	22.20
1	2	793993.617743	332079.050622	15	14.91	14.40	15.00
1	73	793993.617743	332079.050622	17	14.39	14.40	19.90
1	4	793995.839907	332080.162514	17	15.15	17.00	36.20
1	72	793996.979087	332069.100095	17	18.76	17.00	29.20
1	1	794001.415387	332074.643411	18	16.01	16.70	21.40
1	44	794001.418063	332073.536900	17	17.24	15.10	16.10
1	5	794006.969459	332077.976396	17	15.10	14.80	21.30
1	26	794008.076527	332080.192109	16	16.01	15.05	20.70
1	18	794011.413787	332080.200180	16	16.67	13.60	12.50
23	2	793856.297838	332282.317593	26	24.72	30.30	73.20
23	49	793855.206833	332273.462823	22	19.96	16.80	32.10
23	48	793857.437020	332271.255185	20	17.54	15.60	32.00
23	28	793857.418285	332279.000754	20	17.97	12.30	29.50
23	39	793851.869582	332273.454751	22	19.20	15.90	49.40
23	60	793858.525349	332281.216464	19	17.69	13.40	31.20
23	14	793861.854570	332284.544066	24	19.05	15.90	23.60
23	21	793857.396873	332287.852833	22	18.02	15.20	29.50
23	19	793854.056946	332288.951270	21	18.92	14.20	19.20
23	8	793844.023782	332297.779131	19	15.60	13.20	16.50
23	43	793844.063928	332281.181485	19	14.44	13.20	18.50
23	66	793845.184374	332277.864647	20	16.32	13.90	17.50
26	4	794086.785282	332193.247349	20	20.37	15.40	44.00
26	52	794083.434634	332198.771831	20	19.05	12.80	10.60
26	43	794069.013344	332182.139161	17	15.32	12.30	26.00
26	57	794075.685185	332183.261824	19	17.00	13.70	12.40
26	72	794079.030477	332179.950365	18	15.84	11.90	17.00
26	20	794092.368803	332184.408716	18	16.17	12.20	23.50
26	60	794099.054033	332179.998822	21	17.17	14.40	25.00
26	15	794101.254772	332189.962813	21	18.26	14.90	56.50
26	59	794099.021899	332193.276964	19	18.88	12.00	43.00
27	54	794077.797554	332229.740696	19	14.11	13.20	18.90
27	72	794082.244553	332230.857977	17	14.88	14.20	29.50
27	61	794076.671744	332235.270561	15	13.17	12.20	18.50
27	10	794073.334487	332235.262484	13	12.24	12.70	18.00
27	34	794076.663710	332238.590096	19	14.38	13.20	12.60

27	41	794072.211355	332239.685838	15	15.38	14.80	23.50
27	52	794087.777189	332243.043067	17	14.76	12.20	12.50
27	35	794090.007384	332240.835429	18	15.75	15.50	18.50
8	2	793713.145757	332597.328246	16	15.20	13.30	21.90
8	3	793718.702466	332599.554723	18	16.03	15.90	28.70
8	4	793719.812201	332600.663924	18	17.62	17.80	37.80
8	18	793718.702466	332599.554723	18	18.28	17.80	11.20
8	29	793707.575659	332600.634312	16	16.64	15.30	21.60
8	44	793706.463246	332600.631620	14	15.15	11.90	11.20
8	28	793700.895827	332602.831178	18	19.01	18.10	24.20
8	30	793702.013595	332600.620852	18	17.41	17.20	16.30
8	27	793699.794125	332598.402451	18	17.12	16.93	21.40
8	12	793714.268880	332592.904903	16	15.90	14.20	12.60
8	11	793700.927958	332589.553074	21	22.74	20.10	42.70
8	13	793703.160816	332586.238932	20	19.60	17.20	21.60
8	20	793713.169856	332587.369667	17	17.20	16.40	25.30
8	21	793716.512450	332585.164725	13	11.54	12.50	21.30
8	19	793716.504417	332588.484252	16	13.02	13.80	11.60
8	25	793720.948714	332590.708037	16	14.35	13.19	14.70
8	26	793723.157474	332597.352474	13	14.66	12.60	23.20
8	17	793708.709493	332591.784934	14	12.64	12.60	18.15
8	6	793706.473957	332596.205585	12	13.97	12.20	17.10
8	10	793706.473957	332596.205585	13	12.74	12.20	22.00
9	42	793755.240683	332670.460148	17	14.94	16.86	23.50
9	46	793754.120234	332673.776982	14	17.49	12.58	16.40
9	49	793753.002464	332675.987307	25	22.88	23.84	24.80
9	48	793744.105843	332674.859255	28	23.38	28.40	72.00
9	53	793748.539421	332681.509081	14	11.49	13.73	13.40
9	1	793754.101483	332681.522546	14	12.66	13.89	35.00
9	41	793749.681298	332669.340174	29	25.59	28.70	20.00
9	7	793738.554494	332670.419755	17	16.33	15.89	13.40
9	13	793740.781998	332669.318631	13	13.66	12.21	14.40
9	15	793740.784676	332668.212122	15	13.27	12.21	11.50
9	35	793743.044322	332653.832891	15	13.49	13.69	13.60
9	17	793738.581279	332659.354665	13	12.86	14.50	20.50
9	39	793750.801747	332666.023340	24	23.34	22.03	23.70
9	40	793753.013179	332671.561271	20	18.26	20.60	24.70
9	22	793754.157735	332658.285855	15	13.07	14.57	11.50
9	23	793756.379882	332659.397750	18	16.64	15.80	20.80
10	47	793629.920908	332511.925255	17	15.20	13.80	14.70
10	46	793631.030645	332513.034454	11	13.42	13.80	14.80
10	40	793624.358843	332511.911803	20	18.60	19.58	35.00
10	43	793629.944994	332501.966683	18	17.24	17.74	24.20
10	45	793625.500694	332499.742905	16	14.76	12.12	18.40
10	48	793631.041350	332508.608421	16	15.86	13.90	15.00
10	22	793636.592710	332513.047906	21	21.70	22.26	26.20
10	55	793636.595387	332511.941398	21	20.45	24.00	22.20

10	52	793639.948684	332505.310421	29	27.92	29.20	42.00
10	60	793642.170834	332506.422311	20	19.63	20.00	21.00
10	65	793643.253807	332518.596591	17	14.62	15.50	19.20
10	64	793638.796126	332521.905353	22	21.51	22.70	35.90
10	66	793643.261836	332515.277067	13	13.47	12.00	10.10
10	67	793643.253807	332518.596591	19	19.13	14.40	12.00
10	68	793642.141394	332518.593900	13	11.63	13.20	13.10
10	69	793631.014587	332519.673502	22	25.68	25.20	35.40
10	72	793622.112607	332520.758486	19	18.18	17.40	12.80
10	5	793638.830918	332507.520747	20	20.35	22.81	20.50
13	27	793548.704077	332516.154904	17	14.92	16.50	24.70
13	54	793552.057368	332509.523928	16	14.00	14.90	19.50
13	36	793547.613069	332507.300155	16	12.19	14.30	20.60
13	32	793548.728157	332506.196337	17	12.97	13.60	20.10
13	31	793540.951971	332501.751480	14	12.83	12.20	23.50
13	30	793545.404296	332500.655731	16	13.15	13.00	21.10
13	28	793548.736183	332502.876815	16	12.67	12.80	15.50
13	25	793548.736183	332502.876815	17	14.22	12.40	10.50
13	20	793547.615744	332506.193647	17	11.85	13.30	26.00
13	53	793543.144691	332515.034947	16	12.39	14.80	22.40
13	48	793542.042980	332510.606228	16	11.68	14.70	17.00
13	49	793542.032279	332515.032258	16	14.06	15.00	13.40
13	45	793537.582629	332515.021499	21	15.81	21.30	38.30
13	42	793542.026928	332517.245272	20	15.19	19.90	27.40
13	50	793537.563901	332522.767050	19	16.63	18.90	31.00
13	39	793535.347103	332519.442148	15	12.84	12.70	17.40
13	24	793547.613069	332507.300155	13	10.16	14.50	11.90
15	40	795330.666952	335760.392566	19	16.81	15.60	17.50
15	28	795332.908055	335753.758897	16	13.21	11.90	14.00
15	2	795332.916209	335750.439331	26	22.98	20.80	44.60
15	19	795334.047632	335742.696407	23	19.36	21.80	42.10
15	27	795327.354224	335750.425668	27	24.28	23.40	36.40
15	45	795325.148456	335742.674548	26	24.85	20.50	36.20
15	53	795317.329062	335755.933688	22	19.13	17.40	37.60
15	44	795311.769796	335754.813504	24	19.61	17.00	52.00
15	32	795316.224819	335752.611389	17	18.11	17.60	35.20
15	14	795325.104968	335760.378904	18	19.40	16.90	21.80
16	10	795430.785430	335759.532013	22	18.71	12.40	10.00
16	41	795433.007506	335760.644003	33	27.96	22.60	24.00
16	54	795438.558619	335765.083763	22	18.24	17.00	13.90
16	58	795428.601418	335742.928700	16	18.66	12.20	16.10
16	63	795435.251335	335752.903808	18	18.42	12.40	16.30
16	3	795427.442799	335761.736859	19	16.23	15.90	18.00
16	9	795427.434642	335765.056428	32	31.85	32.00	34.00
16	30	795425.209846	335765.050961	14	16.75	13.80	25.00
16	55	795419.669610	335756.185110	27	23.32	15.60	21.50
16	22	795427.464550	335752.884674	29	27.71	23.40	18.60

17	40	795327.468372	335703.951734	22	22.40	20.50	21.60
17	37	795329.690449	335705.063721	25	20.38	21.60	44.00
17	38	795320.788552	335706.148387	16	17.51	12.20	11.90
17	6	795321.914537	335700.618508	17	19.07	12.30	10.00
17	12	795316.363420	335696.178759	21	23.85	17.10	29.00
17	10	795323.037805	335696.195151	26	26.71	14.20	11.70
17	8	795324.166507	335689.558750	24	22.16	19.10	19.20
17	51	795325.284340	335687.348437	17	18.36	14.80	21.80
17	20	795327.511852	335686.247379	18	19.16	12.20	17.00
17	13	795327.506417	335688.460423	21	22.64	20.70	75.60
18	4	795398.672697	335699.700515	21	20.20	16.20	21.70
18	11	795398.672697	335699.700515	14	16.59	14.70	26.00
18	39	795398.642796	335711.872266	23	23.38	15.80	16.00
18	40	795389.743613	335711.850404	16	14.95	14.10	12.60
18	14	795390.866884	335707.427046	18	18.05	16.30	18.40
18	37	795391.968409	335711.855870	29	28.89	20.10	33.00
18	60	795384.192497	335707.410650	20	23.01	20.60	26.40
18	67	795383.069226	335711.834008	33	30.66	25.10	63.10
18	69	795377.520828	335706.287732	21	19.39	14.40	10.20
18	48	795383.096408	335700.768781	26	24.97	23.20	35.50
18	52	795377.545290	335696.329028	15	13.77	12.20	32.00
18	20	795380.898792	335689.698090	35	35.70	27.20	35.00
18	43	795378.654970	335697.438283	20	22.48	14.90	22.90
18	51	795382.019344	335686.381254	19	19.85	16.60	18.40
18	19	795385.351102	335688.602497	19	16.97	14.90	17.00
4	1	793905.279774	332727.255815	14	14.63	13.70	16.80
4	2	793913.074709	332723.955148	18	16.05	14.50	15.30
4	3	793910.860604	332719.523717	26	21.95	25.60	37.00
4	5	793906.416311	332717.299917	18	15.10	15.00	12.30
4	7	793899.741831	332717.283749	22	21.53	20.20	53.10
4	8	793900.843523	332721.712485	21	18.39	15.40	23.10
4	10	793903.076391	332718.398344	20	19.30	18.90	23.10
4	9	793895.268054	332727.231563	20	19.64	18.00	16.40
4	12	793899.736470	332719.496770	21	19.70	18.20	14.30
4	13	793895.284137	332720.592501	24	20.45	23.20	17.90
4	14	793899.717707	332727.242342	24	21.30	20.40	15.00
4	17	793904.167360	332727.253121	18	17.30	14.65	11.00
4	22	793913.066667	332727.274679	27	23.98	27.75	27.10
4	24	793914.173719	332729.490395	19	17.60	14.71	10.30
4	28	793918.626053	332728.394664	22	20.50	20.63	20.40
5	60	793869.773673	332689.548247	22	18.75	21.50	13.30
5	63	793870.891446	332687.337921	19	17.81	15.10	13.70
5	67	793865.332059	332686.217940	21	18.61	20.40	37.00
5	61	793877.571286	332685.141066	19	17.13	12.70	14.40
5	59	793876.437434	332693.990452	19	18.68	18.13	49.30
5	58	793878.672980	332689.569800	18	16.73	16.00	10.10
5	54	793880.873687	332699.533780	24	19.66	22.50	26.10

5	56	793871.974380	332699.512225	19	16.87	16.00	22.10
5	55	793871.971700	332700.618735	16	14.09	14.25	12.50
5	49	793868.650540	332693.971593	22	17.43	18.30	22.00
5	45	793870.888766	332688.444431	18	15.24	12.90	14.10
5	74	793867.562245	332684.010309	19	16.45	17.10	31.70
5	70	793869.779033	332687.335227	22	21.56	21.30	21.60
5	69	793872.022618	332679.595045	18	18.91	12.60	11.30
5	68	793868.688058	332678.480453	17	14.18	13.50	28.70
5	71	793863.128670	332677.360472	18	16.74	13.20	13.40
5	72	793860.901164	332678.461594	25	20.99	25.50	37.00
5	50	793865.353497	332677.365860	18	17.89	17.60	15.30
5	33	793865.350817	332678.472370	23	21.10	22.20	40.00
5	42	793864.203567	332692.854306	18	16.50	14.70	12.70
5	35	793863.091154	332692.851612	17	17.17	16.70	20.20
5	43	793857.529087	332692.838141	22	19.25	17.20	37.00
5	41	793865.313300	332693.963510	20	19.13	18.00	55.60
7	65	794187.080078	332579.665243	23	22.34	22.10	24.90
7	63	794185.978389	332575.236497	17	17.62	16.00	14.00
7	70	794188.195177	332578.561427	14	13.89	12.80	15.00
7	71	794183.737464	332581.870180	14	14.43	13.70	27.00
7	62	794188.195177	332578.561427	18	17.52	12.60	12.50
7	61	794185.970343	332578.556035	18	17.28	12.80	17.00
7	60	794182.622365	332582.973996	28	28.31	31.90	53.50
7	58	794188.176404	332586.307015	21	17.57	20.40	28.90
7	57	794190.369054	332599.590558	25	24.19	24.20	54.50
7	54	794194.842859	332589.642730	18	15.92	16.30	40.30
7	75	794182.606274	332589.613071	19	18.33	15.10	25.90
7	22	794189.275411	332591.842274	27	25.07	25.40	57.90
7	42	794189.262001	332597.374837	21	19.87	18.80	27.30
7	47	794193.708986	332598.492135	23	23.23	20.00	25.80
7	45	794185.946206	332588.514647	24	21.16	21.30	50.80
7	46	794192.599251	332597.382926	16	12.68	12.80	22.00
7	38	794197.062329	332591.861148	24	19.32	21.70	42.20
7	40	794194.826767	332596.281806	20	18.36	14.10	24.60
7	33	794189.264683	332596.268324	24	23.55	18.40	13.00
7	68	794193.730442	332589.640034	20	19.12	19.50	28.00
20	21	793824.210282	332670.627131	18	18.65	14.50	15.70
20	59	793824.234395	332660.668544	16	15.60	14.20	13.00
20	53	793829.799141	332659.575502	14	12.00	13.40	19.90
20	4	793827.566277	332662.889644	18	16.01	14.40	22.10
20	12	793829.812537	332654.042954	16	17.88	15.90	29.80
20	43	793834.238077	332664.012315	13	13.96	12.20	16.40
20	17	793836.465583	332662.911193	24	21.02	22.46	57.00
20	69	793836.454865	332667.337232	15	12.61	13.60	15.20
20	20	793828.662614	332669.531396	18	15.79	14.80	18.30
20	9	793830.890120	332668.430273	18	18.17	16.40	17.60
20	5	793831.991816	332672.859006	19	18.78	14.70	19.30

20	22	793827.528766	332678.380779	15	16.09	14.00	15.70
20	25	793833.109588	332670.648680	20	18.63	16.70	33.60
20	44	793827.528766	332678.380779	17	15.54	16.50	14.40
20	47	793827.542163	332672.848231	15	14.19	14.27	16.00
20	66	793835.337093	332669.547557	24	19.80	22.60	32.40
20	56	793824.210282	332670.627131	19	18.49	13.70	17.50
21	35	794017.848056	332639.007146	16	15.55	12.30	39.50
21	55	794021.185302	332639.015231	16	15.50	15.30	28.50
21	42	794023.412813	332637.914110	19	17.46	15.40	36.20
21	64	794025.632281	332640.132523	23	20.71	21.30	50.70
21	24	794030.087303	332637.930281	17	17.19	16.40	45.70
21	5	794032.317495	332635.722649	18	15.63	12.40	23.40
21	8	794027.870516	332634.605357	16	16.08	14.20	35.00
21	23	794032.333581	332629.083581	25	23.74	23.50	38.60
21	41	794017.885587	332623.515989	19	18.67	15.90	15.40
21	17	794024.543993	332630.171227	17	15.01	12.70	20.10
21	65	794023.423536	332633.488065	19	17.86	16.50	20.50
21	58	794016.765130	332626.832828	17	14.92	14.30	17.70
21	56	794017.869503	332630.155056	18	17.08	14.70	22.00
21	47	794016.757088	332630.152361	20	16.65	16.40	27.00
21	54	794010.104042	332621.284102	15	13.61	12.50	12.50
21	59	794012.318150	332625.715537	20	18.16	17.80	28.00
21	45	794014.540299	332626.827438	20	20.66	19.70	24.20
21	75	794014.540299	332626.827438	21	20.50	19.60	39.90
21	1	794012.310108	332629.035070	19	17.50	16.20	14.50
21	6	794018.973875	332633.477285	12	10.40	12.10	16.30
22	25	793869.610185	332757.045358	17	14.37	14.20	12.40
22	35	793870.714556	332760.367583	18	15.42	16.60	27.50
22	43	793870.727958	332754.835032	21	18.48	20.30	23.40
22	65	793867.377318	332760.359498	18	16.22	14.50	19.90
22	8	793866.280988	332753.717744	15	14.30	13.50	11.70
22	26	793865.165895	332754.821559	16	13.81	12.10	13.70
22	65	793866.259545	332762.569824	18	15.93	16.70	20.40
22	54	793860.700162	332761.449840	17	14.52	14.40	13.50
22	1	793867.371957	332762.572518	19	16.12	17.20	25.20
22	56	793862.906224	332769.200799	16	15.10	15.50	14.00
22	21	793862.900863	332771.413819	14	14.05	11.90	22.40
22	64	793869.580700	332769.216968	20	18.67	14.70	10.80
22	42	793870.698473	332767.006643	25	22.51	22.40	61.00
22	29	793875.153485	332764.804402	17	16.67	15.30	23.00
22	62	793872.928660	332764.799012	17	14.77	14.30	27.50
22	9	793879.597775	332767.028202	19	18.64	14.90	35.60
22	71	793881.822600	332767.033591	18	16.08	15.90	20.00
22	46	793884.031342	332773.678042	18	16.70	17.50	38.80
22	19	793887.379303	332769.260086	13	14.91	14.20	10.60
22	31	793881.833323	332762.607551	20	18.10	17.80	34.50
22	2	793887.414151	332754.875454	17	14.11	12.70	19.80

25	20	793959.761226	332738.452980	15	14.50	13.40	16.90
25	61	793956.442752	332730.699319	18	15.84	15.20	31.90
25	38	793949.770951	332729.576637	17	15.74	14.10	16.90
25	56	793953.124278	332722.945658	19	17.70	14.90	45.20
25	3	793959.788036	332727.387873	19	18.18	15.30	16.30
25	57	793956.453476	332726.273276	26	21.37	25.70	51.90
25	12	793954.247415	332718.522311	16	17.28	12.60	22.40
25	47	793970.920218	332724.095293	18	16.30	16.20	25.10
25	6	793965.355467	332725.188328	13	14.60	14.40	22.00
25	74	793963.130640	332725.182937	17	16.26	15.20	28.00
25	66	793967.577614	332726.300229	15	15.85	14.20	12.90
25	10	793965.347424	332728.507860	15	13.01	12.80	33.20
25	44	793959.771950	332734.026937	24	20.04	25.20	43.90
6	31	794232.783055	332541.047844	16	13.78	13.68	13.90
6	8	794236.133718	332535.523368	15	13.25	13.80	14.20
6	9	794232.796465	332535.515279	18	17.13	16.40	36.90
6	44	794232.777691	332543.260869	20	18.80	16.50	12.30
6	6	794232.801829	332533.302253	21	19.34	22.30	23.20
6	10	794228.341430	332537.717520	17	19.66	22.00	45.30
6	2	794221.669606	332536.594830	19	16.13	15.20	33.00
6	14	794234.991798	332547.692314	23	20.71	20.00	38.70
6	18	794227.207557	332546.566927	24	22.34	22.19	23.20
6	21	794230.542128	332547.681528	19	18.25	16.68	40.00
6	28	794232.772327	332545.473895	24	19.68	25.60	48.00
6	20	794235.005209	332542.159749	13	12.28	12.76	10.50
2	1	793919.251200	332470.245790	30	27.69	33.00	66.00
2	13	793932.262180	332472.047713	19	16.92	14.00	16.20
2	14	793932.266466	332470.277297	29	28.39	30.30	35.20
2	16	793932.271019	332468.396229	18	16.20	13.20	17.50
2	17	793930.393305	332462.859099	20	17.81	16.00	14.40
2	18	793928.497645	332464.735588	18	16.55	12.00	20.20
2	19	793922.931280	332466.492541	18	15.94	14.50	14.00
2	23	793924.826672	332464.726702	22	17.96	16.20	22.00
2	28	793919.273700	332460.951103	21	19.80	23.50	35.00
2	33	793922.913333	332473.906160	17	15.49	12.40	11.00
2	40	793910.018150	332470.223439	17	16.49	16.90	36.00
3	71	793998.186391	332489.579648	20	18.47	15.00	10.00
3	70	793998.186391	332489.579648	22	21.81	25.00	16.00
3	67	793997.084692	332485.150910	21	19.64	19.00	26.00
3	73	793994.830386	332497.317143	21	19.51	18.90	11.40
3	68	793995.948161	332495.106815	20	15.45	13.40	15.00
3	42	793983.714263	332493.970674	16	12.77	12.50	13.00
3	41	793982.617923	332487.328915	17	18.18	17.80	23.50
3	54	793984.840076	332488.440813	22	18.55	20.70	46.60
3	51	793988.174645	332489.555405	20	20.23	19.40	33.60
3	39	793991.618793	332445.413698	19	16.03	14.40	15.00
3	35	793992.732549	332444.863136	18	17.60	18.00	17.90

3	64	793991.620400	332444.749792	22	24.62	30.50	50.00
3	63	793991.617989	332445.745652	19	17.37	16.00	14.00
3	58	793981.610526	332443.950995	26	21.25	24.20	28.00
3	57	793977.161396	332443.718920	19	18.23	17.20	27.00
3	52	793982.720264	332445.060199	27	25.17	25.00	21.70
14	50	793765.884335	332409.348225	19	16.07	15.30	25.70
14	21	793773.681948	332404.941025	23	23.40	21.30	45.70
14	75	793767.015487	332401.605352	26	26.39	20.10	47.60
14	12	793771.470501	332399.403097	16	13.67	12.40	18.60
14	35	793762.571179	332399.381570	16	14.17	12.10	14.60
14	17	793760.349025	332398.269680	18	19.05	14.30	21.50
14	26	793755.896688	332399.365426	17	17.50	15.60	18.90
14	22	793758.108136	332404.903353	12	13.56	15.30	15.50
14	57	793753.658476	332404.892589	19	16.47	15.60	31.10
14	74	793749.211492	332403.775317	17	16.60	16.00	24.20
14	58	793756.993044	332406.007171	17	14.60	12.20	35.60
14	65	793753.645093	332410.425134	18	14.18	12.50	16.20
14	64	793763.656828	332410.449352	23	23.30	20.00	40.40
14	60	793765.870952	332414.880771	20	15.02	12.30	13.40
14	71	793760.338319	332402.695716	21	22.75	22.40	26.20
19	6	793846.814842	332523.515200	19	18.85	16.70	26.60
19	13	793849.045028	332521.307565	16	15.56	14.50	12.70
19	38	793853.492008	332522.424846	19	18.28	17.20	26.70
19	55	793851.269857	332521.312951	19	17.48	16.20	24.80
19	40	793857.928275	332527.968166	15	13.93	12.90	17.00
19	25	793853.470581	332531.276925	22	21.51	22.10	28.40
19	51	793856.802468	332533.498023	19	16.38	15.50	28.60
19	8	793857.890776	332543.459304	15	15.44	13.50	17.00
19	48	793851.232360	332536.804088	19	17.84	17.40	34.50
19	69	793851.232360	332536.804088	15	13.40	13.20	13.30
19	12	793849.031636	332526.840114	18	16.03	14.50	14.50
19	4	793849.028958	332527.946624	17	16.40	15.90	16.20
19	70	793849.036993	332524.627095	16	15.57	12.90	13.10
19	9	793849.028958	332527.946624	21	18.13	17.40	30.50
19	53	793847.911186	332530.156951	17	15.48	13.80	25.20
19	52	793850.122624	332535.694886	22	22.04	25.40	24.30
19	68	793851.227003	332539.017108	20	16.55	16.40	32.00
19	47	793852.344774	332536.806781	16	14.04	14.80	23.60
19	14	793848.999495	332540.118232	18	17.56	15.80	13.60
19	39	793845.651538	332544.536193	19	15.10	14.40	21.20
19	60	793845.656895	332542.323174	17	15.84	13.30	19.60
24	37	793939.078311	332551.401485	19	15.79	14.80	32.00
24	57	793949.103446	332545.893175	19	16.44	15.00	22.00
24	33	793943.546728	332543.666686	23	18.75	17.70	38.50
24	17	793948.015145	332535.931886	20	15.12	13.60	17.50
24	35	793952.464806	332535.942661	24	19.20	17.70	36.50
24	59	793950.253372	332530.404720	18	14.43	12.60	10.00

24	50	793949.138277	332531.508537	23	18.41	20.60	27.50
24	25	793929.085330	332543.631669	17	17.24	17.20	38.00
11	61	796219.297152	335383.036826	19	17.55	14.80	17.90
11	45	796213.705159	335395.194960	21	15.74	12.70	27.40
11	40	796214.842076	335385.238934	27	26.82	24.20	70.00
11	70	796212.619984	335384.126929	22	23.15	16.80	22.90
11	71	796209.282761	335384.118716	18	17.15	12.10	29.10
11	43	796209.271868	335388.544833	18	17.68	15.30	16.30
12	61	796133.336823	335506.757269	17	16.70	14.60	11.50
12	62	796136.690381	335500.126310	20	18.23	18.00	21.60
12	42	796128.892647	335504.533260	21	22.03	20.70	21.80
12	60	796127.772071	335507.850108	19	22.41	16.50	22.40
12	18	796131.106565	335508.964851	17	16.77	12.19	19.50
12	38	796129.985989	335512.281699	16	18.80	12.31	22.50
12	4	796134.438335	335511.186122	21	22.88	25.23	44.20
12	37	796141.115493	335510.096021	22	21.36	22.26	36.20
12	44	796140.003087	335510.093283	18	15.56	14.80	14.60

Appendix 21: Field photos













